Urban Air Mobility: Deconstructing the Next Revolution in Urban Transportation - Feasibility, Capacity and Productivity

by

Vishwanath Bulusu

A dissertation submitted in partial satisfaction of the
requirements for the degree of
Doctor of Philosophy

in

Engineering - Civil and Environmental Engineering

in the

Graduate Division

of the

University of California, Berkeley

Committee in charge:

Professor Raja Sengupta, Chair
Professor Alexandre M. Bayen
Professor Per-Olof Persson

Summer 2019

Urban Air Mobility: Deconstructing the Next Revolution in Urban Transportation - Feasibility, Capacity and Productivity

Abstract

Urban Air Mobility: Deconstructing the Next Revolution in Urban Transportation - Feasibility, Capacity and Productivity

by

Vishwanath Bulusu

Doctor of Philosophy in Engineering - Civil and Environmental Engineering

University of California, Berkeley

Professor Raja Sengupta, Chair

Owing to a century of innovation in aircraft design, for the first time in history, air transport presents a potential competitive alternative to road, for hub-to-door and door-to-door urban services. In this dissertation, we first study the feasibility of uncongested air transport, for moving people and goods in an urban area, based on three metrics - enroute travel time, fuel cost and carbon dioxide (CO_2) emissions. We estimate the metrics from emission standards and operational assumptions on vehicles based on current market data and compare electric air travel of near future to predominantly gasoline road travel of today. For passenger movement, air is faster than road for all distances. It fares better on fuel cost and emissions for longer distances (specific transition distances are stated in the main text). For consolidated movement of goods, air is at par or better than road dependent on the type of aircraft used. Finally, for movement of unconsolidated goods, air far outperforms road on all three metrics.

To enable the feasible air-based services, a typical metropolitan region's airspace needs to accommodate traffic orders of magnitude higher than the manned airspace of today, while staying uncongested to deliver the afore-mentioned benefits. Hence we also develop methods to study the urban airspace capacity. We use our methods to evaluate the airspace capacity for a specific use case of goods movement under 400 feet (low altitude airspace) and find that with today's technologies at least 10,000 free routed small Unmanned Aircraft Systems (sUAS) flights per day can be safely enabled in the San Francisco Bay area. Better

onboard technologies would only improve this number. Furthermore, our methods can be extended to evaluate the metropolitan airspace capacity to accommodate other use cases including movement of passengers and goods in a much wider band of airspace.

Finally, we look at the energy efficiency, travel time and throughput trade-off between speed and direction control. We find that while maintaining a similar decent throughput, direction control is more energy efficient for enroute tactical resolution unless aircraft can be built with very high hover energy efficiency. However, speed control has a lower impact on travel time extension. Hovering capability additionally offers high flexibility for the type of operations that can be enabled in an urban airspace. Hence, the findings of this dissertation also have policy implications for the aircraft design industry for enabling Urban Air Mobility (UAM).

It is quite noteworthy that all our results are based on a road-friendly urban design. Changes in design that facilitate easier access to air-based hub-to-door and door-to-door services, would only make the case stronger for UAM as the next revolution in urban transportation.

To my parents - Rajya Lakshmi and Chandi Prasad
for their unconditional love and unwavering support

&

To my mentor and consortem culpae - Raja
for being the guiding light whenever I needed one

Contents

List of Figures

List of Tables

Acknowledgments

I would first like to thank my advisor, Professor Raja Sengupta. It is said - Never seek a guru. When the pain in you becomes a cry, a guru will find you. Raja found me when I needed to be found. He taught me the true meaning of research and for that I am forever indebted. I hope to continue our collaborations and work towards a better tomorrow. I also thank the rest of my thesis committee: Professor Per-Olof Persson and Professor Alexandre M. Bayen for their insightful comments, recommendations and encouragement as and when I needed them.

Thank you Professor Valentin Polishchuk, one of my major research collaborators, for invaluable insights and contributions in my early research career. I hope to continue pursuing our transformational ideas for the future of urban air traffic. Furthermore, I extend my acknowledgements to my fellow researchers, Leonid Sedov, Zhilong Liu, Dounan Tang, Alexander Kurzhanskiy and Rohan Datta, for their technical contributions that made this research possible. I also acknowledge my mentors and colleagues at NASA Ames - Eric Mueller, Min Xue, Banavar Shridhar, Gano Chatterji and Todd Farley for providing technical, financial and moral support to my academic pursuits.

The moral support one receives, outside one's academic environment is as important, if not more. I am therefore forever indebted to my wonderful Woodhouse friends - Madhyama Subramanian, Aaditya Ramdas, Leila Wehbe, Mayur Mudigonda, Sandeep Mehta, Pulkit Agrawal and Siva Bandaru; my fellow meditators - Ashwin Mudigonda, Susan Purcell, Sangeeta Agrawal and Ali; my life mentor Joe Lurie and my god-grandmother Nancy Nielsen, for all the fun, support and good times. I also salute and express my heartfelt gratitude to Sadhguru and Simran Ji, for rekindling spirituality in my life, when I needed it the most. Please give me the strength to journey on.

The journey of a thousand miles begins with one step. My journey began with three. First was my school life at St. John's, Marhauli, Varanasi. I bow to Jaya Mam and Jyotsna Mam for seeing my potential that I myself could not and pushing me towards it. I also express my gratitude to all my teachers who were the closest friends and guides growing up. Second was my undergraduate life at NIT, Trichy. It taught me what it meant to be a fearless explorer. That adventure wouldn't have been possible without the encouragement of Professor K. Muthukkumaran and Professor P. Jayabalan. I also could not have wished for a better guide than Professor Pradipta Banerji at IIT, Bombay, without whom, I might have never made it to Berkeley. The third step was my Masters at Cal. I thank Professor Armen Der Kiureghian and Professor Filip C. Filippou for recognizing me for what I could be. As I grew through these phases my one constant companion was my tabla and my love for percussion which wouldn't have been possible if not for the ten years of training from my guru Shri Pradeep Kumar Verma. I am forever indebted to you Sir.

Last but not the least, no words of gratitude do enough justice to the two most important people in my life - My parents, Rajya Lakshmi and Chandi Prasad Bulusu, for raising me to be the person I am, loving and supporting me unconditionally, through the best, worst and the hardest times, placing their unwavering trust in me and sharing my every joy and sorrow. I love you so much!

Chapter 1

Introduction

Transportation systems move people, goods and services (henceforth collectively referred to as entities), from one place to another, via Air, Land (Rail and Road) and Water and other secondary modes like pipelines, cables and space. In a nutshell, all transportation operations can be classified into three types, namely - hub-hub, hub-door/door-hub, and door-door.

Hubs handle large-scale movement of entities, such as airports, harbors, railway stations, bus terminals, gas stations, supermarkets, etc. Doors are places handling small-scale movement of entities, like individual houses, farms, offices and so on. Air, rail, road and water enable hub-hub operations. But hub-door and door-door operations are conducted till date, primarily via roads.

Founded by Henry Ford on June 16, 1903, the Ford Motor Company produced its first automobile - the Model T in 1908. The same year, the Wright Brothers made their first public flight and carried the first airplane passenger. Within two decades, Sikorsky Aero Engineering Corporation was founded by Igor Sikorsky on May 23, 1923. It produced the Sikorsky R-4 - the first stable, single-rotor, fully controllable helicopter to enter full-scale production. Yet over the past century, the automobile became a consumer product but the aircraft/helicopter did not. With one simple goal that a company should produce products that its employees can afford, Henry Ford's revolution changed the face of urban transportation (figure 1.1), putting every American home on a motorable road.

However, owing to a century of innovation in aircraft design, for the first time in history, air transport presents a potential competitive alternative to road, for hub-to-door and door-to-door urban services. This dissertation explores that potential. We do this in three steps. First, in chapter 2, we explore the feasibility of air transport, for moving people and goods in an urban area, based on three metrics - enroute travel time, fuel cost and carbon dioxide (CO_2) emissions. We estimate the metrics from emission standards and operational assumptions on vehicles based on current market data and compare electric air travel to

Figure 1.1: Columbus Circle New York City - from 1905 to 2015, Image Courtesy: fineprintnyc (left), 2luxury2 (right)

gasoline road travel. Apart from optimistic market studies such as the one conducted by Uber[40] and sporadic academic research into emissions based sustainability of goods movement by air[32], research into the potential of urban mobility via air as the next fundamental evolution of transportation is lacking and this dissertation provides the first stepping stone in that direction.

Second, in chapter 3, we estimate the capacity of urban airspace to accommodate goods movement at or below 400 feet Above Ground Level (AGL) altitude, as a function of safety. Airspace capacity is a vastly explored concept in manned aviation[64, 65, 50, 58] but barely utilized practically. All practical capacity considerations are primarily tied to a manual air traffic controller till date. Benefits of automated aircraft and air traffic management could vastly improve this capacity. Studies exploring unmanned air traffic capacity in metropolitan airspace are again few, a good example being the Metropolis study that explored a hypothetical Personal Aerial Vehicle (PAV) traffic system in Paris. This research therefore complements such studies and further provides one of the first capacity estimates for low altitude urban airspace.

Third, in chapter 4, we study the productivity of the below 400 feet AGL urban airspace as a function of onboard flight control (speed control vs direction control). We first look at the variation of inflow and outflow rates to determine the maximum steady state throughput in a given area of airspace with traffic flying in all directions. Then we compare the energy consumption of speed control vs direction control while maintaining the throughput to identify which control is more optimal. This effort is novel in two ways. First, enroute throughput is a widely explored concept in road traffic but not utilized to the same depth and extent in air traffic. This effort starts bridging that gap. Second, all throughput studies explore flows where outflow and inflow do not obstruct each other. In other words, there is

a sense of global direction. This also means that gridlocks can be resolved. However, this is not true for free flow air traffic in an urban airspace where flights are dispersed in all directions. This means that inflow in an area can obstruct the outflow from it eventually leading to sudden instability which may be impossible to resolve unless the inflow is curtailed.

We find that air is indeed a feasible alternative to road. Airspace capacity chapter evaluates when the airspace gets congested for one particular use case. Airspace Productivity chapter finds that direction control is the best strategy unless aircraft can be designed with very high hover energy efficiency. The methods developed in this dissertation can be extended to other UAM use cases and can inform important policy decisions as discussed in the concluding chapter.

1.1 Research Objective

This dissertation explores feasibility, capacity and productivity of urban airspace to accommodate hub-door and door-door traffic in a metropolitan region, thereby providing a viable alternative to traffic that has primarily been moved by roads till date. It focuses on the following research questions:

1. Is Air a feasible option for hub-door and door-door services of today?
2. When can airspace get congested in a metropolitan region? In other words, what is the metropolitan Airspace Capacity?
3. While airspace remains uncongested, what type of airborne control increases productivity without compromising safety? Is Speed control better or Direction control?

1.2 Dissertation Outline

Chapter 2 evaluates the feasibility of moving people and goods via air using three enroute metrics - travel time, fuel cost and emission. Chapter 3 presents our approach to airspace capacity and evaluates a sample capacity for under 400 feet goods movement in the San Francisco Bay Area. Chapter 4 shows a region agnostic method to evaluate the productivity of the metropolitan airspace for a given level of safety. Chapter 5 summarizes key findings from this dissertation, discusses policy implications and possible future research.

Chapter 2

Airspace Feasibility

Is air transport a feasible alternative to road transport for hub-to-door and door-to-door urban services today? This chapter answers that question based on enroute travel time, fuel cost and CO_2 emissions. We compare automobiles on urban roads to aircraft of the near future in urban airspace. We first explore the evolution of consumer aircraft and automobiles over the past century that begets the comparison. Then we introduce the metrics that capture the trade-offs a consumer has to make, when choosing a mode, followed by the results on feasibility. Only unimodal trips are compared. The chapter concludes with a summary of the results.

2.1 Introduction

The revolution in small consumer aircraft design over the past decade has created an opportunity for large scale hub-door and door-door urban operations to be conducted via air. Companies like DJI and 3DR, first made sUAS aka drones a consumer product. Consequently, drone-based services like photography, package delivery, surveying, surveillance, news-gathering, law enforcement, search and rescue and so on are now within the reach of an average consumer. This industry, predicted by Forbes to be worth a billion dollars in 2015, produced a combined revenue (consumer and commercial) of $4.5 billion in 2016[29], from the goods and services sector.

What about moving people? With rapid innovation in electric propulsion and Personal Aerial Vehicle (PAV) (2-4 passenger) design, fuel efficiency and emission numbers have already improved and are expected to get better. For example, the eVTOL Airbus Vahana is expected to produce thrice the mileage of the most efficient gas powered Cessna and over seven times the mileage of the Robinson R44 Raven II helicopter. At the same time it will produce close to two-thirds the CO_2 emissions of either (see section 2.2 for numerical details). eVTOLs are therefore expected to lead the UAM era [71].

Parallely, automobiles have also undergone a revolution. Electric and hybrid (part gasoline and part electric) propulsion have made the automobile fuel economy five-fold and two-fold respectively and reduced CO_2 emissions compared to gasoline. However, they still make up only around 2% of automobile sales globally and in the USA. We therefore believe that they will take a long time to substantially replace the existing gasoline fleet on roads. In comparison, UAM enabling aircraft are primarily envisioned as electric[93]. Hence, we use electric aircraft and gasoline automobile as the representative vehicles for air transport and road transport respectively.

We use three enroute metrics for comparison - 1) travel time (min), 2) fuel/energy cost ($), and 3) CO_2 emissions (lbs). These are elaborated upon in section 2.3. The relative performance of air travel depends on whether the trip involves moving passengers, consolidated goods or unconsolidated goods. Hence, we analyze each of these three urban movement types and consider air transport a feasible alternative if it fares at par or better on most of the metrics. Urban air traffic operations will start in an airspace which is uncongested today. Road traffic on the other hand is already quite congested much of the time. Hence, we compare uncongested electric air travel to both uncongested and congested gasoline road travel. Section 2.3 lists all the assumptions made for each type of urban movement and section 2.4 presents the detailed analysis of the metrics. Section 2.5 summarizes our findings.

2.2 Background

UAM studies have shown improvements in urban passenger air travel time for both hub-door[3] like and door-door[4] services with specific trip designs. Uber[40] estimates its future air taxis to be competitive to its current road based rideshare services based on time, direct operating costs and emissions. Our work complements these efforts for passenger movement.

The maximum permitted uncongested freeway speed in a US metropolitan region is usually 65 mph. On congested roads, the speeds come down to about 30 mph[80]. Similarly, the US average fuel economy for cars comes down from about 30 mpg to roughly 20 mpg due to congestion [1]. In comparison, urban air travel is envisioned to be most fuel efficient at speeds of about 125-150 mph[40] with operations at or below 5000ft altitude.

A Cessna 150 that can fly at a comparable cruise speed gives a mileage of close to 18 mpg which is more than twice that of a helicopter like the Robinson R44. An all electric Airbus Vahana will give thrice that mileage (using an energy density conversion of 34.44 kWh/gal for aviation fuel[25]) while producing less CO_2 per kWh. These improvements in aircraft motivate our work.

For goods, we differentiate between consolidated (e.g. - mail delivery) and unconsolidated (e.g. - grocery trips) movement. Published research comparing urban goods movement by

air and roads is quite limited. Goodchild and Troy[32] come closest with their comparison of emissions for drones vs delivery trucks. Following a similar approach for consolidated goods, we compare a standard UPS Diesel Truck against a drone that can deliver similar packages by air, normalizing the fuel and emission numbers by weight and distance. For unconsolidated goods, we compare a sedan trip to a grocery store a mile away from home against the same trip needs met by drones.

2.3 Modelling and Preliminaries

Metrics

For passenger and goods (consolidated and unconsolidated) movement, we base our comparisons on -

1. Travel Time
2. Fuel Cost
3. Emissions

We normalize these metrics as elaborated in the next section. Only enroute statistics are analyzed to cover a broader class of operations, agnostic to specific locations and network design.

Assumptions

Passenger trips

For passenger movement, all comparisons are made in two ways - as a ratio of the metric (Road/Air, orange lines in figures) and as a difference of the metric (Road-Air blue lines in figures). For road movement, we assume uncongested speed(v_{Ru}), congested speed(v_{Rc}), uncongested fuel economy(M_{Ru}) and congested fuel economy(M_{Rc}) of 65 mph, 30 mph, 30 mpg and 20 mpg, respectively. For air movement, we assume a cruise speed(v_{Au}) of 150 mph and the airspace is assumed to be uncongested.

Market studies of eVTOL viability use highly optimistic power consumption numbers and Lift-to-Drag (L/D) ratios, owing to the lack of data from real certified aircraft or feasible eVTOL models tested for design missions. L/D ratios above 13 are considered in these studies[40]. A rather efficient fixed-wing general aviation aircraft (Cirrus SR22T) has a best-range L/D ratio of 10. In consultation with aircraft designers and aerospace engineers, we found that it is highly unlikely that any eVTOL configuration for long range urban

passenger movement will have better L/D than even current-technology fixed wing aircraft, let alone fixed wing aircraft with same level of advanced technology.

To explain this better, for an aircraft in level cruise, the L/D ratio is given as:

$$L/D = Wv/P \tag{2.1}$$

where, W is the weight of the aircraft, v is the cruise speed and P is the cruise power. If all three terms on the right are known, the L/D ratio of the aircraft in cruise can be calculated. However, released specifications of eVTOL under development or even those that have been tested only state the W and v values. They provide information on the total installed power but not on how much is actually used, nor do they provide the actual L/D numbers. If we assume the L/D values as projected in all market studies (13 plus), the computed cruise powers typically tend to be less than 20% of the total installed powers of these designs. Hence, they don't seem realistic.

We therefore instead use insights from eVTOL models as developed by Johnson and Silva at NASA Ames[48] (henceforth referred to as NASA eVTOL models/designs) and combine those with design specifications of flight tested eVTOL aircraft to compute the cruise power to be used for our study. The L/D ratios of the all electric NASA eVTOL models vary from roughly 5.3 to 9.3, with the most optimal (design size + cruise efficiency) model's value at 7.2.

The Airbus A^3 Vahana Beta is the 2-seater version of the Vahana Alpha that has flown over 50 full scale test flights[74]. Its design specifications include a maximum take off weight of 815 kg with an optimal cruise speed of close to 150 mph. It has 8 propellers each rated at 45 kW. Since aircraft are built with redundancy, we assume only half of this installed power (180 kW) is utilized during the hover phase of flight. For the cruise phase of flight since its L/D numbers are not available publicly, we assume the optimal NASA eVTOL number of 7.2 to compute the cruise power at 70.87 kW (substituting W, v and L/D in equation 2.1 and making the appropriate unit conversions). We note that instead if we used L/D of 13 (as per market studies), we would get a cruise power of 41 kW, less than the power of a single propeller. A higher L/D would make this even smaller. Clearly, the L/D ratios of this designed and flown aircraft is not as high. Yet, since we don't know the exact L/D, we also perform a sensitivity analysis by varying the L/D to 5 and 10 and utilizing the corresponding Vahana cruise power values of 102 kW and 51 kW.

We assume a flight profile as shown in figure 2.1. The eVTOL takes off hovering in place to 100 feet at 100 fpm. Then it ascends while cruising to its cruise altitude, cruises close to destination, descends while cruising to a hover and then lands while hovering. The in place hover take-off and landing phases therefore take overall 2 minutes while the extra energy utilized in slant ascent to the cruise altitude (4000 ft in the NASA eVTOL designs) while

accelerating to the cruise speed is assumed to be offset by the energy saved in descent while decelerating to a hover for final landing. We compare statistics only for enroute travel. By enroute, we refer to portion of the journey from start of trip (take off for air and movement start for road) to end of trip (landing for air and movement end for road).

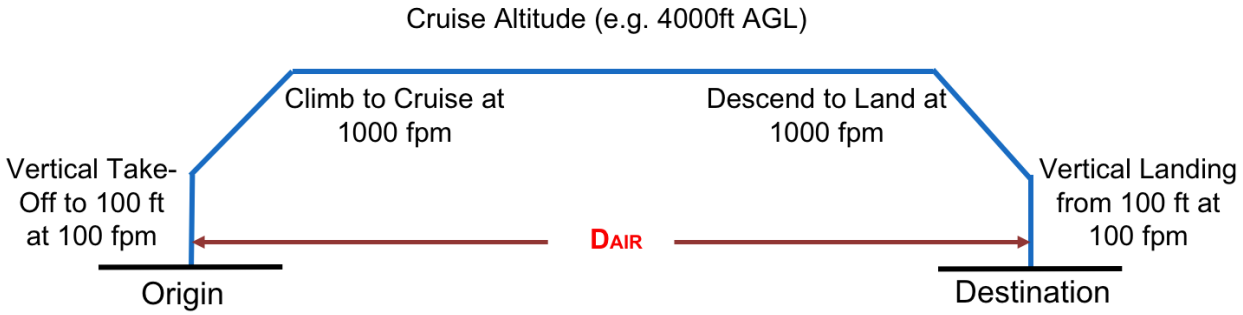

Figure 2.1: eVTOL flight profile for passenger movement.

Our first set of results only compare the vehicle configurations as is without accounting for the passenger occupancy. UAM passenger services as a shared transportation mode will tend to maximize utilization rates, unlike cars on the road today which are predominantly singly occupied. To account for this discrepancy, we perform a second sensitivity analysis by normalizing our fuel costs and emission numbers on a per passenger basis. For road movement, we use a US average passenger occupancy of 1.54 (O_R)[91]. The chosen aircraft (Vahana) is a pilotless 2-seater. Hence, we choose an occupancy of 2 (O_A) for it. Furthermore, the NASA eVTOL models were designed for 6 passengers, including the pilot. Such aircraft might be preferred even more to improve the utilization rates. Hence, we add that design to the list of test cases for comparison using an occupancy of 5 passengers for it. We note that the enroute distinction above ensures that the wait time constraint is not included, the assumption being that given the diversity of vehicle sizing, the vehicle appropriate to the available number of passengers will be used.

For gasoline and electricity we use fuel costs of \$3/gal(c_R) and \$0.12/kWh(c_A) respectively based on US averages. For electric fuel, we also account for the battery charge-discharge efficiency of 90%(η). In other words, the energy used by the eVTOL is assumed to be only 90% of the energy delivered while charging from the grid.

Finally, for emissions, we use CO_2 emission rates of 19.59 lbs/gal (e_R) and 0.474 lbs/kWh (e_A) (California ISO (CaISO)) for gasoline and electricity respectively. We also account for the additional emissions in moving fuel from primary source to delivery by multiplying the above emission rates by primary-to-delivery ratios of 1.28[6](μ_R) and 1.67 (CaISO grid system efficiency)(μ_A), respectively.

Road movement is typically more circuitous compared to direct aerial routes. Hence, for

air movement, we use the haversine (great circle) distance(D_{Air}), while for road movement we assume circuity factors (f) of 1.20 (US average [7]), 1.35 (Silicon Valley average [4]) and 1.42 (Uber average based on their trip data[40]. Hence, the road distance $D_{Road} = f.D_{Air}$.

The metrics for comparison are computed as follows:

The travel time, T for each mode is given by -

$$T = D/v \tag{2.2}$$

where, D is substituted as is for air and as $f.D$ for road.

The energy consumed for road in gallons is given by -

$$E_{Road} = D_{Road}/M_R \tag{2.3}$$

where, M_R is substituted for uncongested and congested conditions as needed.

The energy consumed for air in kWh is given by -

$$E_{Air} = (P_{Hover}.T_{Hover} + P_{Cruise}.T_{Air})/\eta \tag{2.4}$$

where, the hover and cruise, power and times and the charging efficiency are as stated earlier.

Given each of the energies, they are multiplied by the respective unit energy costs to get the total energy cost.

The emissions for each mode are given by -

$$CO_2 = E.e.\mu \tag{2.5}$$

where, e and μ are the respective emission rate per unit energy and primary-to-delivery ratios, respectively.

Results are first presented for the three metrics, using the Vahana design based assumptions above, for each of these circuity factors for direct travel distances from 1 to 100 miles. It is to be noted that the US average accounts for more direct road routes in rural areas and Uber's average is for a very specific niche of trips. The Silicon Valley average is the best representative among the three of circuity factors in a metropolitan area. Hence, we only present the sensitivity analysis results for a circuity factor of 1.35. Also, we don't analyze distances shorter than a mile.

Consolidated Goods Trips

We assume a standard diesel UPS truck[61]. It weighs 11000 lbs. with a maximum storage capacity of 12000 lbs. and makes 200 stops per day on an average. With a mileage of 10.2 MPG and about 80-100 miles driven per day, it consumes roughly 10 gallons of fuel. We further assume that it moves 5000 lbs of packages daily on average.

Since, no efficient drone exists in the market currently that can deliver packages over long distances from hub to door, we choose DJI S900 as a representative. We pick the necessary values from its specification sheet[24]. It produces 12A current at 24V for 18 min of flying time and can carry a payload of 10lb. At its maximum speed it can cover a distance of 10 miles in that time.

Unconsolidated Goods Trips

Unlike a big truck delivering packages, there are other hub-door and door-door trips that move consumer goods in smaller quantities. An Uber Eats trip, a pizza delivery, a quick shopping trip to buy groceries or other household products, delivery of emergency medical supplies and so on are all examples of such smaller unconsolidated goods trip that typically originate and end within the confines of an individual city within a larger metropolitan region. At least one fifth ($\tilde{2}0\%$) of vehicle trips in the US fit this criteria as per the US Department of Transportation[91].

We use the same DJI S900 drone as above to evaluate a typical unconsolidated goods trip. For road movement, an average gasoline based Sedan with a mileage of 25MPG is assumed (average of the congested and uncongested road mileages)[26]. We first evaluate a consumer trip to a store a mile away for a gallon of milk (8.6lbs) and present our travel time, fuel cost and emissions analysis for that.

A typical shopping trip or a food/essentials delivery via a car would still have some consolidation effect, albeit not to the extent of a UPS truck per se. For example, a person might shop for multiple items in the same trip. Unlike the car, a single drone has limited capacity. So those multiple items need to be delivered by multiple drones. To account for this mini consolidation advantage from the car, we also analyze our metrics by varying the car trip goods weight from 1 to 50 pounds.

2.4 Results

Passenger Trips

Figures 2.2,2.3 and 2.4, each show two comparisons for travel time - 150 mph by air (best speed with minimal reduction in fuel efficiency[40]) against uncongested (free) and congested

road travel. We are only analyzing distances from 1 mile to 100 miles. Air travel time is less by around one-third compared to free road conditions across the three circuity conditions.

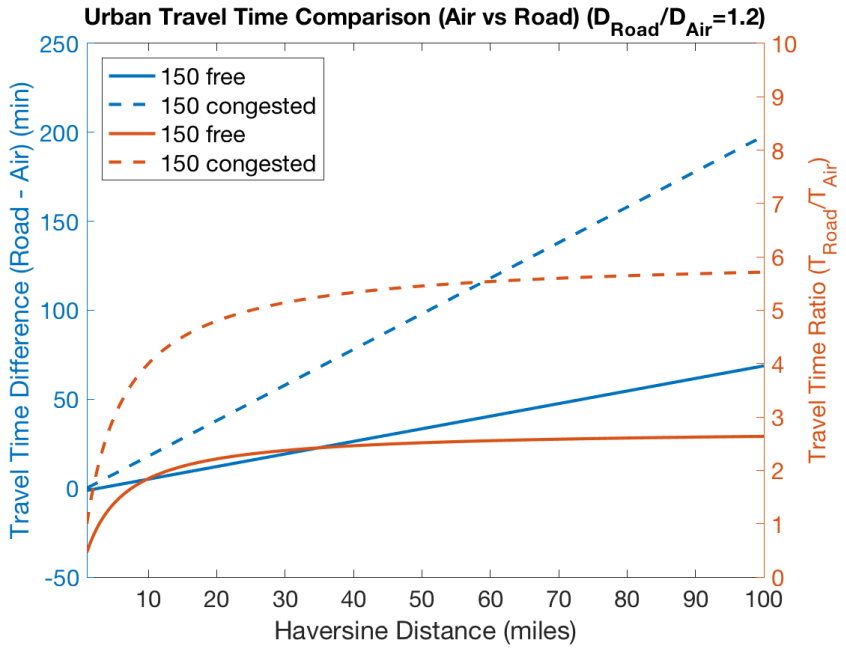

Figure 2.2: Enroute Travel Time Comparison - Road vs Air. Orange - Travel Time ratio, Blue - Travel Time difference

Congestion on roads more than doubles the advantage of air to road. For example, at a circuity factor of 1.20, for a 50 mile (haversine distance) long trip, air time is 22 min compared to 55 min by uncongested road and 120 min when the road is congested. This translates to a time saving of 33 min and 98 min for free and congested road conditions respectively. As the circuity factor is increased to 1.35, the corresponding time savings are increased to 42 min and 115 min. For a circuity factor of 1.42, these savings are even more pronounced at 44 min and 120 min. However, it is noteworthy that air only has a time advantage over distances of roughly 2 miles. This is because these distances are covered by road in the time the eVTOL takes to take-off and land.

Energy/fuel cost comparison is shown in figures 2.5, 2.6 and 2.7. Air fares better enroute compared to roads for longer travel segments. These savings are more than doubled with congestion on road. For example, for a 50 mile air trip, at a circuity factor of 1.20, fuel spent enroute costs \$1.89 and \$4.89 less by air than uncongested and congested roads respectively. At a circuity factor of 1.35, these savings increase to \$2.64 and \$6.01 and furthermore to \$2.99 and \$6.54 at a circuity factor of 1.42. However, at a circuity factor of 1.2, for uncongested trips under 15 miles and congested trips under 8 miles, road fuel costs beat air. We call these the transition distances. As the circuity factor is increased, air becomes cheaper than

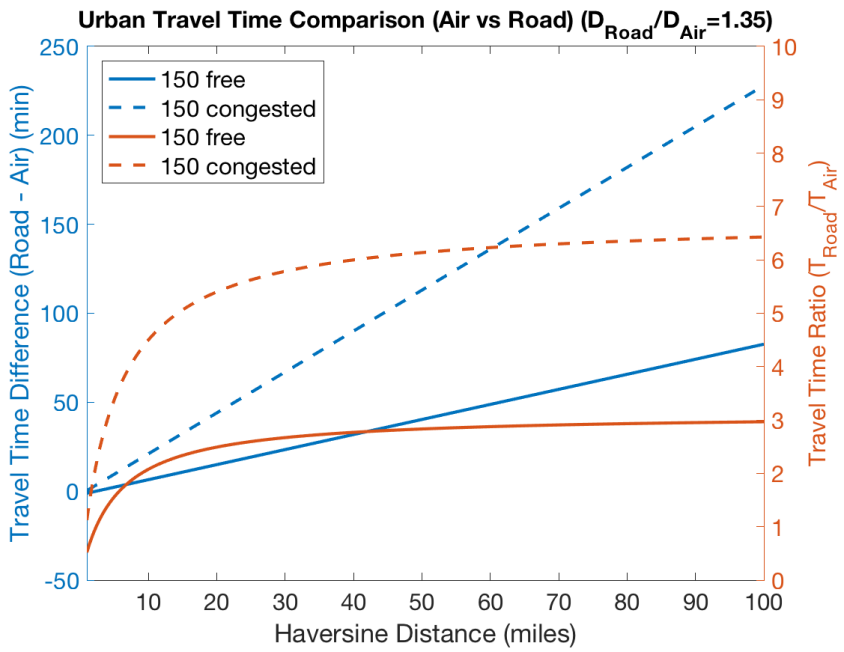

Figure 2.3: Enroute Travel Time Comparison - Road vs Air. Orange - Travel Time ratio, Blue - Travel Time difference

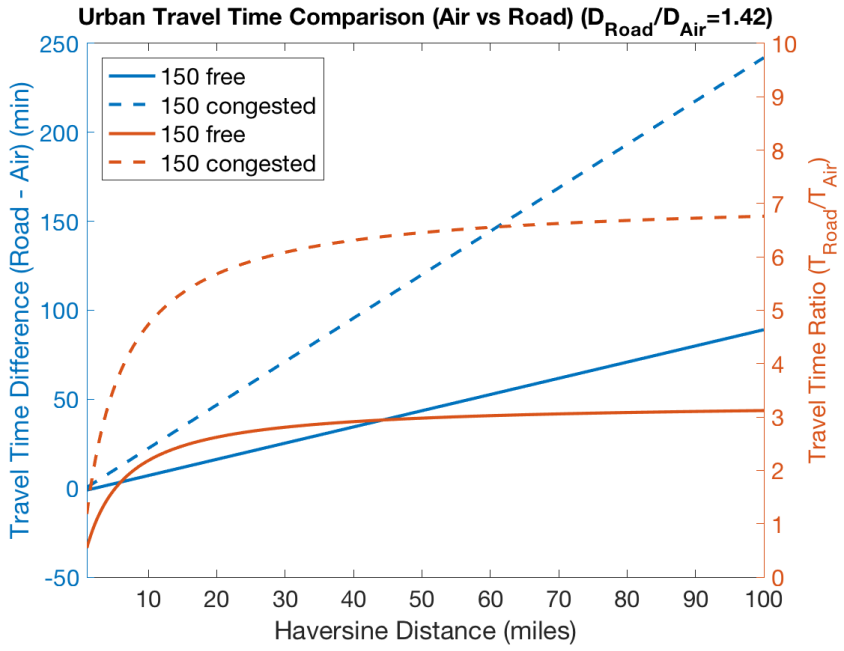

Figure 2.4: Enroute Travel Time Comparison - Road vs Air. Orange - Travel Time ratio, Blue - Travel Time difference

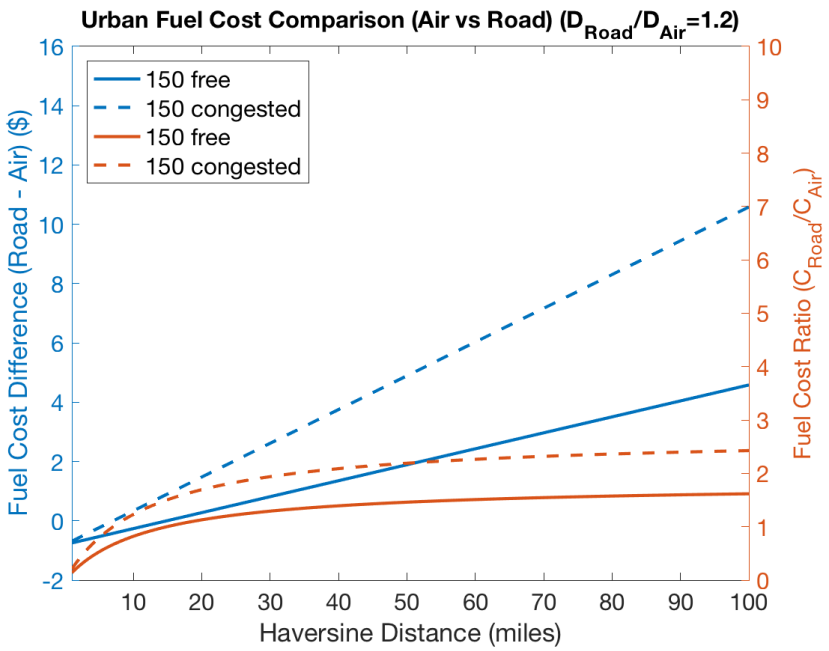

Figure 2.5: Enroute Fuel Cost Comparison - Road vs Air. Orange - Fuel Cost ratio, Blue - Fuel Cost difference.

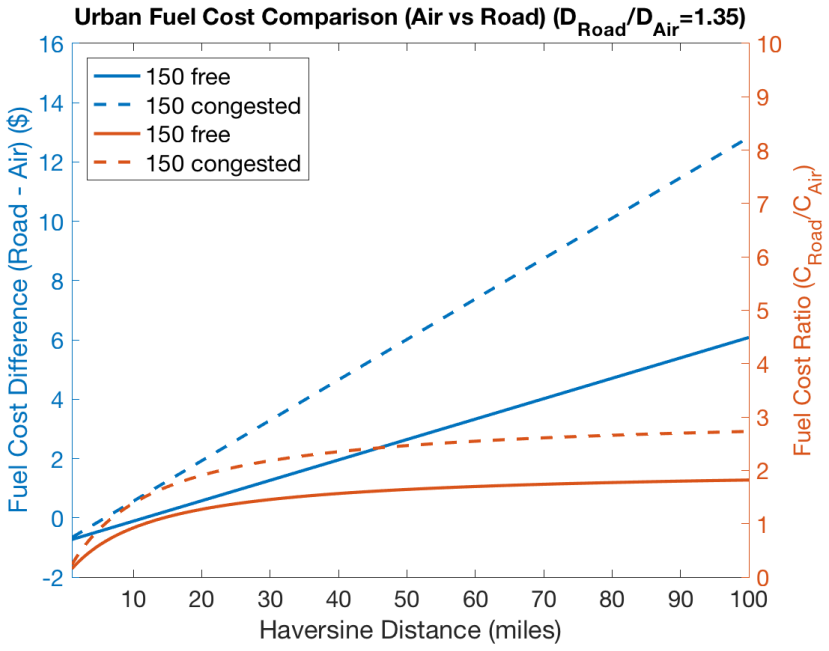

Figure 2.6: Enroute Fuel Cost Comparison - Road vs Air. Orange - Fuel Cost ratio, Blue - Fuel Cost difference.

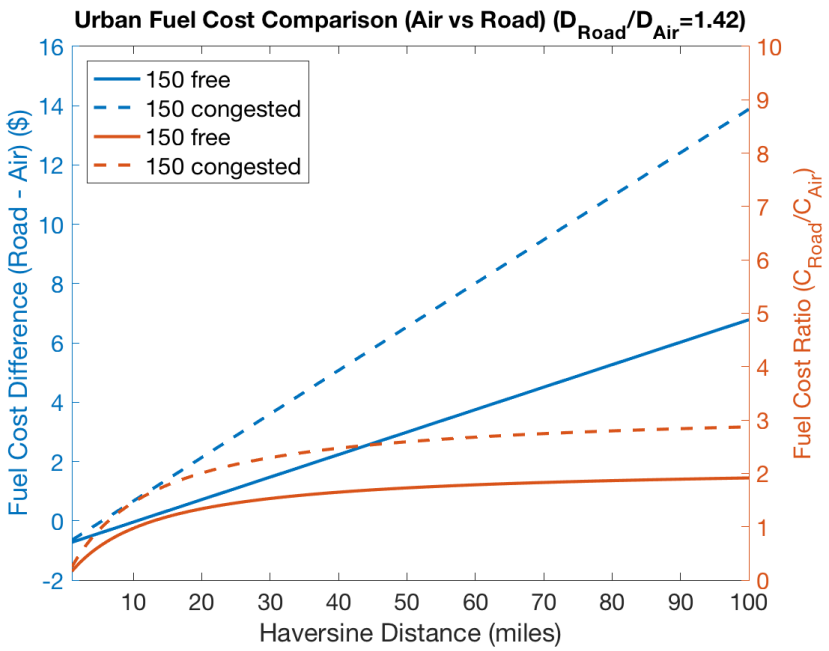

Figure 2.7: Enroute Fuel Cost Comparison - Road vs Air. Orange - Fuel Cost ratio, Blue - Fuel Cost difference.

road at shorter transitions distances.

Next we compare CO_2 emissions as shown in figures 2.8, 2.9 and 2.10. We find that beyond 8 miles, at a circuity factor of 1.20, it is greener to travel by air. If the roads are congested, this becomes true beyond 5 miles. A higher circuity factor further reduces these transition distances. Again for a 50 mile trip example, at a circuity factor of 1.20, travel by air generates 23.12 lbs less of CO_2 emissions with the savings almost doubled to 48.21 lbs when the roads are congested. At a circuity factor of 1.35, the savings against uncongested and congested roads are 29.40 lbs and 57.62 lbs, respectively. These savings are further improved to 32.32 lbs and 62.01 lbs at a circuity factory of 1.42.

For the rest of our analysis, we only consider a circuity factor of 1.35 as a best measure of travel distance extension (road vs air) in metropolitan areas. The fuel cost and emission trade-offs depend on the L/D ratio of the eVTOL. We demonstrate this by varying the L/D ratio. The assumed design weight and cruise speed are kept unchanged for the Vahana.

For a very low cruise efficiency (L/D = 5 - figure 2.11), a 50 mile travel by air only saves \$1.18 and \$4.56 over uncongested and congested road travel, respectively (compared to \$2.64 and \$6.01 earlier at L/D = 7.2 in figure 2.6). A high cruise efficiency with L/D = 10 (figure 2.12) increases these savings to \$3.58 and \$6.94.

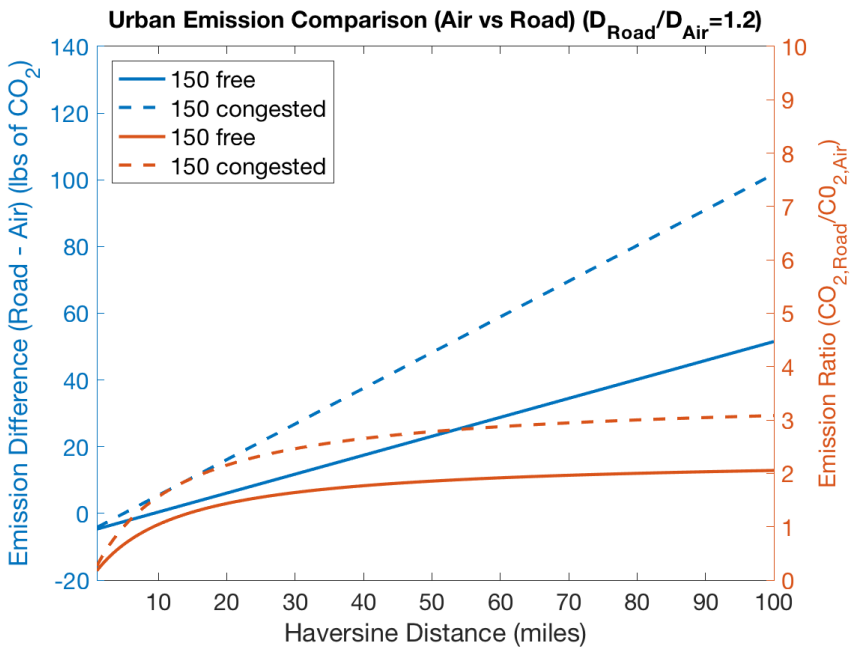

Figure 2.8: Emission Comparison - Road vs Air. Orange - Emission ratio, Blue - Emission difference.

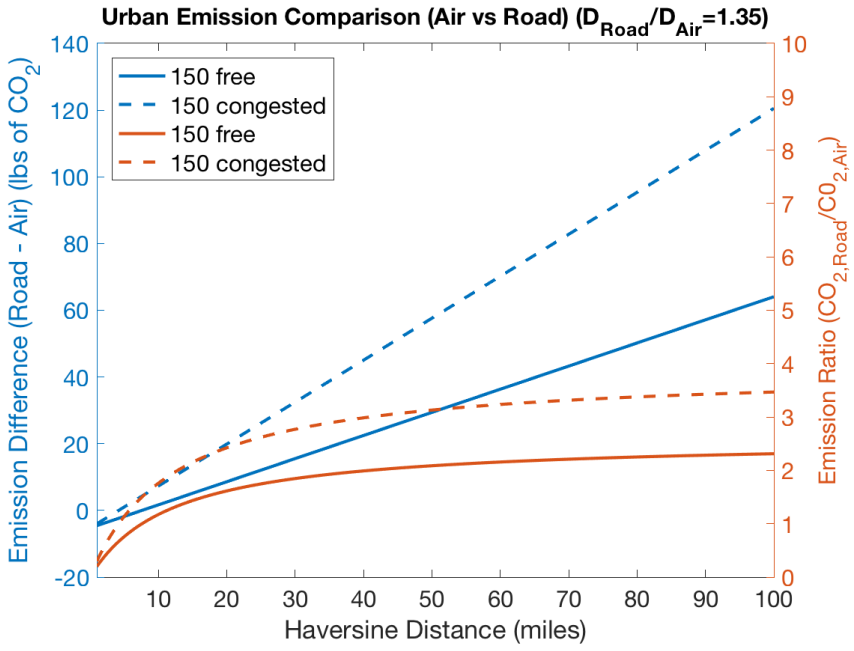

Figure 2.9: Emission Comparison - Road vs Air. Orange - Emission ratio, Blue - Emission difference.

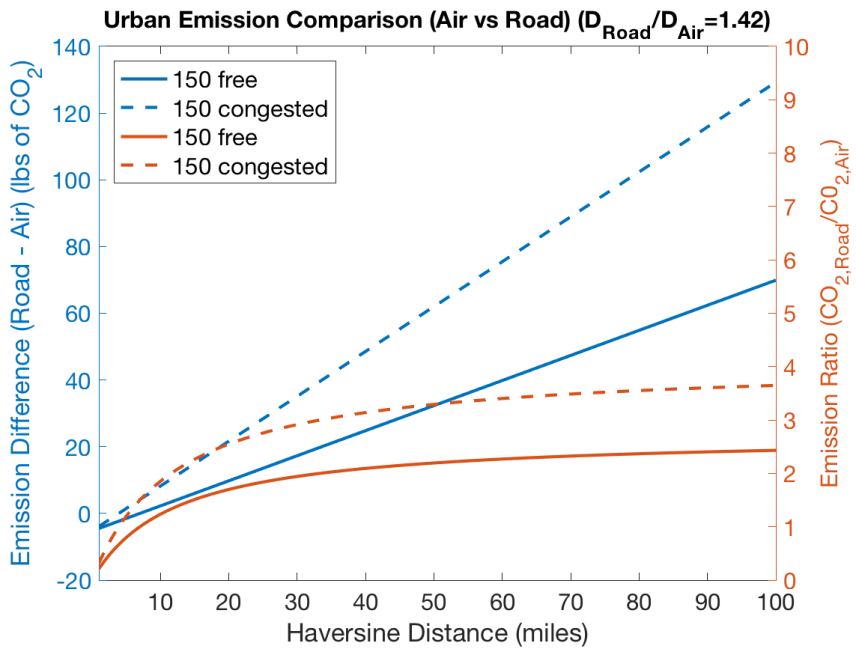

Figure 2.10: Emissions Comparison - Road vs Air. Orange - Emission ratio, Blue - Emission difference.

A similar trend is seen for CO_2 emissions too but the differences are more pronounced. Low cruise efficiency (figure 2.13) saves 19.82 lbs and 48.04 lbs of CO_2 for a 50 mile trip by air against uncongested and congested road, respectively. Earlier (L/D = 7.2 in figure 2.9) these savings were 29.40 lbs and 57.62 lbs. A very high cruise efficiency (figure 2.14) makes the aircraft quite greener by saving 35.49 and 63.72 lbs of CO_2.

All the results till now used a vehicle to vehicle comparison. The savings therefore can be thought of as pertaining to the operator side. However, as stated earlier, eVTOL aircraft are expected to operate at much higher utilization rates than cars on roads today. Hence we want to understand the trends as pertaining to the consumer or the customer by computing the metrics on a per passenger basis. Since we are looking at only enroute statistics (take off to land by air and wheels move to wheels stop by car), the travel time comparison only depends on speed which remains unchanged with occupancy. Hence, the savings are as before. We only analyze the impact on fuel cost and emissions. We keep the design parameters of the base case unchanged with L/D = 7.2.

Assuming an occupancy of 1.54 for cars and 2 for the 2-seater aircraft, compared to uncongested and congested road, air again performs better albeit now at even shorter distances. There are fuel cost and emission savings for all distances beyond a mile. Both the fuel cost and emission savings double with congestion on roads. For example for a 50 mile trip, $2.32

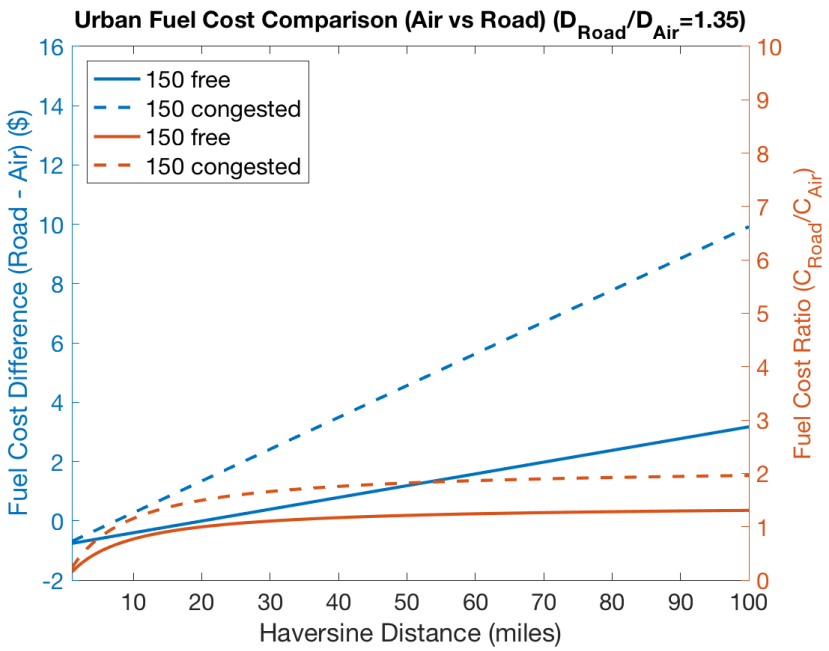

Figure 2.11: Enroute Fuel Cost Comparison - Road vs Air. L/D = 5. Orange - Fuel Cost ratio, Blue - Fuel Cost difference

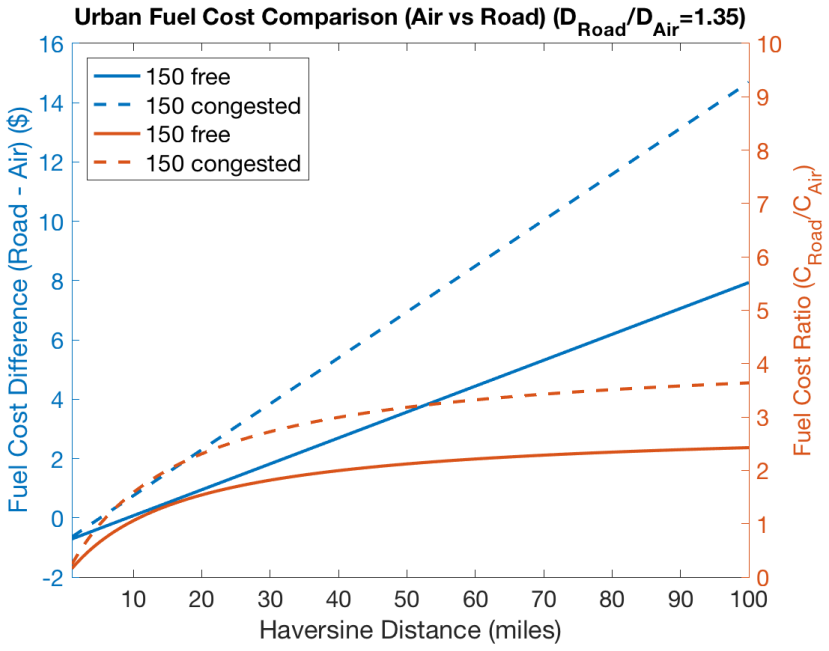

Figure 2.12: Enroute Fuel Cost Comparison - Road vs Air. L/D = 10. Orange - Fuel Cost ratio, Blue - Fuel Cost difference

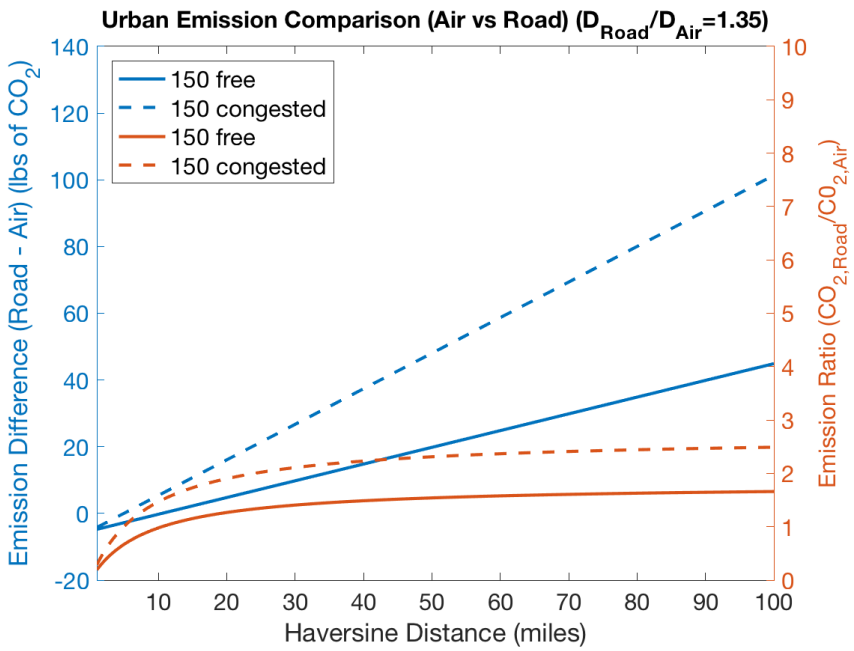

Figure 2.13: Emission Comparison - Road vs Air. L/D = 5. Orange - Emission ratio, Blue - Emission difference

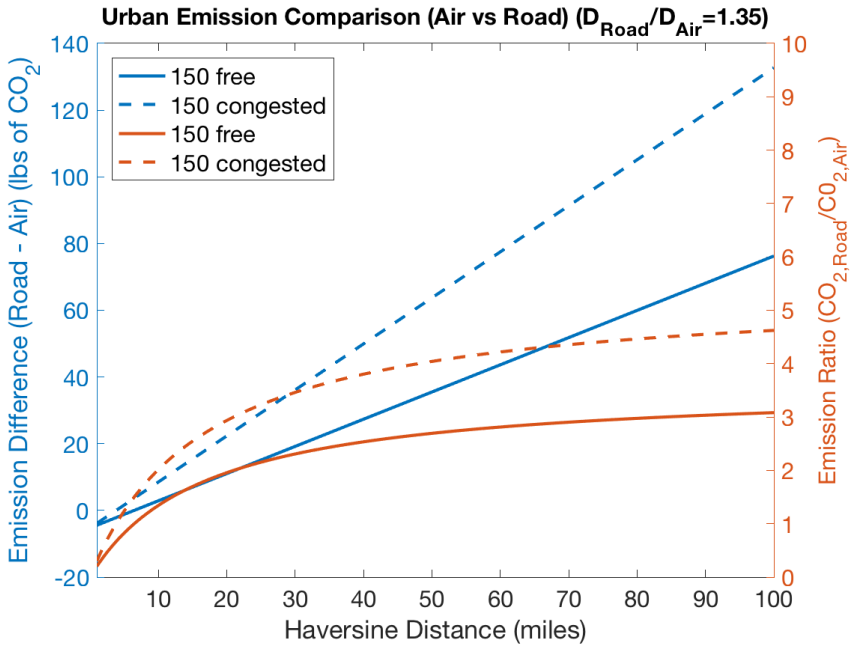

Figure 2.14: Emission Comparison - Road vs Air. L/D = 10. Orange - Emission ratio, Blue - Emission difference

(uncongested road) and \$4.52 (congested road) are saved in fuel costs and the corresponding CO_2 emissions are less by 23.13 lbs and 41.46 lbs per passenger.

The chosen aircraft design is only a 2-seater. Aircraft that can carry a lot more passengers might produce more savings per passenger from consolidation. But they are also bulkier and these savings could get offset by increases in electric aircraft weight due to larger batteries needed. To test how the trends change, we perform the same analysis with the 6 passenger NASA eVTOL model that had an L/D of 7.2. However, since that aircraft design assumes a pilot, we only use an occupancy of 5 to evaluate per passenger fuel costs and emissions.

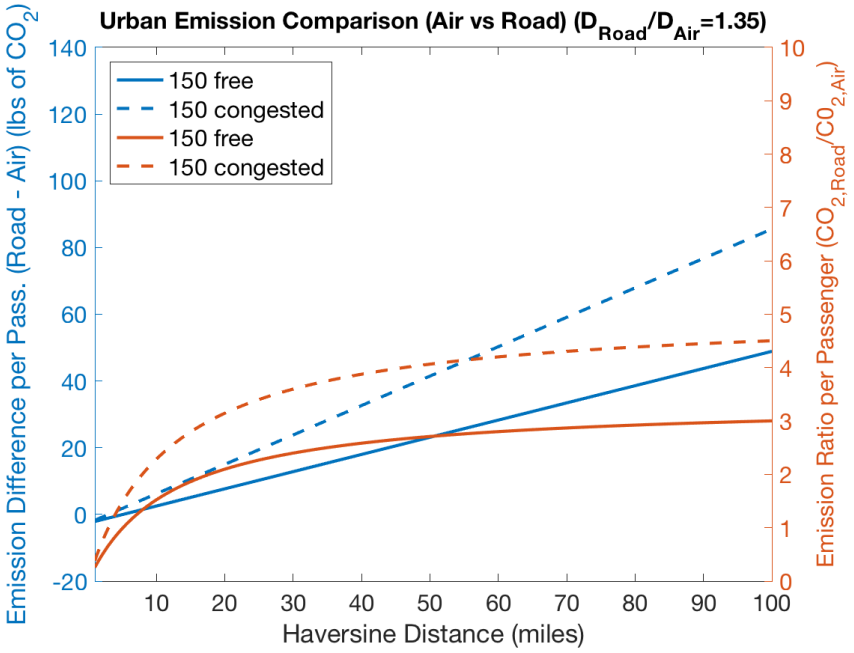

Figure 2.15: Emission per Passenger Comparison - Road (Occupancy = 1.54) vs Air (Occupancy = 2). Orange - Emission ratio, Blue - Emission difference

We find the per passenger trends strikingly similar. For example, for a 50 mile trips, fuel cost savings per passenger by air compared to uncongested and congested road are \$2.38 and \$4.58, respectively. (For the 2-seater the corresponding numbers were \$2.32 and \$4.52). The CO_2 emissions difference per passenger is 23.52 lbs and 41.86 (also very similar to 23.13 lbs and 41.46 lbs for the 2-seater). Even here the per passenger fuel costs and emissions are better by air for all distances. There are at least two implications of this. First, a per passenger normalization seems a better way to compare the feasibility of different vehicle designs. Second, a bulkier aircraft may not necessarily gain the benefits of consolidation with respect to our chosen metrics with a similar design efficiency.

Overall, air fares better compared to roads for moving passengers based on enroute transit times, energy costs and emissions.

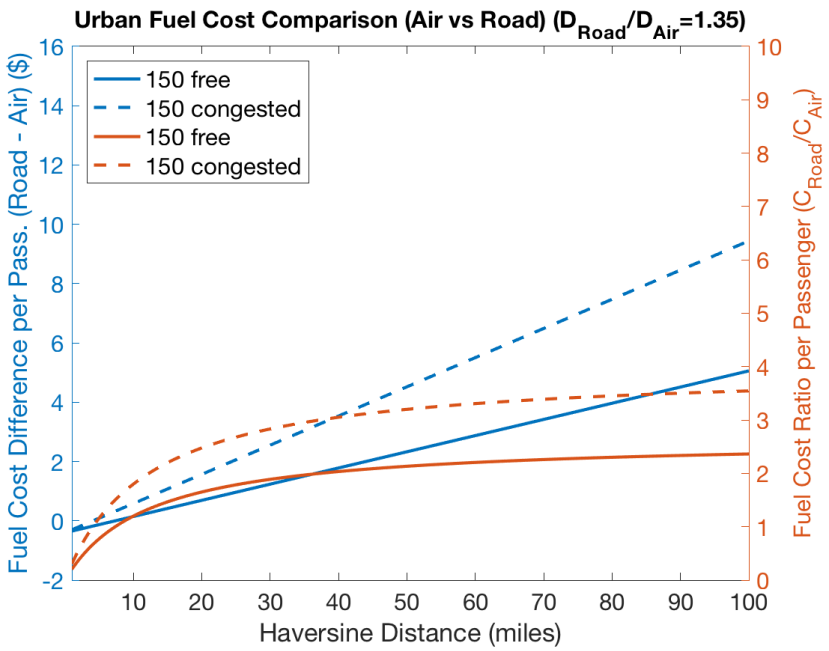

Figure 2.16: Enroute Fuel Cost per Passenger Comparison - Road (Occupancy = 1.54) vs Air (Occupancy = 2). Orange - Fuel Cost ratio, Blue - Fuel Cost difference

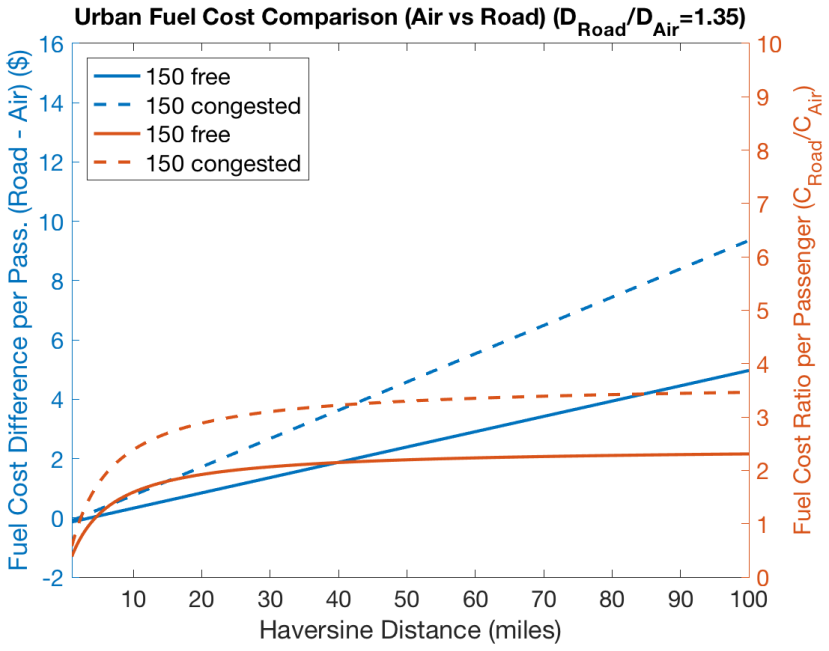

Figure 2.17: Enroute Fuel Cost per Passenger Comparison - Road (Occupancy = 1.54) vs Air (Occupancy = 5). Orange - Fuel Cost ratio, Blue - Fuel Cost difference

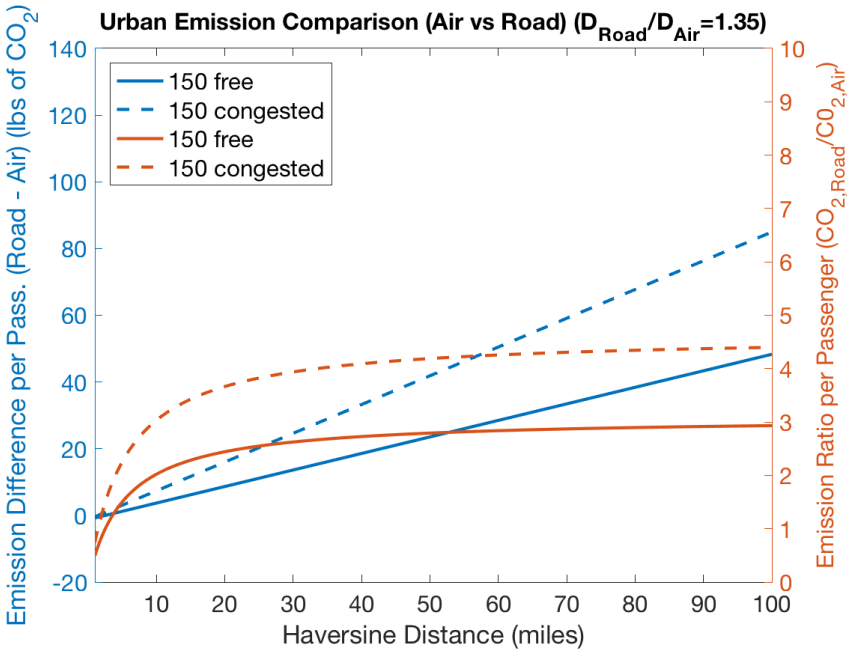

Figure 2.18: Emission per Passenger Comparison - Road (Occupancy = 1.54) vs Air (Occupancy = 5). Orange - Emission ratio, Blue - Emission difference

Consolidated Goods Trips

We assume that instead of a delivery truck distributing packages over a network, the package can be carried directly from the distribution center to any address. Hence, the travel time benefit of air vs road becomes trivial. For the remaining two metrics, we evaluate as below.

A standard diesel UPS truck weighing 11000 lbs. with a maximum storage capacity of 12000 lbs. makes 200 stops per day on an average. With a mileage of 10.2 MPG and about 80-100 miles driven per day[83], it consumes roughly 10 gallons of fuel[61]. If we assume that it moves only 5000 lbs of packages daily on average, it spends about 6.517kJ/lb/mile of energy and 0.00128 lbs of CO_2/lb/mile of emissions. The metrics here are normalized by package weight and distance. We also express the fuel cost directly in terms of energy here instead of the dollar value for comprehensibility as otherwise the number becomes quite negligible.

A stated in under assumptions, we choose DJI S900 as a representative. It produces 12A current at 24V for 18 min of flying time and can carry a payload of 10lb. At its maximum speed it can cover a distance of 10 miles in that time. It spends about 3.11 kJ/lb/mile of energy and 0.00075 lbs of CO_2/lb/mile of emissions. Hence, on face value drones have the potential to fare better in terms of energy consumption and emissions.

However, a delivery truck is more efficient in terms of vehicle miles traveled and hence the above benefit may not be necessarily existent if we sum up the fuel costs and emissions over total distances traveled (which themselves will vary based on the specific distribution network). For this we look at the results of Goodchild and Troy. [32] studied the tradeoff between delivery by drones and trucks based on Vehicle Miles Travelled (VMT) and Emissions. They divided LA County into 330 service zones with a main depot at the center. They used truck emissions from California Air Resources Board (CARB) database for a standard diesel truck and compared with drones with varying Average Energy Consumption (AEC) (Wh/mile). The study found that even though trucks would travel 98.45% less distance per recipient than drones on average, drones would still produce less emissions if their AEC is less than 25 Wh/mile. Our representative vehicle above has an AEC of roughly 9 Wh/mile for carrying a 10 lb package. Hence, our analysis also fits a specific network design study. Therefore, we can again conclude that air is at par or better than roads for consolidated goods movement.

Unconsolidated Goods Trips

Food, household items, groceries, emergency medical supplies, etc. are a few examples of a vast variety of unconsolidated goods that are frequently moved in an urban area. We therefore study a simple example and then extend the results to range of goods weights to cover the above variety.

First, we evaluate a sample shopping trip. Assume a consumer trip to a store a mile away for a gallon of milk (8.6lbs). As explained for consolidated goods movement, travel time benefits here are also trivial. Now an average gasoline based Sedan with a mileage of 25MPG, spends about 10466 kJ for carrying that gallon of milk (in addition to the driver and the roughly 3000 lb sedan) consuming \$0.24 in fuel costs and producing 2.0063 lbs of CO_2 emissions.

In comparison, the above drone (as used in the previous section) for the same trip would spend 26.75kJ, consuming \$0.001 in electricity costs and produce on average 0.007 lbs of CO_2. Hence, the car spends and produces, roughly 250 times the energy and 300 times the emissions respectively, compared to a drone on the same trip.

However, unconsolidated goods with a wide variety of weights can be moved by a car. But a drone is limited in capacity. There is also a mini consolidation effect in a car. For example, in the example of the shopping trip, a consumer could buy a few different items instead of just a gallon of milk. For movement by air, each item has to be separately moved. Again the time benefit here is trivial. We show the variation in fuel cost and emission ratios in figures 2.19 and 2.20, respectively.

The goods weight difference is negligible compared to the car weight. So the difference

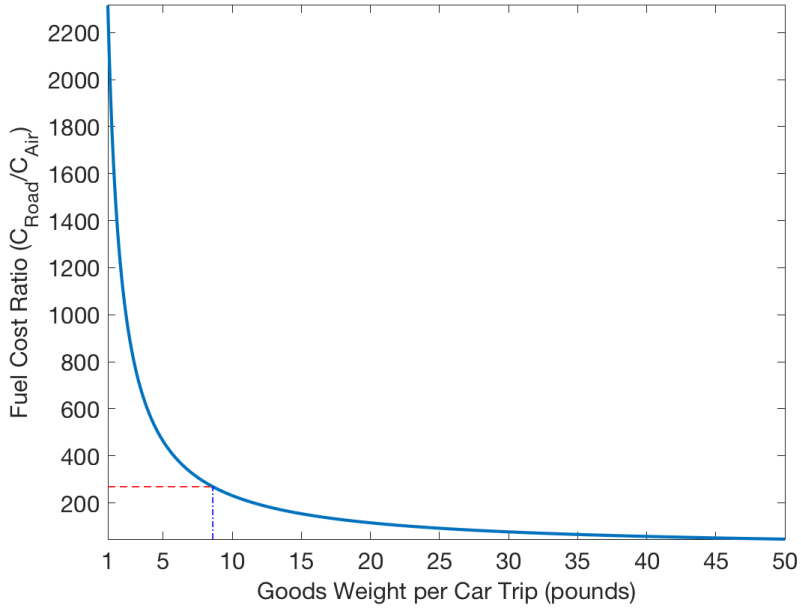

Figure 2.19: Fuel Cost comparison with varying Goods Weight - Road vs Air. The red and blue dotted lines show the sample shopping trip in text.

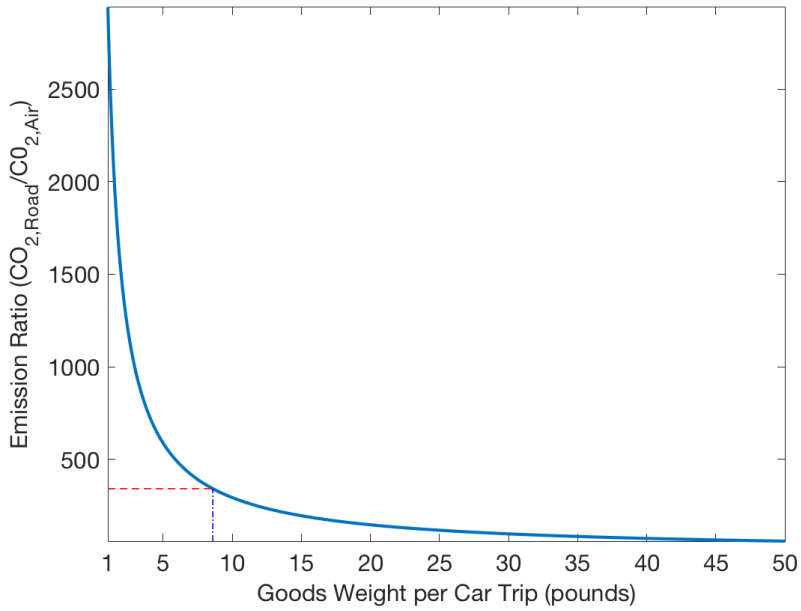

Figure 2.20: Emissions comparison with varying Goods Weight - Road vs Air. The red and blue dotted lines show the sample shopping trip in text.

in fuel consumption of the road trip will also be negligible for a given distance. The fuel cost and emissions by road practically stay the same. However, each item has to be separately delivered if a drone is used. Therefore, the advantage of drones reduces as the total weight of unconsolidated goods moved increases. Yet, even for 50 pounds of unconsolidated goods, a car would spend 45 times more fuel costs and produce 60 times more emissions than if the same goods were moved by air. We note that over 200 single deliveries by drone would still amount to lesser energy costs and emissions than a single car trip. This clear advantage owes to the fact that for unconsolidated goods movement by cars and other light and heavy motor vehicles, extensive energy is spent on moving the vehicle itself. Drones on the other hand provide the advantage of fitting form to need. Air therefore beats road even for unconsolidated goods movement.

2.5 Conclusions

This chapter described an analytical process to determine the feasibility of urban travel by air compared to road. The results show that for each of the three different kinds of movement, namely - Passenger trips, Consolidated Goods trips and Unconsolidated Goods trips, electric air travel fares at par or better than gasoline road travel, in an *uncongested airspace*. Since, aircraft are more than twice as fast as automobiles on uncongested roads, enroute travel time is improved across the board.

For a 50 mile passenger movement, road takes at least 33 min and 98 min longer than air depending on whether it is uncongested or congested. An operator also saves at least \$1.89 and \$4.89 respectively in fuel costs and produces 23.12 pounds and 48.21 pounds less CO_2 emissions respectively for the same trip. However travelling by road is cheaper, for an under 15 mile movement in uncongested conditions and for a roughly 8 mile or shorter movement in congested conditions. It is greener for up to 8 mile distance in uncongested conditions and up to 5 miles in congested conditions. The savings are further increased and the transition distances (when air becomes at par or better than road) become shorter as the circuity factor of road travel compared to air travel increases.

Additionally, we also performed a sensitivity analysis by varying the aircraft cruise efficiency and also compared different aircraft by normalizing the metrics on a per passenger basis. We found that improving the L/D of the aircraft has a pronounced effect on the fuel cost and emission savings. Normalizing the metrics on a per passenger basis proved effective for comparing aircraft with different designs.

Consolidated goods movement by small aircraft also fares at par or better than diesel delivery trucks, if the average energy consumption of the aircraft is less than 25 Wh/mile. For unconsolidated goods movement, air is about 250 times and 300 times better than road in terms of fuel cost and emission benefits respectively.

Therefore, to summarize the findings on airspace feasibility and answer the opening question of the chapter - Air is a feasible alternative to roads for hub-door and door-door urban movement, as it fares at par or better on enroute travel time, fuel costs and CO_2 emissions, *when the airspace is uncongested*.

Chapter 3

Airspace Capacity

When can airspace get congested in a metropolitan region? In other words, since air fares at par or better than roads when the airspace is uncongested, we seek to quantify the capacity of the metropolitan airspace to accommodate the aerial traffic while staying uncongested. This chapter presents a threshold based mathematical definition to estimate capacity. Airspace capacity is then measured by simulating unmanned traffic over urban areas and estimating metrics focused on safety. The aviation industry envisions UAM operations encompassing the movement of people and goods segregated into two distinct altitude bands. As part of Federal Aviation Administration (FAA)'s ongoing integration of Unmanned Aircraft Systems (UAS) into the National Airspace Syste (NAS), under 55 pounds goods movement, defined by FAA as part 107 sUAS operations are restricted to at or below 400 feet AGL and up to a speed of 100 mph[27]. All other enroute operations are as of now expected to be accommodated in the rest of the open airspace above 400 feet with integration into controlled airspace where needed and possible. The latter research is still in its nascent stages. Hence, in this chapter and the rest of the thesis, we focus on goods movement via future sUAS traffic in low altitude (under 400 feet) airspace. However, wherever applicable, we point out the use as is, any required modifications and potential future extensions of our methods to the rest of the airspace and operations. The chapter concludes with a summary of the findings.

3.1 Introduction

The urban airspace today is used by far lesser aircraft than it can accommodate. The next phase of unmanned aviation with Beyond Visual Line Of Sight (BVLOS) operations is expected to fill that same airspace with traffic, orders of magnitude higher. So, how many small unmanned aircraft can the existing low-altitude airspace accommodate under a given set of technological capabilities, operational requirements, protocols and conditions such as safety, stability, performance efficiency and noise levels?

In this chapter, we present an analytical process and quantify the airspace capacity dependent on safety. We present a threshold based definition [15] of airspace capacity (Section 3.4) and use a simulation paradigm to establish the results (Section 3.7). For a given metric, there is a certain acceptable value up to which the airspace is considered operable. The number of aircraft at which the metric exceeds that acceptable value with high probability is the metric-specific capacity, the threshold at which the probability phase transition occurs. Given a set of metrics with respective acceptable limits, the minimum of all the metric-specific capacities is then the airspace capacity.

We think of the amount of air traffic in this chapter and related work [18, 15, 20, 19] as the number of sUAS flights per day in a metropolitan region. Metropolitan regions are an appropriate geographical scale for major sUAS use cases like package delivery or digital scanning services. We present analyses of the San Francisco Bay Area in the United States (additionally Norrköping region in Sweden was also studied in associated published work[19]), and consider up to 200,000 flights per day because our analyses suggest 100,000 flights per day as possible for the Bay Area just for package delivery [18].

Capacity in manned aviation is primarily informed by safety, though there are other considerations as well. Therefore the analytical work here also focuses on safety. The safety of unmanned aviation will be informed by the technology applied to it. This technology will have an unmanned traffic management (UTM) [77] component in the network core (the cloud), and a collision detection, resolution, and avoidance (CDRA) [59] component on the network edge (outside UTM), i.e., on-board each UAS. An analytical process aiming to establish a feasible volume of unmanned air traffic needs to pick metrics for safety, parameters modeling the technology, and develop a computational process that puts numbers to the safety metrics, as a function of the technology parameters. Our computational process is a simulator described in section 3.6-3.6.

Safety metrics in the literature (see section 3.2) pertain to the number of aircraft conflicts, forced conflicts, average proximity, closest approach distances, number of losses of separation and compounds of these such as dynamic density [68, 52]. Some of these are extrinsic and others intrinsic [87]. Amongst these, we value the aircraft conflict cluster size measure proposed by Durand [33] and Bilimoria[12] and the number of losses of separation more highly in the context of unmanned aviation. These metrics are described in detail in section 3.5.

To model technology, we make the following assumptions. We consider sUAS with strictly Vertical Take Off and Landing (VTOL) capability. They take off, fly directly from origin to destination and land. This models the evolution of the system if everyone was allowed to fly their most preferred route. All sUAS fly at a uniform speed at the same level because with an under 400ft restriction on commercial sUAS operations [27] in urban areas, there is very little room for multiple levels. Thus our setup is two dimensional and any conflicts and

collisions may happen only due to loss of minimum separation.

However, the resolution can use the third dimension. Compared to regular aircraft, sUAS are very small. We model this by allowing very close collision proximity (from 2.5m (best) to 20m (worst)). They are also highly maneuverable. Hence, for conflict resolution, we use vertical avoidance by modelling altitude control within a range such that the horizontal velocity is maintained. We aim at establishing capacity for the most basic system with minimal feasible assumptions. Hence, we ignore sensor and navigational uncertainties (such as deviations from trajectory, delays in aircraft detection, etc), static (e.g. buildings) and dynamic (e.g. manned aircraft) obstacles, wind and air worthiness violations (aircraft failures).

The structure of the chapter is as follows. We first present a review of related work under section 3.2. Our traffic density estimates, metrics and Capacity definition are presented under sections 3.3, 3.5 and 3.4 respectively. The conflict detection and resolution algorithm used, the simulator requirements and details of the sample simulator used are discussed in 3.6. In 3.7 we discuss our capacity estimates based on safety for San Francisco Bay Area. We also evaluate an additional metric for performance efficiency. The results provide further insights from the distributions of the efficiency numbers to emphasize the effect of lack of management on fairness in the system. Section 3.8 concludes the chapter with a summary of the findings.

3.2 Literature Review

The simplest notion of airspace capacity is the maximum number of aircraft that can traverse an airspace in a given time under a set of requirements. Capacity estimation approaches in literature evaluate this from controller and pilot workload[64, 65, 50, 58]. Capacity is derived from air traffic complexity measures such as Monitor Alert Parameter (MAP)[94], the maximum number of aircraft an Air Traffic Control (ATC) controller can handle at any given time and Dynamic Density (DD)[62, 84], a weighted summation of factors that affect the air traffic complexity. These are defined based on an assumption of a structured airspace and Air Traffic Management (ATM) that includes monitors, sectors and airways[68, 52, 55]. Capacity is then estimated using fast time and real time simulation methods [88].

Most of this structure doesn't exist in low-altitude airspace where the future sUAS traffic is expected to show up. Moreover as unmanned aviation begets the need for automation, these extrinsic measures may need to be modified for automated traffic. A second more intrinsic approach (in the sense of Vidosavljevic [87]) for UAS traffic is presented in [18]. The safety of future sUAS traffic is measured from the expected conflict cluster size statistics derived from an aircraft cluster based analysis as defined and discussed by Durand[33] and Bilimoria[12]. On board systems must resolve these conflicts as the UAS fly. Multi-aircraft de-confliction algorithmic research [59, 75, 89, 81, 49, 51, 66], parametrizes the computa-

tional complexity of conflict resolution on the number of aircraft to be jointly de-conflicted. Hence, the cluster size metric captures computational complexity as a function of air traffic complexity.

Furthermore, the manned aviation capacity estimates are highly subjective owing to the dependency on manual controller judgment during the experiments, who are also assumed to be the bottleneck of the system. The Eurocontrol Care-Integra is another novel approach that addresses this by modeling the ATM system as a combination of several information processing agents, each with an associated information processing load (IPL) [41]. The system reaches capacity when one of the agents overloads. This overload threshold is easy to determine for machine agents but needs subjective judgment for human agents. However, this approach determines the bottleneck in the system instead of assuming it. Our capacity estimation approach is therefore inspired by this. We base our capacity on the metrics themselves that need to be satisfied. The metrics and their acceptable limits account for the type of controller and hence the approach can handle a hybrid management – human, automated or both.

Future sUAS operations may be free flight by nature i.e. individual flights could prefer responsibility for determining their own courses independent of a global plan or system. UAS Traffic Management (UTM) should therefore support user preferred flight trajectories to the extent possible. Any chosen metrics should account for this. 'Self-separation' design concepts and decentralized control strategies that transfer some of the separation responsibility to the cockpit have been proposed for manned aviation [59, 57, 37]. ATM architectures with the same objective for manned free flight were also researched by Bilimoria et al. at NASA as part of their Distributed Air/Ground Traffic Management (DAG-TM) concept[34, 56, 57, 13]. DAG-TM is characterized by distributed information sharing, decision-making and/or responsibility among a triad of agents: the Flight Deck (FD), Air Traffic Service Provider (ATSP), and Airline Operational Control (AOC). From a UTM perspective, this is analogous to the on board autopilot (FD), the UTM service provider (ATSP) and the UAS operator/command center (AOC).

Krozel et al.[56] show that following types of metrics can be potentially used to evaluate any UTM architecture for free flight (the sample measures used[56] for manned ATM are listed in parenthesis): Safety (number of actual conflicts and conflict alerts), Performance (Change in direct operating cost), Stability (number of forced conflicts (domino effect)) and DD (aircraft density, average proximity and average point of closest approach). Of these, we focus on the first two for sUAS traffic in this chapter. Further a recent MITRE report [67] proposes a maximum loss of 1 sUAS flight per 100000 flight hours over urban areas. Hence, this forms the basis of our chosen metrics described in section 3.5.

Next comes the choice of a CD&R algorithm. CD&R methods [59] in aviation literature have been primarily developed for large aircraft flying at higher altitudes and lower densities

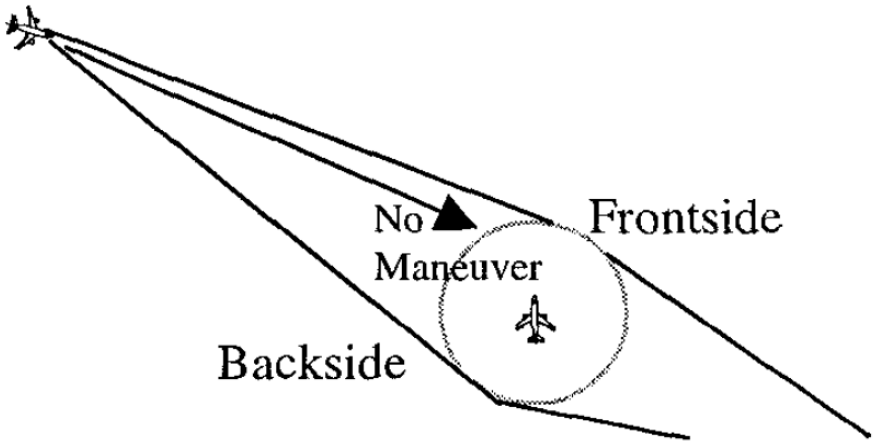

Figure 3.1: CD&R geometry based on choosing the lower cost choice between the frontside and backside maneuver [56]

than the expected future sUAS traffic. An example of a simple rule as used by Bilimoria et al.[56] is shown in Figure 3.1. However, owing to their size and maneuverability, sUAS provide a unique opportunity for simpler conflict resolution algorithms. Proposed future sUAS operations [8] might be done primarily by aircraft that have VTOL capability and high vertical acceleration rates. Hence, a simple velocity or altitude control is worth studying for safety of sUAS traffic. In section 3.6, we present a CD&R algorithm based on altitude control.

Given the metrics and a CD&R algorithm, we next need to measure the low altitude airspace capacity. We have developed a capacity estimation approach for sUAS traffic based on phase transition thresholds of chosen metrics beyond their allowable limits [15]. In this chapter, we use that definition to produce results for our chosen metrics. The capacity definition is reproduced in section 3.4.

Finally, we need a simulator that can simulate sUAS traffic densities so that the allowable limits of chosen metrics are reached with reasonable confidence. Many advanced simulation and evaluation tools developed for ATM (like BlueSky, TMX, ACES, AEDT, FACET) are overly complicated for our purposes – they take into account interaction with a variety of actors (air traffic controllers, the military, etc.) that are an overkill for the study of fundamental low-altitude UTM questions of traffic behavior and capacity.

Depending on the development of UTM, some of the factors present in ATM simulators (e.g., hazardous weather, community effect via noise and pollution, existence of no-fly zones) should be simulated/evaluated also in UTM, as the research progresses. Naturally, there are also features that are not relevant for ATM (and therefore are rightly absent from the

ATM simulators) while being of high importance to UTM. One example of such a factor is geo-data on near-ground obstacles, public and private land ownership and rights of way. Unlike conventional aircraft which stay primarily above 1000 feet in urban areas, except near airports, future sUAS operations are expected to occur below 400 feet. Simulation of safety from near ground static and dynamic obstacles and avoidance of exclusion/non-permitted flying zones therefore become necessary components of a sUAS traffic capacity generating simulator.

Lastly, ATM and its simulators are focused mostly on scheduled and deterministic traffic. Aircraft take off and land in distinct and well defined areas. For UTM, this will change in future when, in the words of Dr. Kopardekar [53],"every home will have a drone and every home will serve as an aerodrome". Given the diversity and unpredictability (temporal and spatial) of its operations, randomness is a much bigger player for future UAS traffic. To include this stochastic component, we look at some past approaches. A probabilistic setup which can be called *Dutch model* was used in PhD thesis of Hoekstra [36], developed by Jardin [44], and more recently explored within the Metropolis project by TU Delft [38]. In this model the aircraft are distributed *uniformly* in the given airspace. The direction of flight is also uniformly distributed in 0...360°; in [38] the different direction cones are separated by altitude. This uniform spatial distribution may not necessarily translate to the UAS traffic.

We instead use a population density model in this work. Flights' endpoints are sampled from the population density (neither the vehicles locations nor their headings are distributed uniformly) in line with the 'every home aerodrome' vision [53]. As in the basic version of the Dutch model, the flights occupy a single level, so the setup is essentially two-dimensional while the resolution uses the third dimension (see current restrictions on operations under 400ft [27]; see also Tompa et al.[90] for the "horizontal-maneuvers" TCAS work).

3.3 Traffic Density Estimates

The BVLOS phase of unmanned aviation will entail flights from service provider to service consumer and back. Metropolitan regions typically hold both provider and consumer, making them the appropriate geographical scale for this analysis of unmanned aviation. For example, the under 400 feet sUAS traffic portion of package delivery is likely to be the last mile from hub to door or door to door, e.g., from the regional hub of the delivery company or it's local pickup center to the premises of the recipient. As a representative value, if Amazon were to deliver packages in the San Francisco Bay area by flying them directly from its fulfillment center to homes, the average flight length would be about 25 miles as per our computations (see figure 3.2). We focus on the San Francisco Bay Area to understand the future, just as the Metropolis project[87] used Paris.

The various UAS airspace proposals by the FAA, NASA, and private corporations envis-

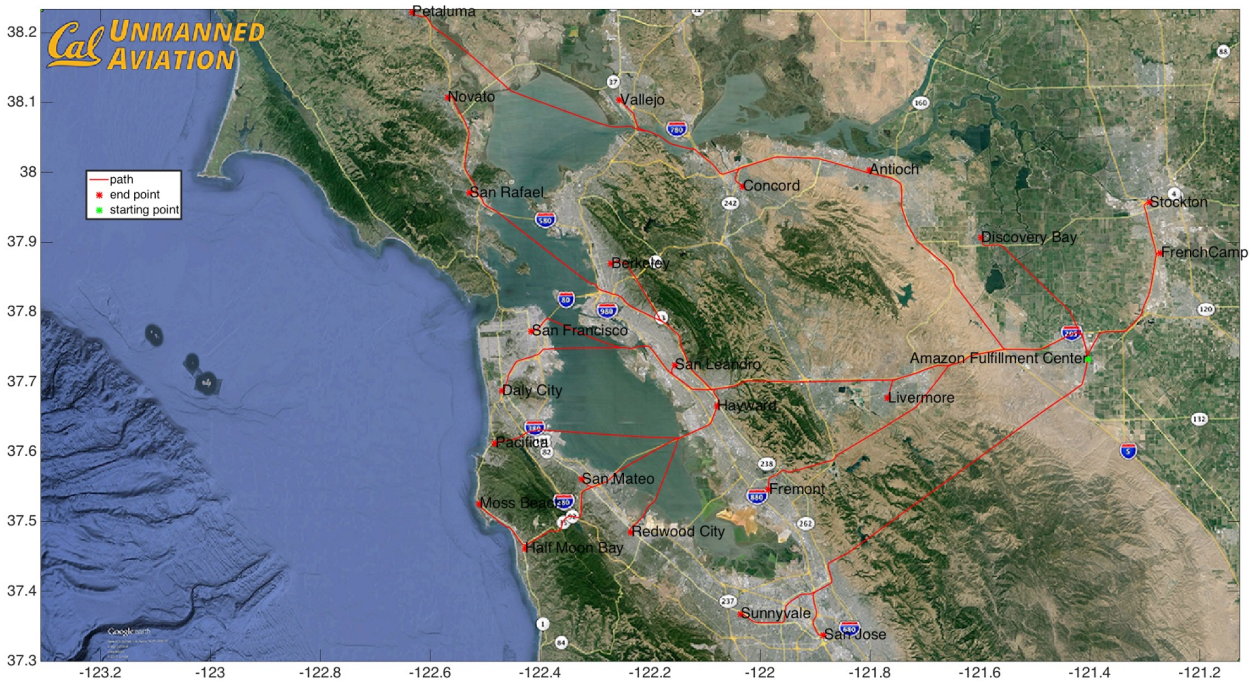

Figure 3.2: Package delivery airways computed from Amazon Fulfillment Center avoiding high density population areas [18]

age below 55 pounds unmanned flight, under 400 ft within class G airspace. Therefore we estimate current flight volumes in this airspace today by collecting data. On any given day, over bay area, there are roughly 60 helicopter flights and about 60 other recreational flight operations. Hence todayâĂŹs VFR air traffic below 1200 feet is nominally 100 flights per day. We choose this as our lower limit traffic density.

Industries like package delivery[78, 8] give us insight into the upper limits of traffic density. FedEx[28] and UPS[42] together deliver approximately 28 million packages every day in the US. If ten percent of that is delivered in California and only ten percent of that were to be delivered by UAS, California would see about 280,000 UAS flights per day. Since about half the state economy is in Northern California, we postulate 140,000 flights up north. Assuming 40,000 of that goes north of the Bay Area (sparsely populated), we obtain about 100,000 unmanned flights per day for package delivery in the Bay Area at maturity. Other sUAS use sectors may add more leading us to postulate the highest order of Bay Area unmanned flight at between 100,000 and 1,000,000. We simulate up to 200,000 sUAS flights a day.

We however note that the goods and passenger traffic in the above 400 feet band of airspace would add a lot more traffic. However, the amount of such traffic and its distribution will depend on the demographics of the population served. As the industry advances further, subsequently estimates like the above for sUAS traffic will become more readily

available. Hence the capacity estimation method and the metrics developed in this work can be extended with necessary modifications.

3.4 Capacity Definition

A metric M is a family of random variables parametrized by an integer which in our case represents the expected number of aircraft. The metric evaluated for a specific integer n is denoted by $M(n)$. We require that M is non-decreasing, i.e. for $n' > n$, $\mathsf{P}\{M(n') < M(n)\}$ tends to 0 as n increases (i.e. $M(n')$ majorizes $M(n)$).

For an airspace, given a metric M with an acceptable level M', the metric-specific airspace capacity is the number of aircraft N, such that an additional aircraft makes the probability that the metric exceeds its acceptable level, very high. In other words, the number of aircraft N is the *metric-specific airspace capacity*, if for any small $\epsilon > 0$ and some $\eta \in (0, 0.5)$, $\mathsf{P}\{M(\lfloor N - \epsilon \rfloor) > M'\} < \eta$ and $\mathsf{P}\{M(\lceil N + \epsilon \rceil) > M'\} > 1 - \eta$.

Typically, more than one metric must be simultaneously considered when evaluating the capacity of an airspace. Hence, we expand our definition over the set of metrics under consideration.

Let $M_S = \{M_1, M_2, \ldots, M_k\}$ be the set of metrics defined on a set of aircraft A for a given airspace. Each M_i, $i \in [1, k]$, is evaluated for a given number of aircraft n and must be a non-decreasing function as per our convention. Let M_i', $i \in [1, k]$, be the acceptable levels of the corresponding metrics. Then we can define the number of aircraft N_i as the *metric-specific airspace capacity*, if for any small $\epsilon > 0$ and some $\eta \in (0, 0.5)$, $\mathsf{P}\{M_i(\lfloor N_i - \epsilon \rfloor) > M_i'\} < \eta$ and $\mathsf{P}\{M_i(\lceil N_i + \epsilon \rceil) > M_i'\} > 1 - \eta$. The overall *capacity of the airspace* is then $N = \min(N_i)$.

A weak form of the definition would allow N to be a phase transition range. Suppose, each N_i is a range $[N_{i,l},\ N_{i,r}]$. Then N_i is the *metric-specific airspace capacity range*, if for any small $\epsilon > 0$ and some $\eta \in (0, 0.5)$, $\mathsf{P}\{M_i(\lfloor N_{i,l} - \epsilon \rfloor) > M_i'\} < \eta$ and $\mathsf{P}\{M_i(\lceil N_{i,r} + \epsilon \rceil) > M_i'\} > 1 - \eta$. The overall *capacity range of the airspace* is then $N = [min(N_{i,l}),\ max(N_{i,r})]$.

This airspace capacity definition includes deterministic cases. For example, let us evaluate the capacity N of a holding airspace around an airport. Let the metric M be the negative of average miles in trail separation between the aircraft in the holding pattern. For simplicity, we will assume the holding airspace is a circle and two aircraft can only be in sequence and not next to each other. For a given number of aircraft n, $M = -C/n$, where C is the circumference of the circle. Let the acceptable average separation be M'. Then the capacity of the holding airspace is $N = \lfloor -C/M' \rfloor$. If the number of aircraft in the holding pattern is even one less than N, $\mathsf{P}\{M > M'\} = 0$. If the number of aircraft in the holding pattern is even one more than N, $\mathsf{P}\{M > M'\} = 1$.

The above example shows a sharp transition in probability. N is therefore a sharp phase transition threshold. The first formulation above is therefore a strong form definition of airspace capacity. It forces N to be a single number. For more complex metrics, this N needs to be evaluated based on air traffic simulation that computes the metrics by varying the traffic densities. As the number of aircraft n becomes large, the airspace capacity may not necessarily be a single number and hence the *capacity range* definition applies.

This capacity definition is agnostic to the type of traffic (eVTOLs, large UAS, sUAS, etc). Even though in this chapter we only focus on sUAS traffic, this definition is applicable to evaluate other kinds of passenger and goods air traffic as is.

3.5 Metrics

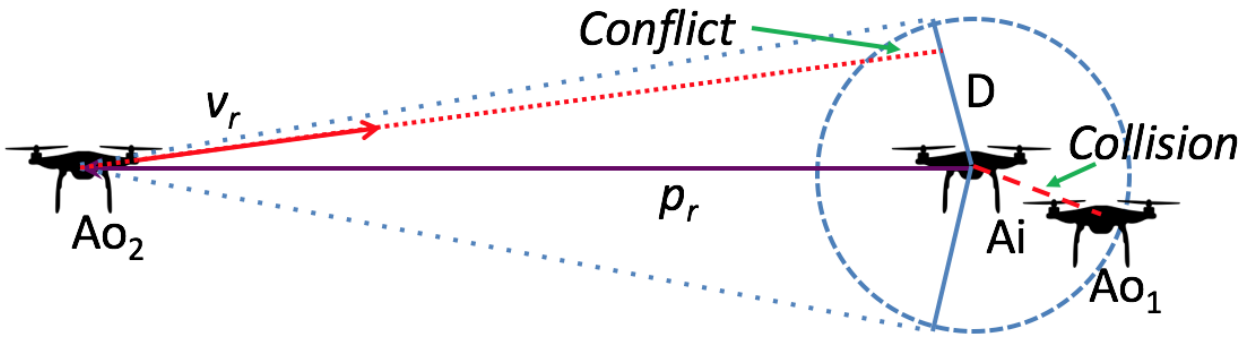

Figure 3.3: Conflict and Collision. Ao_1 & Ao_2 - Own sUAS, Ai - Intruder sUAS. The aircraft are shown in relative frame of reference

We first define the notion of a collision and conflict. Any sUAS should stay out of a minimum separation exclusion zone (a cylinder with radius D and height D) around another sUAS (Figure 3.3 shows the top view. The vertical cylinder is shown in figure 3.6). A *collision* is the loss of this minimum separation between any two sUAS. Given their projected paths in the horizontal plane, if an sUAS will eventually enter within the minimum separation of another sUAS, the two aircraft are in *conflict*. However, this means that two aircraft could be potentially in conflict even if they are miles apart. So, to make it more realistic, we add an additional notion of *conflict distance*. We derive it by adding a buffer to the minimum distance required for a safe manuever to avoid the minimum separation exclusion zone. The conflict distance is therefore equal to the sum of D, buffer distance and the product of sUAS speed and minimum time for avoidance (avoidance time derivation for a specific conflict detection and resolution (CD&R) is shown under 3.6).

Based on the above definitions, we use the following metrics for estimating the low-altitude airspace capacity for sUAS traffic:

Safety

Conflict Cluster Size

In a graph theoretic manner, we think of sUAS as nodes, with an edge between any two sUAS within conflict distance of each other (see figure 3.4). A conflict cluster is then a graph component and conflict cluster size is the number of vertices in the component. Cluster size statistics become component statistics in random geometric graphs [31]. This provides rich theoretical support for a metric sensible in aviation.

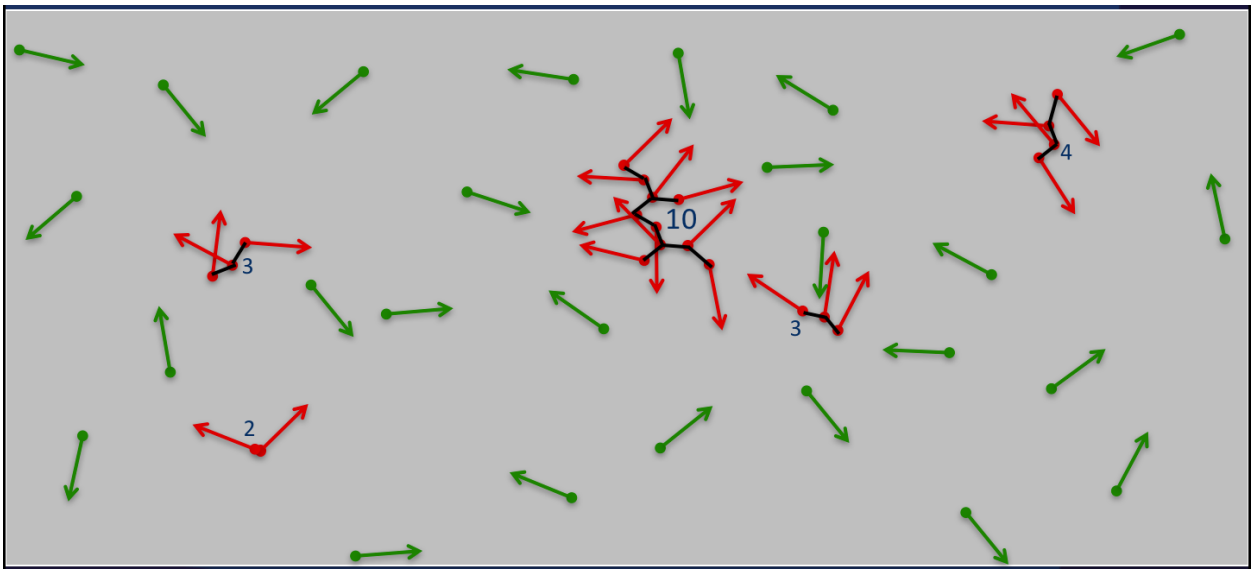

Figure 3.4: Abstraction of an airspace snapshot as a graph with cluster sizes indicated. (Aircraft within conflict distance are shown by red dots. The conflict pairs are connected by a black line. The arrows indicate the heading of the aircraft.)

We propose the conflict cluster size metric be distinguished in unmanned aviation because it is an architectural separator between UTM and on-board CD&R, i.e., the intelligence in the network core and that on the network edge. Architectural separations, when sensible, are enormously valuable, as they decouple industries and decompose system design problems. Conflict cluster size can separate UTM and CD&R because it determines the computational complexity of many CD&R algorithms [59, 75, 89, 81, 49, 51, 66]. The running time of these algorithms grows with the number of aircraft to be jointly de-conflicted, i.e. conflict cluster size.

While pilot ability or workload may be the dominant consideration in manned CD&R, computational complexity should be its surrogate for UAS CD&R. The separated design philosophy based on conflict cluster size is then as follows. The purpose of any UTM would be to ensure that on-board CD&R experiences problems of low complexity, i.e, only small conflict clusters, with high probability. In this view a UTM fails not only when there is a

collision. A UTM should be audited and reviewed each time an on-board CD&R is compelled to resolve a conflict cluster of significant size.

A volume of sUAS traffic is feasible as per this metric when it produces conflict clusters of significant size with low probability. Our task is now reduced to clarifying what size is significant and what probability is low.

An analysis of current air and road transportation suggests conflicts involving 3 or 4 sUAS to be the appropriate limit for on-board CD&R. TCAS and ACAS-X performance both deteriorate significantly when faced with more than two vehicle conflicts [14]. The road transportation system is operated less conservatively, but even there, one observes a three vehicle limit. Drivers solve a three vehicle coordination problem in motion when merging into a freeway or changing lanes. Intersections can require coordination of more than three vehicles but they are brought to a halt with stop signs or traffic lights. Transportation systems almost universally limit on-board CDRA to negotiating at most 3 vehicles through a combination of structure and operational controls. Therefore we focus on the prevalence of conflicts clusters of size greater than 3.

The issue of low probability is more complex. Large conflict cluster sizes are undesirable and must therefore be improbable. The assignment of a tolerable limit on the probability of large conflicts is more a policy exercise than a scientific one. However proper operating regime of an unmanned aviation system is one in which the probability of the undesirable is not only low but also stable, i.e., small increases in the volume of air traffic should not entail large increases in the probability of occurrence of large conflicts (see section 3.7 figure 3.13) . This point has scientific support. Probabilities associated with monotone properties in random geometric graphs, i.e, properties preserved by the addition of edges, exhibit rapid transitions about thresholds [31].

Total Losses of Separation

As the traffic density increases, even with the most robust CD&R methods it is possible that one resolution might result in a much more complex unavoidable loss of separation. Hence, it is also important from a safety stand point to keep a track of the total losses of separation and look at their rate of occurrence. The manned aviation analogue for this is the measurement of Near Mid-Air Collision Rate (NMAC). Following the proposed requirements by MITRE, we propose the second safety metric capturing total losses of separation as the *Total Loss of Flights per Flight Hour* with an acceptable limit of 0.001 as suggested in [67].

Performance

In addition to safety, we also look at loss in efficiency due to longer travel distances and times which then translate into higher operating costs (fuel, wear, etc.) and hence lower

performance. We explore performance in more detail as part of the Airspace Productivity in the next chapter. However, here we use it as an additional metric to demonstrate derivation of airspace capacity from multiple metrics. We use the *Change in Direct Operating Cost* as proposed by Krozel et al.[56] as our performance metric. However, this metric considers the added effect of Cost for Extension of Travel Distance and Travel Time. Since there is no extension of travel time as sUAS do not change their horizontal speed in the analysis in this chapter, we modify it just to *Percentage Extension of Travel Distance* with an acceptable limit of 10%.

We use the above metrics to determine capacity. These can be further extended as research in the field progresses. One example of an additional metric is noise level which has been explored, including by us in a related published work [16, 21]. These metrics are also applicable to other types of urban air traffic albeit the acceptable limits for each may vary.

3.6 Capacity Estimation

Now we proceed to expand on the estimation method we use to establish results for Airspace Capacity. We first present our CD&R algorithm for sUAS followed by a discussion of the Simulation requirements for sUAS traffic and the description of the simulator used in the current work.

Conflict Detection and Resolution

We consider two sUAS A_o (the own sUAS) and A_i (the intruder sUAS), with variables p_o, v_o, u_o and p_i, v_i, u_i respectively having their usual meaning (position, velocity and acceleration control). The kinematic motion of the aircraft is given by

$$\frac{dp_o}{dt} = v_o, \frac{dv_o}{dt} = u_o \tag{3.1}$$

$$\frac{dp_i}{dt} = v_i, \frac{dv_i}{dt} = u_i \tag{3.2}$$

$p(t; t_0)$ denotes the solution of the ODE over the time interval $[t_0, t]$ with initial conditions $p(t_0), v(t_0)$. The relative variables with respect to the intruder aircraft are given by

$$p_r = p_o - p_i,\ \dot{p_r} = \dot{p_o} - \dot{p_i} = v_o - v_i = v_r \tag{3.3}$$

$$v_r = v_o - v_i,\ \dot{v_r} = \dot{v_o} - \dot{v_i} = u_o - u_i = u_r \tag{3.4}$$

The equations of motion therefore reduce to

$$\frac{dp_r}{dt} = v_r, \frac{dv_r}{dt} = u_r \tag{3.5}$$

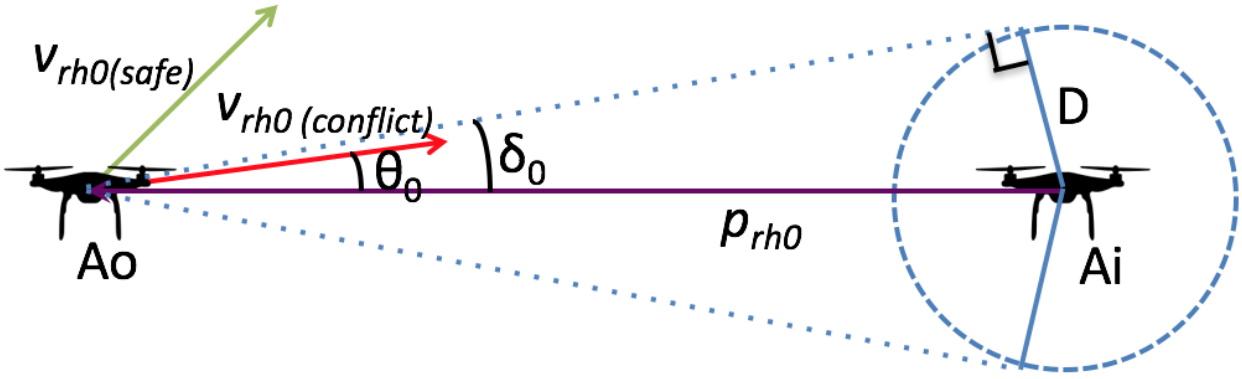

Figure 3.5: Conflict Detection (Top View). A_o - Own sUAS, A_i - Intruder sUAS. The aircraft are shown in relative frame of reference

We additionally use the following subscripts: h – in horizontal plane and v – vertical direction. Hence, $p_r \in \mathbb{R}^3$ can be written as $p_r = [p_{rh}\ p_{rv}]$. Now, for any interval $[0, \tau]$, we define, $d_{closest,h}(\tau) = min\ \|p_r(t)\|,\ t \in [0, \tau]$. We also define the cylinder C_i around sUAS A_i as $p \in \mathbb{R}^3$ such that $\|p_{rh}\| \leq D$ & $\|p_{rv}\| \leq D$. $D \in \mathbb{R}$ is the minimum allowable separation from an sUAS in the horizontal plane and vertical direction.

A_o and A_i are in *collision* at time t if $p_o(t) \in C_i$. A_o and A_i are in *conflict* at time t_0 iff $\exists\ \tau \geq t_0$ such that $d_{closest,h}(\tau) \leq D$ & $p_r(\tau) \in C_i$. Then, we call the time of closest horizontal approach – $t_{closest,h}$.

Define,

$$\alpha = Cos^{-1} \frac{\langle p_{rh}, v_{rh} \rangle}{\|p_{rh}\| \|v_{rh}\|} \tag{3.6}$$

$$\delta = Cos^{-1} \sqrt{1 - \frac{D^2}{\|p_{rh}\|^2}} \tag{3.7}$$

$$\theta = \pi - \alpha \tag{3.8}$$

Conflict Detection Condition

When, $u_{rh}(\tau; 0) = 0$ & $p_{rv}(\tau; 0) = 0$, then for any $t \in [0, \tau]$,

$$\|p_{rh}(t)\|^2 = \|p_{rh}(0)\|^2 + \|v_{rh}(0)\|^2 t^2 + 2\langle p_{rh}(0), v_{rh}(0) \rangle t \tag{3.9}$$

Further we will drop the (t) and use 0 in subscript to denote value at time $t = 0$ for brevity.

For $d_{closest,h}$, $\frac{d\|p_{rh}\|^2}{dt} = 0$, which gives

$$t_{closest,h} = -\frac{\langle p_{rh0}, v_{rh0}\rangle}{\|v_{rh0}\|^2} \tag{3.10}$$

Since, $t_{closest,h} \geq 0, \langle p_{rh0}, v_{rh0}\rangle \leq 0$. This implies that $(Cos\ \alpha)_0 \leq 0$. Hence, $\alpha_0 \geq \pi/2$ or $\theta_0 \leq \pi/2$. Substituting $d_{closest,h}$ and $t_{closest,h}$ in (3.9), we obtain -

$$d^2_{closest,h} = \|p_{rh0}\|^2 - \frac{\langle p_{rh0}, v_{rh0}\rangle^2}{\|v_{rh0}\|^2} \tag{3.11}$$

Since, for conflict, $d^2_{closest,h} \leq D^2$, we get -

$$1 - \frac{D^2}{\|p_{rh0}\|^2} \leq \frac{\langle p_{rh0}, v_{rh0}\rangle^2}{\|p_{rh0}\|^2\|v_{rh0}\|^2} \tag{3.12}$$

The right hand side is $(Cos\ \alpha)^2_0$ and since $(Cos\ \alpha)_0 \leq 0$, we obtain the $conflict$ condition as-

$$\boxed{\frac{\langle p_{rh0}, v_{rh0}\rangle}{\|p_{rh0}\|\|v_{rh0}\|} \leq -\sqrt{1 - \frac{D^2}{\|p_{rh0}\|^2}}} \tag{3.13}$$

Time of Conflict

Next, we find the time interval $[t_1, t_2]$ for which A_o and A_i satisfying (3.13) will be in conflict. Substituting the condition $p^2_{rh} \leq D^2$ in (3.9) and solving the quadratic equation thus obtained we get

$$t_1 = -\frac{\langle p_{rh0}, v_{rh0}\rangle}{\|v_{rh0}\|^2} - \frac{\sqrt{D^2 - \|p_{rh0}\|^2(1 - Cos^2\alpha)}}{\|v_{rh0}\|} \tag{3.14}$$

$$t_2 = -\frac{\langle p_{rh0}, v_{rh0}\rangle}{\|v_{rh0}\|^2} + \frac{\sqrt{D^2 - \|p_{rh0}\|^2(1 - Cos^2\alpha)}}{\|v_{rh0}\|} \tag{3.15}$$

Since, we look for solutions in $[0, \tau]$,

$$if\ t < t_1\ or\ t > t_2,\ \|p_{rh}\| > D \tag{3.16}$$

Conflict Resolution

We make the following assumptions on the system:

- Every sUAS gets a unique start time t_{start} when it enters the cruise altitude.
- An sUAS has higher priority if it has an earlier t_{start}.
- When there is a conflict the lower priority sUAS performs the resolution maneuver.
- When not undergoing a resolution maneuver, every sUAS travels at the same altitude.

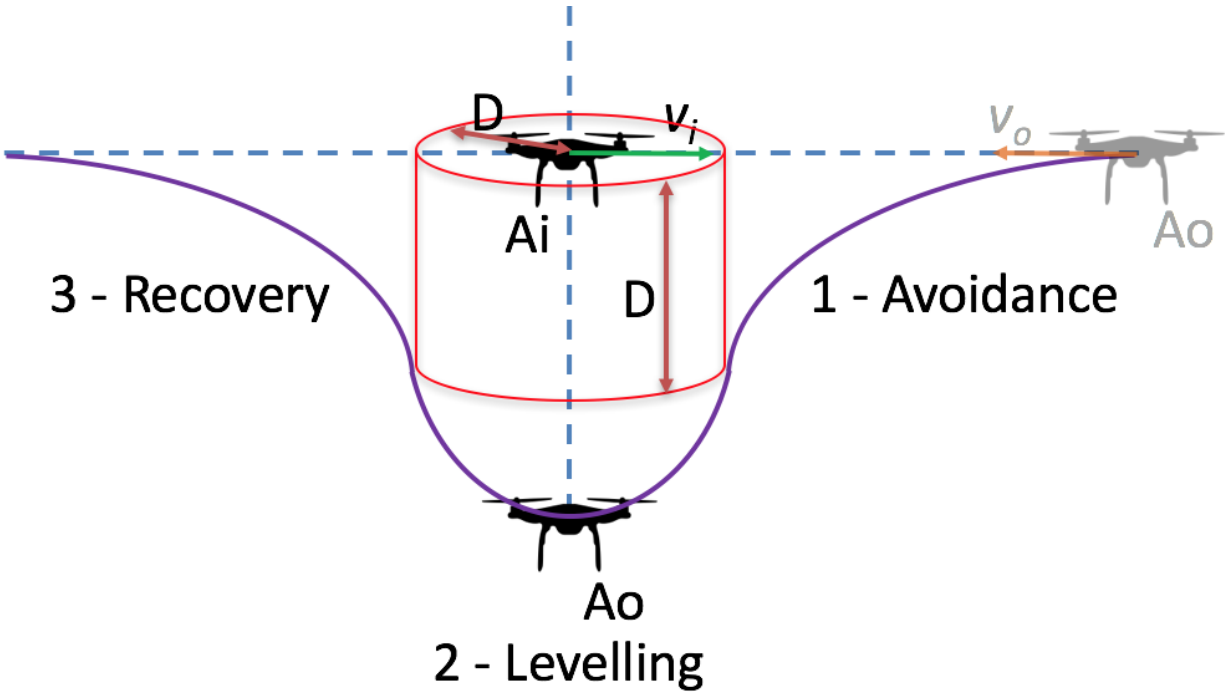

Figure 3.6: sUAS Tactical Resolution (Side View). A_o - Own sUAS, A_i - Intruder sUAS

The resolution in a conflict is that the sUAS with lower priority sinks to a lower altitude to prevent collision, if the time required for resolution is less than the time to imminent collision and then returns to its altitude once the collision is avoided. Figure 3.6 shows the three maneuvers that A_o undergoes to avoid collision, which we call *Avoidance*, *Leveling* and *Recovery* in that order.

We define additional variables as follows:

- a_{down} - Maximum vertically downward acceleration that A_o can apply
- a_{up} - Maximum vertically upward acceleration that A_o can apply

- a_{vd} - Actual vertically downward acceleration that A_o applies
- a_{vu} - Actual vertically upward acceleration that A_o applies

For tactical collision avoidance, we assume that $a_{vd} = a_{down}$. The time durations required for the three maneuvers can now be computed.

$$(Avoidance),\ t_{Avd} = \sqrt{\frac{2D}{a_{vd}}} \tag{3.17}$$

$$(Levelling),\ t_{Lvl} = \frac{2\sqrt{2a_{vd}D}}{a_{vu}} \tag{3.18}$$

$$(Recovery),\ t_{Rec} = \sqrt{\frac{2D}{a_{vd}}} \tag{3.19}$$

where, $a_{vu} = \min\ (a_{up}, \frac{2\sqrt{2a_{vd}D}}{t_2 - t_1})$

A_o will initiate resolution only if,

$$t_{Avd} \leq t_1 \tag{3.20}$$

The time instants for different phases of the resolution are therefore as follows:

$$t_{Start} = t_1 - t_{Avd} \tag{3.21}$$

$$t_{EndAvd} = t_1 \tag{3.22}$$

$$t_{EndLvl} = t_1 + t_{Lvl} \tag{3.23}$$

$$t_{End} = t_{EndLvl} + t_{Rec} \tag{3.24}$$

where, $\{t_{Start},\ t_{EndAvd},\ t_{EndLvl},\ t_{End}\} \in [0, \tau]$

Theorem: For two sUAS A_o and A_i satisfying (3.13) and (3.20), given:

$$\begin{bmatrix} p_r \\ v_r \end{bmatrix} = \begin{bmatrix} p_{r0} + v_{r0}t + \frac{1}{2}u_r t^2 \\ v_{r0} + u_r t \end{bmatrix} \tag{3.25}$$

if,

$$p_{rv0} = 0 \tag{3.26}$$

$$u_r = [0\ 0\ u_v] \text{ for } t \in [t_{Start}, t_{End}] \tag{3.27}$$

where,

$$u_v = \begin{cases} -a_{down}, & \text{for } t \in [t_{Start}, t_{EndAvd}) \\ a_{up}, & \text{for } t \in [t_{EndAvd}, t_{EndLvl}) \\ -a_{down}, & \text{for } t \in [t_{EndLvl}, t_{End}) \end{cases} \tag{3.28}$$

then for $t \in [0, \tau)$,

$$p_o \notin C_i \tag{3.29}$$

Proof-

Recall that $p_o \in C_i$, if $\|p_{rh}\| \leq D$ & $\|p_{rv}\| \leq D$. Since, $t_{EndAvd} = t_1$ & $t_{EndLvl} \geq t_2$, from (3.16), for $t \in [0, t_{EndAvd})$ & $t \in [t_{EndLvl}, \tau)$, $\|p_{rh}\| > D$ i.e. $p_o \notin C_i$.

By construction, for $t \in [t_{EndAvd}, t_{EndLvl}]$, $\|p_{rv}\| > D$ i.e. $p_o \notin C_i$. Hence, for $t \in [0, \tau)$, $p_o \notin C_i$

Resolution Algorithm

We now present the resolution algorithm that executes the tactical collision avoidance for two sUAS described above in a simulation environment.

The *range* around an sUAS that it needs to check for conflicts with other higher priority sUAS is given by

$$range = D + (max\ v_r) \cdot t_{Avd} \tag{3.30}$$

Now, at a given time t in the simulation, let A = [A_1,A_2,...A_n] is the set of sUAS active at time t, p = [p_1,p_2,...p_n] is the set of updated positions of the active sUAS at time t and v = [v_1,v_2,...v_n] is the set of velocities of the active sUAS at time t.

for $i = n$ to 2, step -1 **do**

for $j = i - 1$ to 1, step -1 **do**
$p_r = p_i$ - p_j

if $|p_r| \leq range$ **then**
$v_r = v_j$ - v_i

if $\frac{p_r \cdot v_r}{|p_r| \cdot |v_r|} \leq -\sqrt{1 - \frac{D^2}{|p_r|^2}}$ **then**
Evaluate t_1, t_2*and*t_{Avd}

if $t_{Avd} < t_1$ **then**
Evaluate $t_{Start}, t_{EndAvd}, t_{EndLvl}, t_{End}$
$t_{resolve}(A_i) = t_{End} - t_{Start}$

end if
end if
end if
end for
end for

The $t_{resolve}$ above is the time for which the sUAS will undergo the entire resolution. The actual maneuvers are therefore accounted for in the position update and the $t_{resolve}$ gets updated to 0 once the resolution is over. By virtue of the construction, this algorithm ensures that every two vehicle conflict that is detected and can be resolved gets resolved assuming the higher priority vehicle continues on its path.

It is noteworthy that collisions that will occur in the simulation therefore are all forced. In other words, all resolvable two sUAS conflicts detected will be resolved but collisions will occur if one of the following conditions happens – an sUAS takes off into a conflict for which it does not have enough resolution time (see [17] for measures to prevent takeoffs into conflicts), an sUAS enters a conflict with a different sUAS before finishing its current resolution and therefore cannot avoid a collision with that and finally the higher priority sUAS finds itself in conflict with another even higher priority sUAS and initiates resolution before the lower priority sUAS has finished its own.

Additionally, as mentioned earlier, the conflict distance is the sum of a buffer distance added to the range in (3.30). For a collision distance varying from 2.5m to 20m, the conflict distance varies from roughly 50m to 150m. Hence, for a comprehensive analysis, we look at conflict distances varying from 5m to 300m.

Simulation

To estimate low-altitude airspace capacity, we need to investigate how different metrics behave w.r.t. the sUAS traffic intensity. So, we require a simulator that can simulate at least until the break-point where the metric exceeds its acceptable limit.

First, we have to choose a data structure to store sUAS static and dynamic data. An ideal choice should enable fast access and update times as well as the best possible search complexity adequate to the CD&R algorithm chosen. With the proposed CD&R algorithm in the previous subsection, the repeated distance comparisons consume the most time. A simple linear search would produce a worst case search complexity of $O(n^2)$ in the number of active sUAS at every instant of the simulation time. Use of spatial databases could speed this up at the same time making it easier to incorporate geo-spatial data on static and dynamic near ground obstacles that become more crucial for sUAS with increasing fidelity of simulations.

Next, the simulator requires a trip generator that generates the origin destination pairs for sUAS trips based on the chosen underlying spatial stochastic process and the start times for sUAS trips based on the chosen temporal stochastic process. The trip generator feeds into the aircraft database whenever new trips are generated.

Finally, the simulator requires three other functions – one to define the metrics to be computed, another that runs the CD&R algorithm on the sUAS traffic and evaluates the metrics and a third one for post processing the generated data and results.

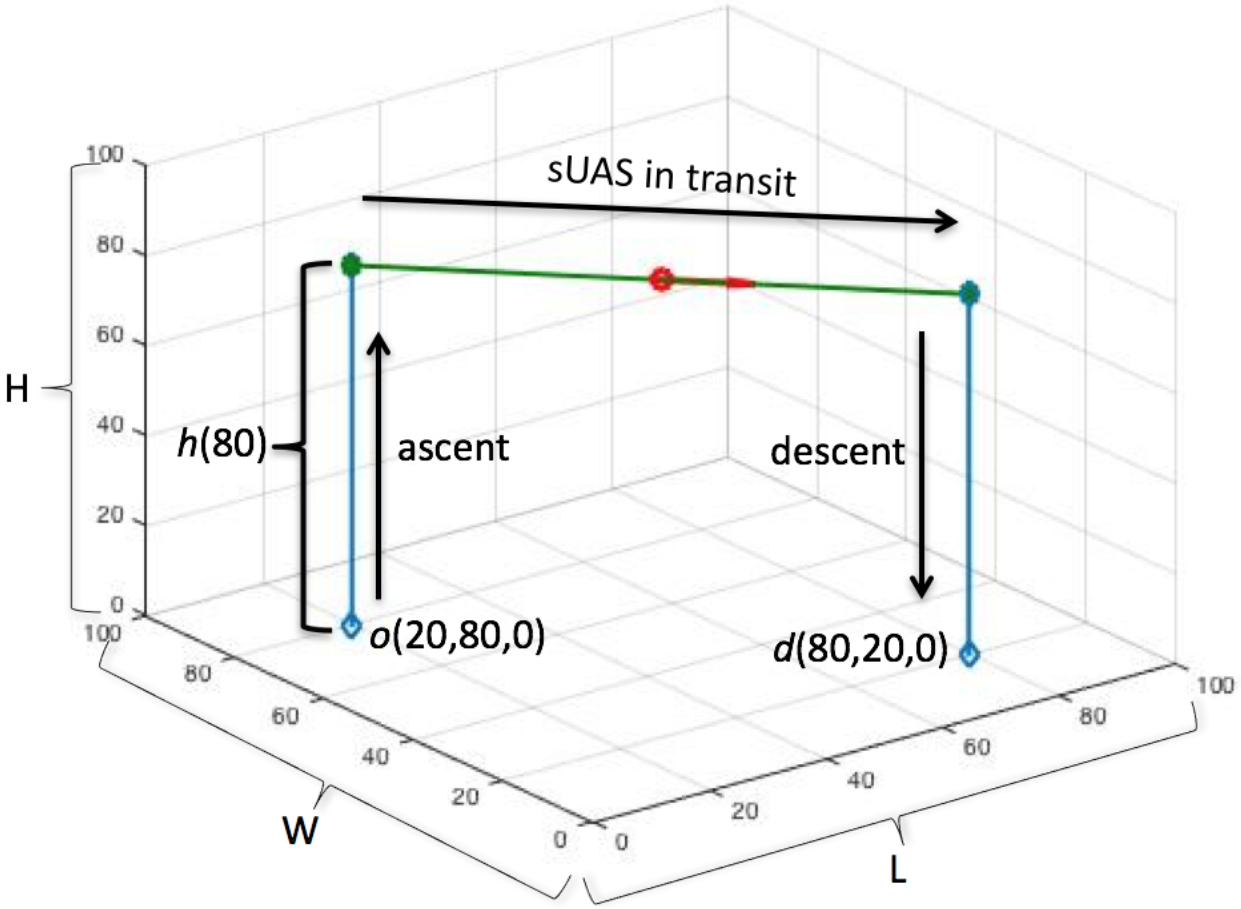

Figure 3.7: A typical sUAS flight path

In our work, we developed a simple simulator meeting most of the above requirements. Following our approach as published in [18], we consider the traffic setup as described in the introduction. Airspace is modeled as a cuboidal volume LWH defined by a rectangular area extruded to a given height H. Each sUAS is a quadruple (o, d, h, t) i.e. it has an origin, destination, height and start time. A typical flight is shown in figure 3.7. Each sUAS is defined as a Matlab class with properties that include the start time, origin, destination and

so on. The flights' origins and destinations were generated randomly based on the population density over the rectangular area. This preserves the actual shape of the geographical area (the San Francisco Bay Area in the sample study - figure 3.8) and the volume of airspace used.

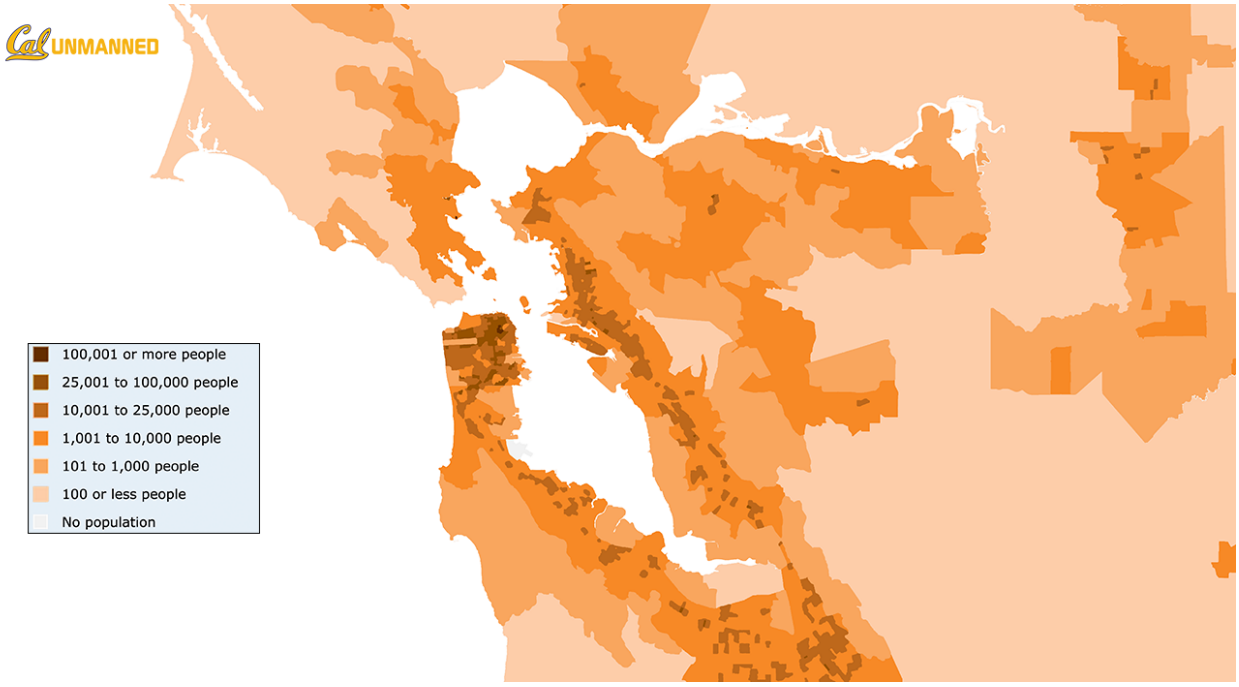

Figure 3.8: Population Density Map. Left: Bay Area [5].

The total number n of flights expected during the day was given, and the intensity of the traffic starting or ending at a point p of the domain was proportional to the population density at p (that is, the starting times of the flights from p form a Poisson process with the rate proportional to the density). At every instant of simulation time, handles to only the active trips were stored and accessed reducing the search space. However to implement the CD&R algorithm, the simple linear search algorithm was used producing a worst case time complexity of $O(n^2)$ in the number of steady state active trips.

We used this setup to run simulations for Bay Area (figure 3.8) varying traffic densities from 100 to 200,000 flights per day. For each density we analyzed all cases of collision distance (2.5m, 5m, 10m and 20m) and conflict distance (varying from 5m to 300m). All sUAS travel at a uniform speed and have a maximum vertical acceleration/deceleration of 0.5g ($\sim 5ms^{-2}$). We now present the results for the different metrics.

3.7 Results

Our simulation data spans traffic densities varying from 100 to 200,000 flights per day. There is a paradigm shift in complexity as traffic density increases to future estimates. Figures 3.9, 3.10, 3.11 and 3.12 visualize this shift with every order of magnitude increase in traffic.

Figure 3.9: Zoomed perspective snapshot of conflicts over Bay Area at 100 flights/day.

Figure 3.10: Zoomed perspective snapshot of conflicts over Bay Area at 1000 flights/day.

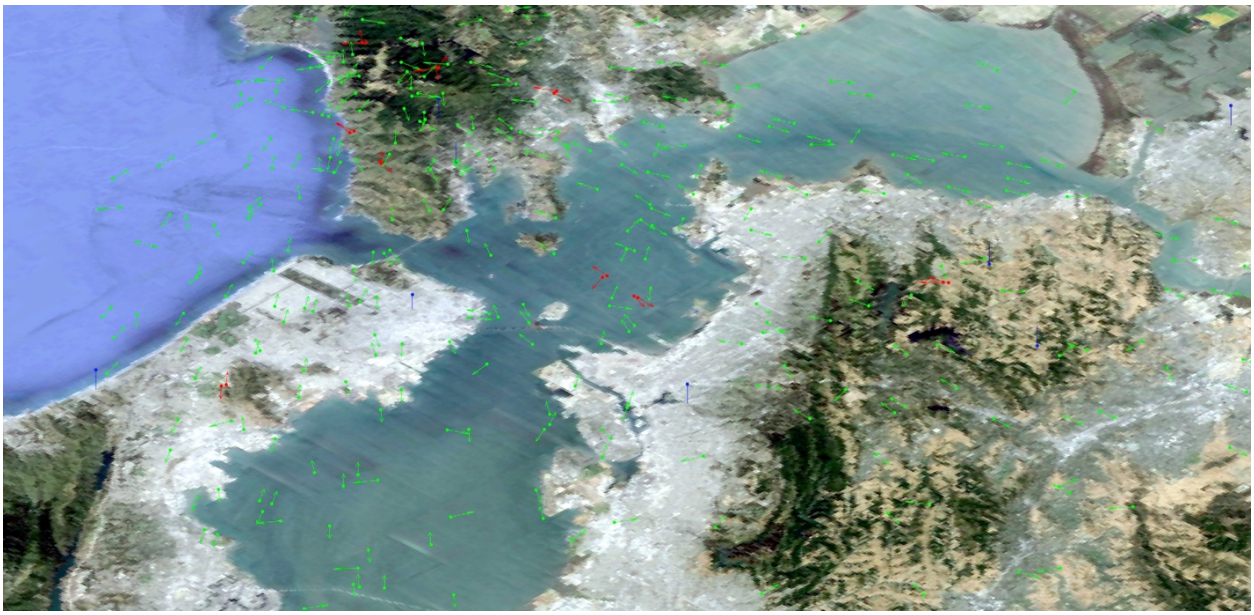

Figure 3.11: Zoomed perspective snapshot of conflicts over Bay Area at 10,000 flights/day.

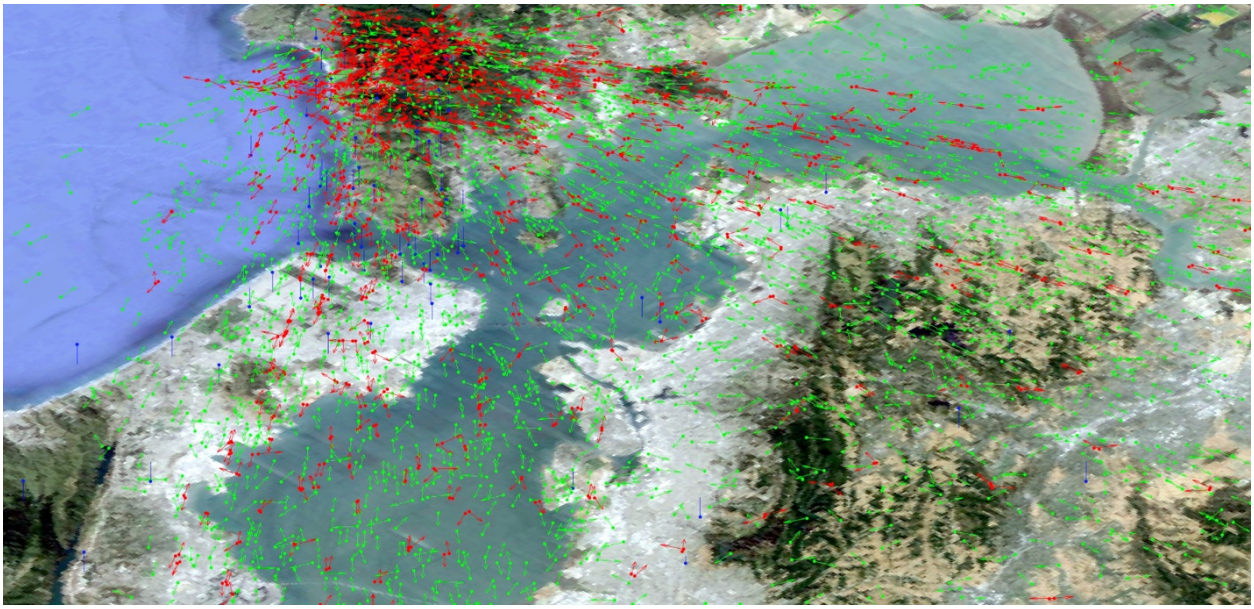

Figure 3.12: Zoomed perspective snapshot of conflicts over Bay Area at 100,000 flights/day.

Since, we first seek to understand the impact of traffic as is, these figures are produced with a conflict distance of 300 m and using a simulation where the CD&R method is turned off. Conflicting aircraft are marked red while the others are marked green. sUAS taking off or landing are shown in blue. The arrows show the flight direction of the sUAS.

There is a dramatic rise in the number of conflicting sUAS as large clusters begin to appear over densely populated areas, primarily over San Francisco city. As stated later in this section, the 99^{th} percentile conflict cluster size observed in these cases goes from a size of 0 (100 flights per day) to 13 (100,000 flights per day)[18].

The results in the rest of this section quantify the airspace capacity estimates from the chosen metrics. They were estimated with the CD&R method running in the simulation. We first present the results for the Conflict Cluster Size metric in figures 3.13. We observe that the transfer from conflict-free to unsafe regime indeed exhibits *threshold* properties akin to phase transition (figure 3.13): small changes in the input parameters lead to drastic changes in the output.

For example, the 300m curve in figure 3.13 shows the probability of occurrence of a cluster of size greater than 3, as being under 0.2 at 20,000 sUAS/day. It crosses 0.8 at 40,000 sUAS/day. Thus we consider the sUAS traffic regime between 20,000 and 40,000 sUAS flights per day a region of rapid transition, and interpret the curve to mean that the amount of sUAS traffic in the metropolitan region under the assumptions of the curve should be kept below 20,000 flights per day. This is the Conflict Cluster Size specific airspace capacity for the 300m conflict distance. Furthermore, figures 3.14 and 3.15 shows the entire band of capacity range in light blue and green over all the combinations of the minimum separation and traffic densities chosen.

In Table 3.1, we present the cluster size distribution statistics. They list the 99^{th} percentile and largest clusters observed for six conflict distances in the Bay Area. We only list the major traffic density jumps. With 100,000 flights a day, with a conflict distance of 300m, the largest clusters observed are of size 16 and the 99^{th} percentile cluster is of 7 aircraft. In our related published work [18], we had observed that the lack of a CD&R system and intent information produced largest and 99^{th} percentile cluster sizes of 96 and 13 respectively for the same conflict distance of 300m and traffic density of 100,000 flights a day. Clearly, the CD&R algorithm used has greatly improved the safety of the system.

Table 3.1: Cluster Size Distribution - Bay Area

	(99^{th} Percentile, Largest) Cluster Size					
Flight Rate (per day)	**50m**	**100m**	**150m**	**200m**	**250m**	**300m**
100	(0, 0)	(0, 0)	(0, 0)	(0, 0)	(0, 0)	(0, 0)
1000	(0, 2)	(0, 2)	(0, 2)	(0, 2)	(0, 2)	(2, 2)
10000	(0, 2)	(0, 2)	(2, 2)	(2, 3)	(2, 4)	(2, 5)
100000	(2, 3)	(2, 5)	(3, 6)	(4, 9)	(5, 12)	(7, 16)

Next, we look at the Loss of Separation Per Flight Hour Metric (figures 3.16 and 3.17).

We observe a threshold around 5000 flights per day for safety being violated (flight loss per flight hour exceeding the allowable limit) with high probability. At high tolerance (very close allowable collision proximity of 2.5m), the capacity regime lies between 10,000 to 30,000 flights per day. As we reduce the tolerance, meaning collisions occur at higher distances, the capacity regime comes down. For the lowest tolerance (20m), the capacity regime lies between 1000 to 5000 flights per day.

The implications of this are two fold. First, it shows that some form of traffic management will become necessary beyond 5000 flights per day. Secondly, it also shows that CD&R algorithms and better trajectory following methods that reduce deviations from flight path and allow for closer acceptable proximity would improve the capacity of the airspace.

We also present the results for the Performance Metric (figures 3.18 and 3.19). Here we

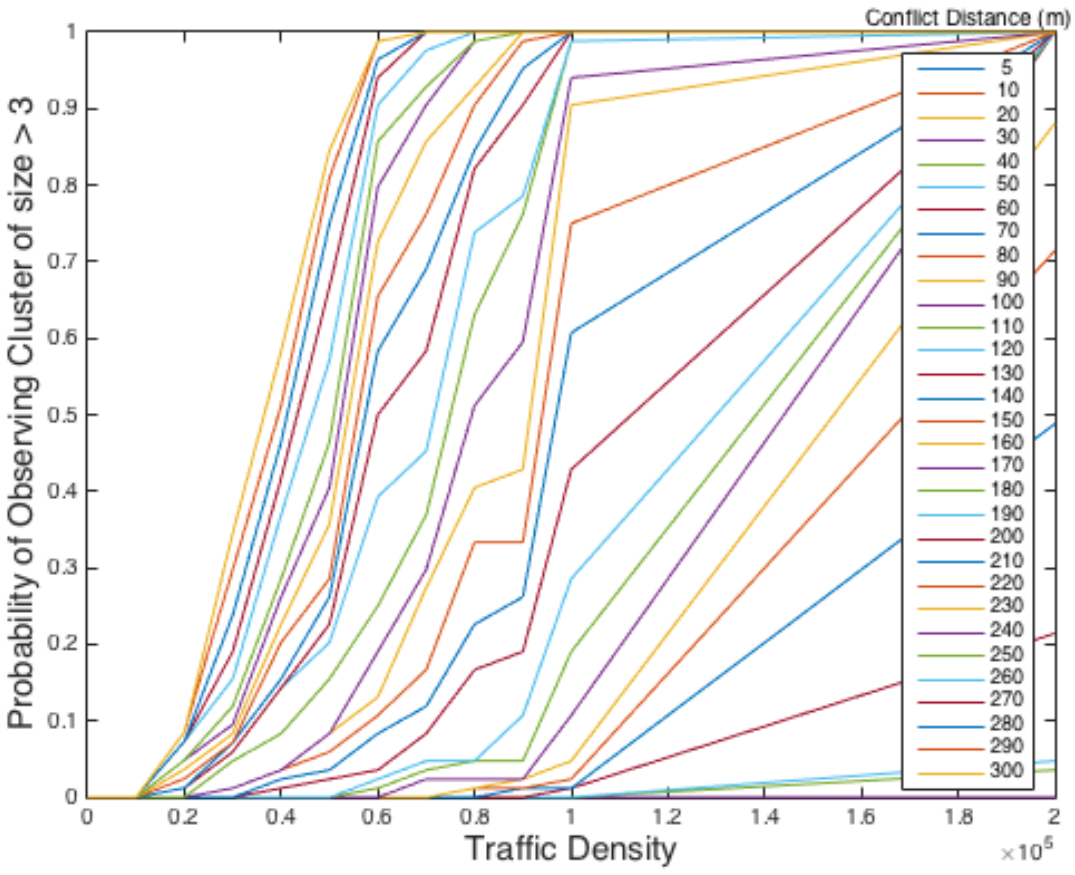

Figure 3.13: Probability of Conflict Cluster Size exceeding allowable limit as a function of traffic density for various collision distances for Bay Area.

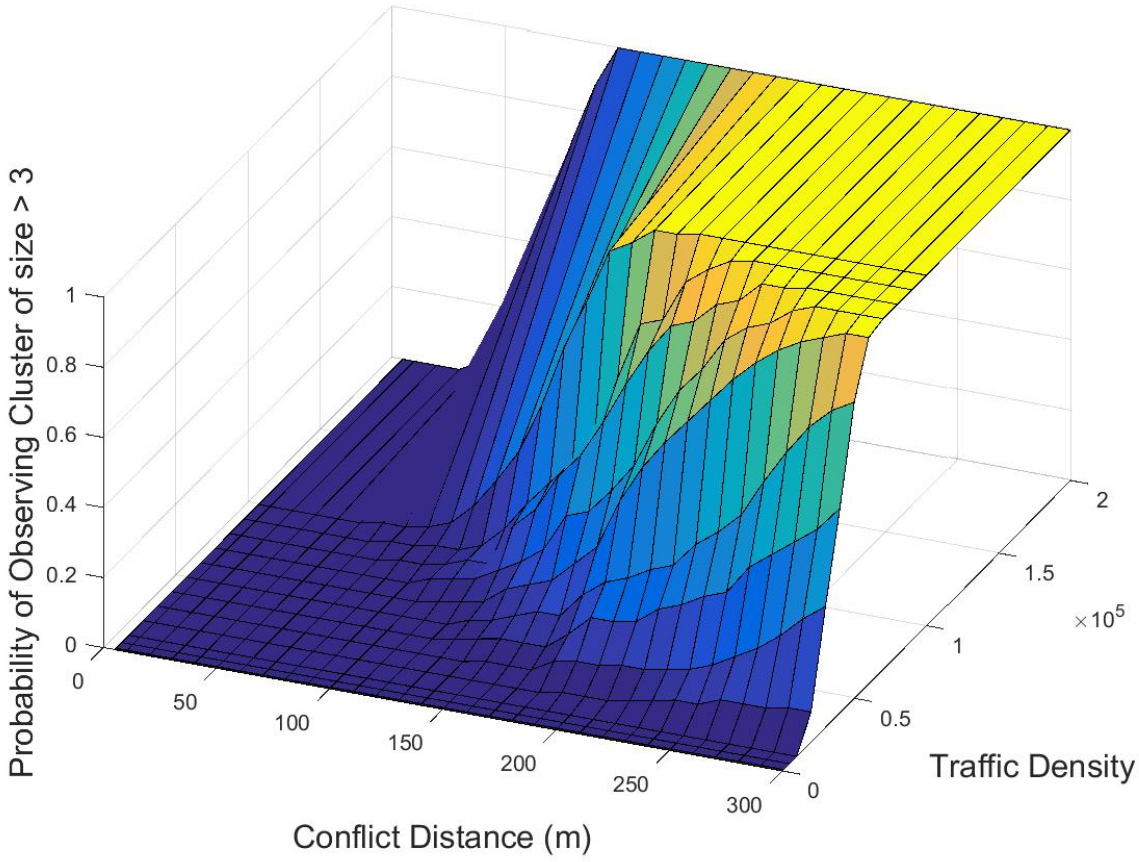

Figure 3.14: Probability of Conflict Cluster exceeding allowable limit as a function of both traffic density and collision distance for Bay Area.

observe that on average, the travel distance of sUAS is not extended more than 10% ever even at 200,000 flights a day. However, when we look at the maximum percentage extension observed, we again see a threshold, albeit at a much higher traffic density (over 80,000 flights a day in the worst tolerance case).

However, on closer observation if we look at the distribution of the percentage extensions, we see that most of the flights do not deviate much and hence the mean always stays below the allowable limit. But a few that get affected, get affected by a lot. We show this behavior by plotting a histogram of the distribution for the 100,000 flights a day case with 20m collision distance tolerance. Figure 3.20 shows that there are over 20 flights which travel more than double the distance. This shows that there is unfairness in the system. Most do not get affected but those who do, get affected severely.

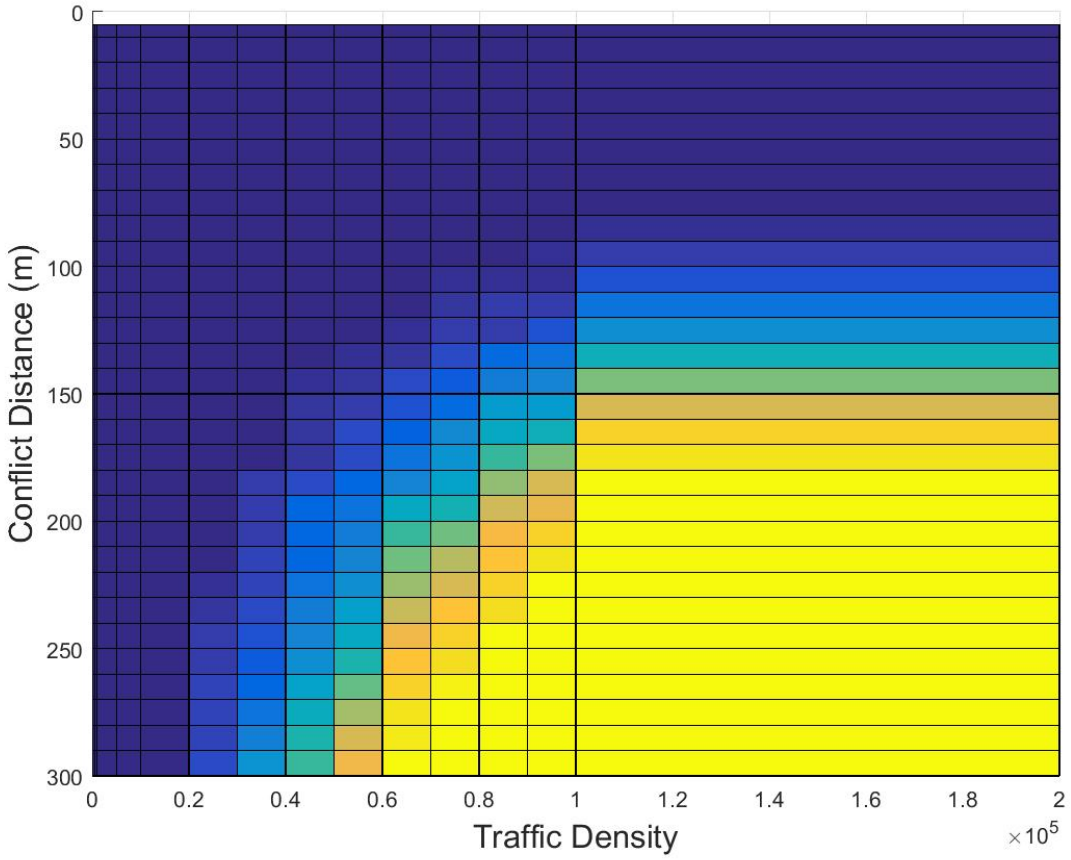

Figure 3.15: Probability of Conflict Cluster exceeding allowable limit as a function of both traffic density and collision distance for Bay Area - Top View

Combining the above metric specific capacities, if we consider the collision distance of 2.5m and the most conservative conflict distance of 300m, the airspace capacity of the San Francisco Bay Area low altitude airspace for sUAS traffic is determined to be at 10,000 flights per day. We also draw two further conclusions. First, safety is a bigger bottleneck than performance with regard to airspace capacity. Secondly, there is airspace management also required to ensure a fair provision of airspace to all users.

Finally, we observe that although defining the traffic per day is a good means to generate traffic and run the simulation, it is not necessarily the best density measure. The primary reason is that it doesn't capture spatial and temporal effects. To elaborate, first one cannot immediately say how many aircraft are there in the air at any given time. Second, the metrics might be exceeded only very locally in areas of highly concentrated traffic but seems

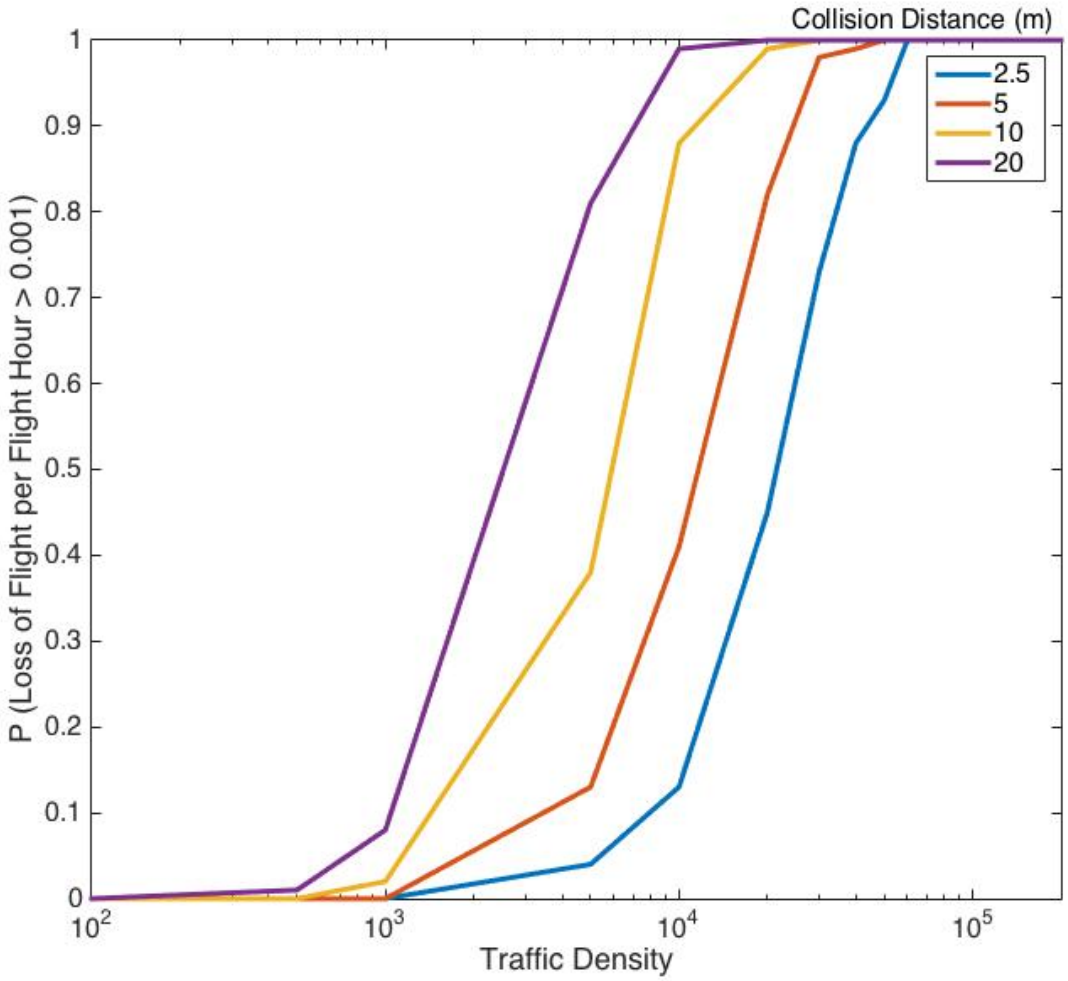

Figure 3.16: Probability of Loss of Flight per Flight Hour exceeding allowable limit as a function of traffic density for various collision distances for Bay Area.

to effect the entire system's capacity. The traffic is distributed over a large metropolitan area and even when thresholds are violated, most of the airspace might not necessarily be as worse. Hence, for each traffic density here, we also measured the 99^{th} percentile and peak traffic density per unit area over a $0.25km^2$ grid (see Table 3.2). In the next chapter, all the Airspace Productivity results are evaluated using traffic flow over this grid size.

3.8 Conclusions

We have estimated airspace capacity for sUAS traffic in the low-altitude airspace under the consideration of Safety. Results show that a capacity of 10,000 sUAS flights per day can be

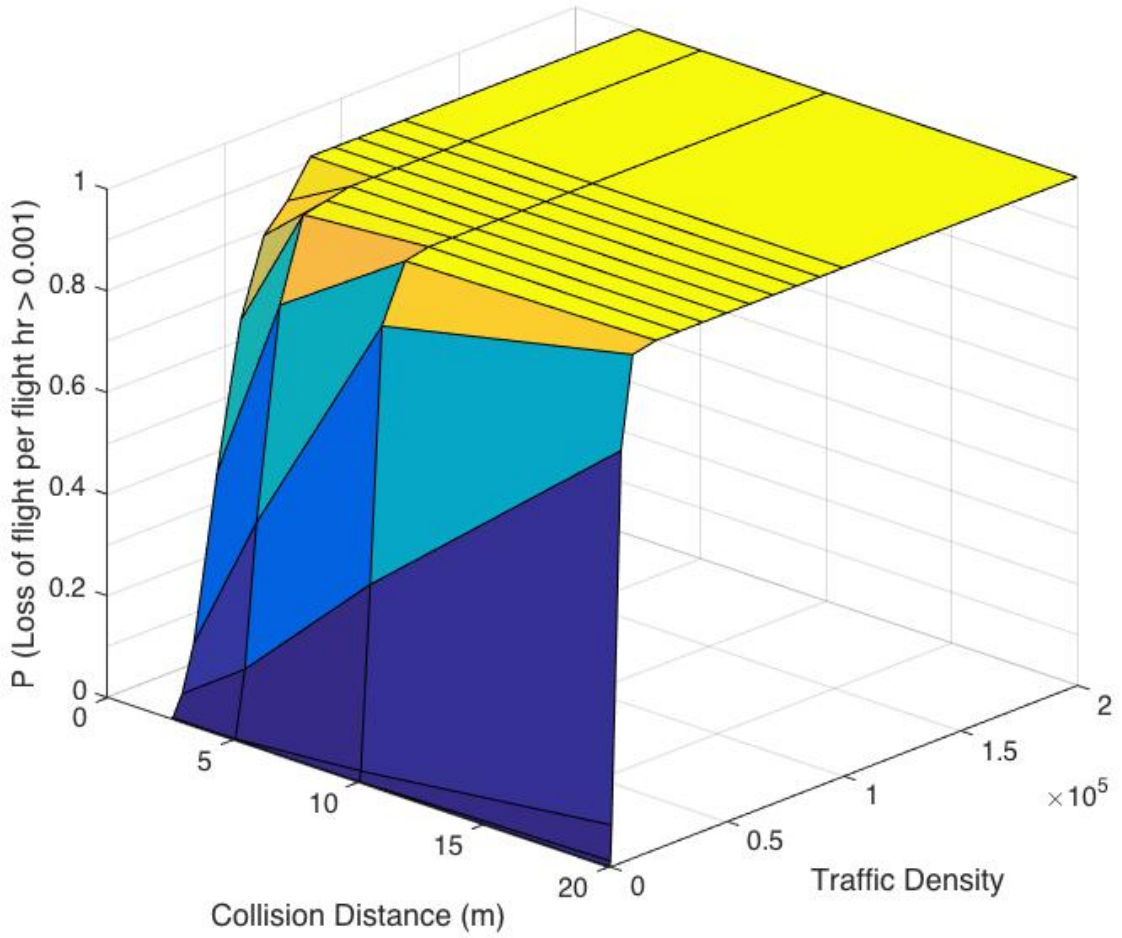

Figure 3.17: Probability of Loss of Flight per Flight Hour exceeding allowable limit as a function of both traffic density and collision distance for Bay Area.

Table 3.2: Spatial Traffic Density Distribution - Bay Area

	Temporal Traffic Density (Flights/day)			
Spatial Traffic Density (Flights/0.25km^2)	**100**	**1000**	**10000**	**100000**
99th Percentile	0	1	2	8
Peak	1	2	11	21

safely achieved over a metropolitan region such as the Bay Area. The probabilities of these metrics exceeding their allowable limits show sharp thresholds at their respective capacities. Modes of operations with traffic densities and tolerances in the blue areas on Figures 3.15,

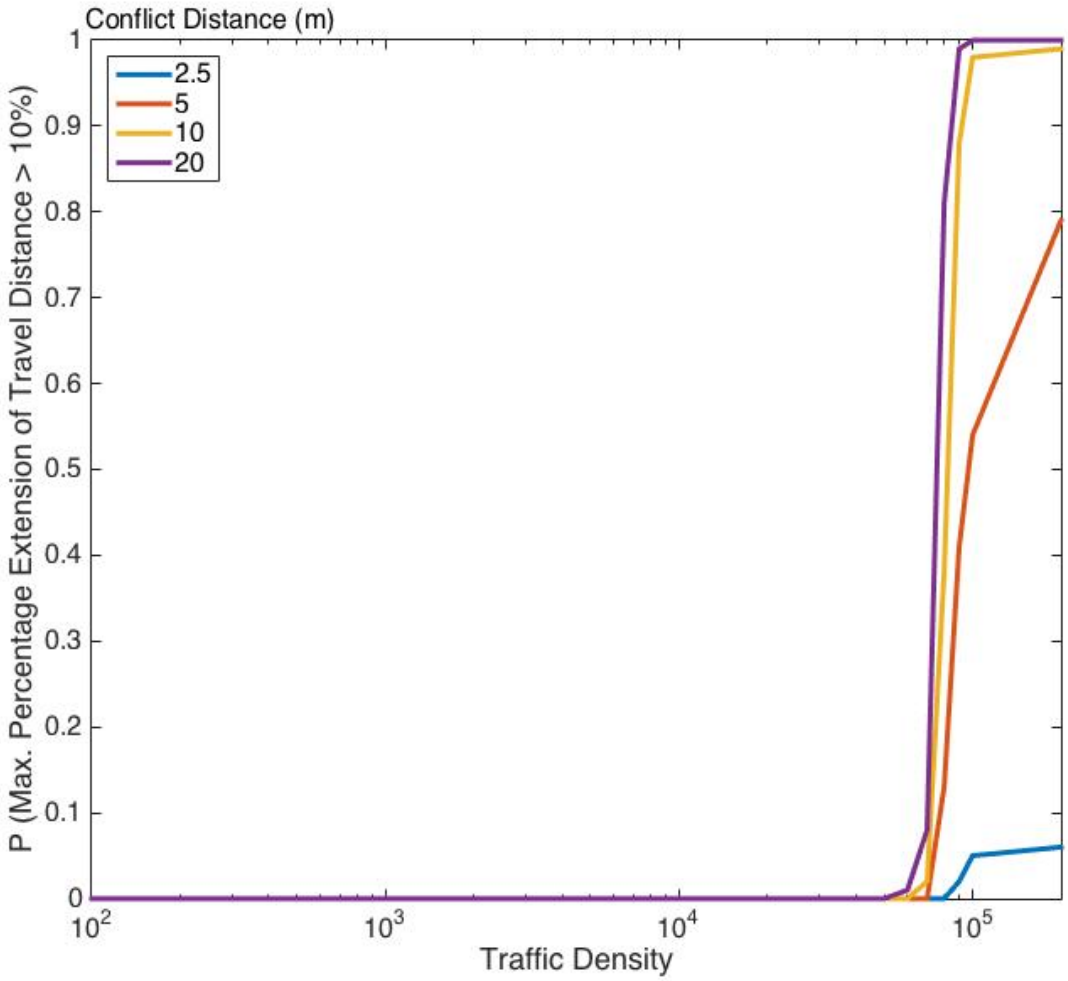

Figure 3.18: Probability of Maximum Extension of Travel Distance exceeding allowable limit as a function of traffic density for various collision distances for Bay Area.

3.17 and 3.19 are very unlikely to exceed the capacity, while operating in the yellow areas will almost surely exceed the airspace capacity. In general graphs like these for a variety of metrics will help the authorities in quantifying the tradeoffs between the allowable density of the sUAS traffic and the conflict detection and resolution capabilities (collision tolerance).

Next, we find that between safety and performance, Safety is a bigger limiting factor for sUAS. Secondly, although average performance may not be bad at high traffic densities but the distributions show that the system becomes highly unfair with those losing performance being severely impacted at high traffic densities. Both of these suggest that some form of traffic management becomes essential in near future if the future unmanned flights need to

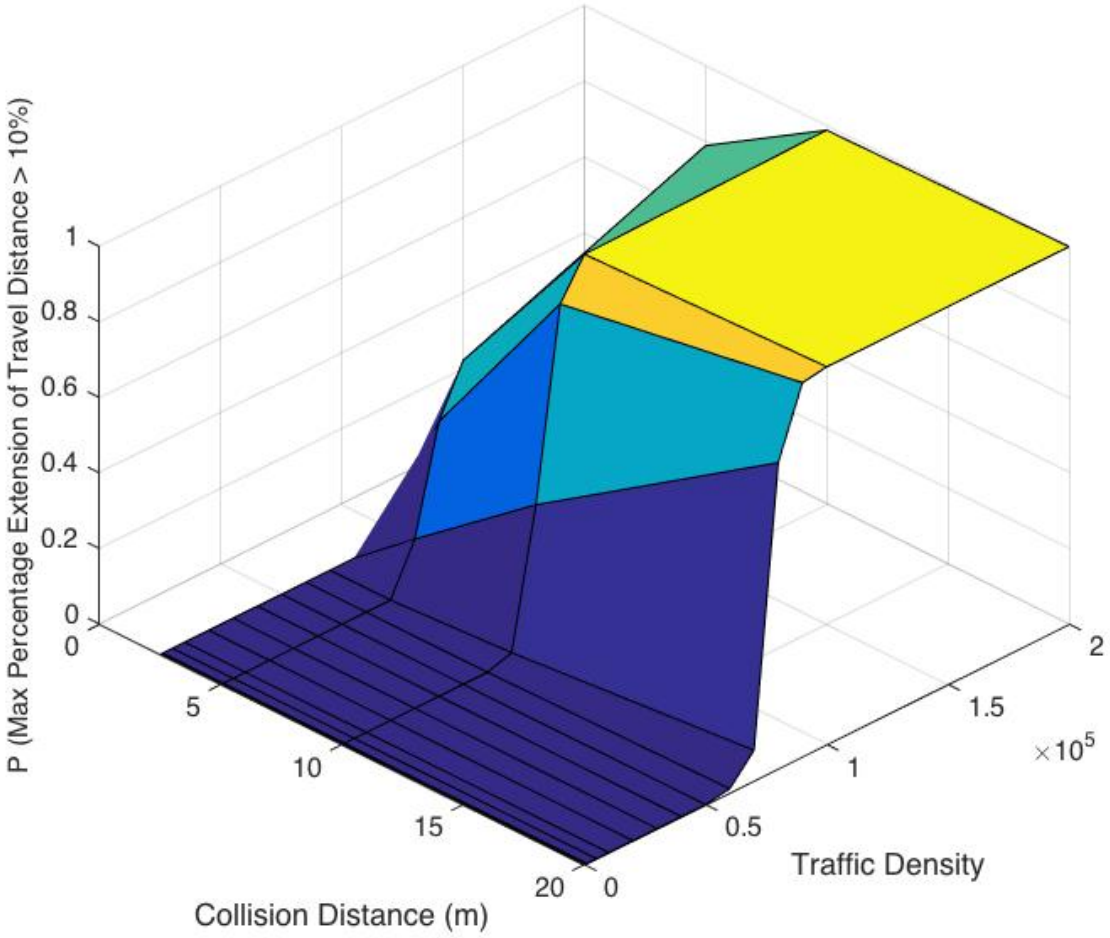

Figure 3.19: Probability of Maximum Extension of Travel Distance exceeding allowable limit as a function of both traffic density and collision distance for Bay Area.

be enabled in the existing airspace.

It is also of interest to estimate the airspace capacity for other values of allowable limits M', and more generally – under a wider range of metrics M. One of the most important concerns that the UTM community is currently facing is to measure the volume of unmanned aircraft that can be accommodated in the existing airspace based on considerations of safety, performance, spectrum required for communication and noise levels. Our definition has enabled us to provide a stepping stone to respond to that concern at least on grounds of safety, performance and noise [16]. Airspace capacity estimates based on the other aforementioned considerations will improve this further.

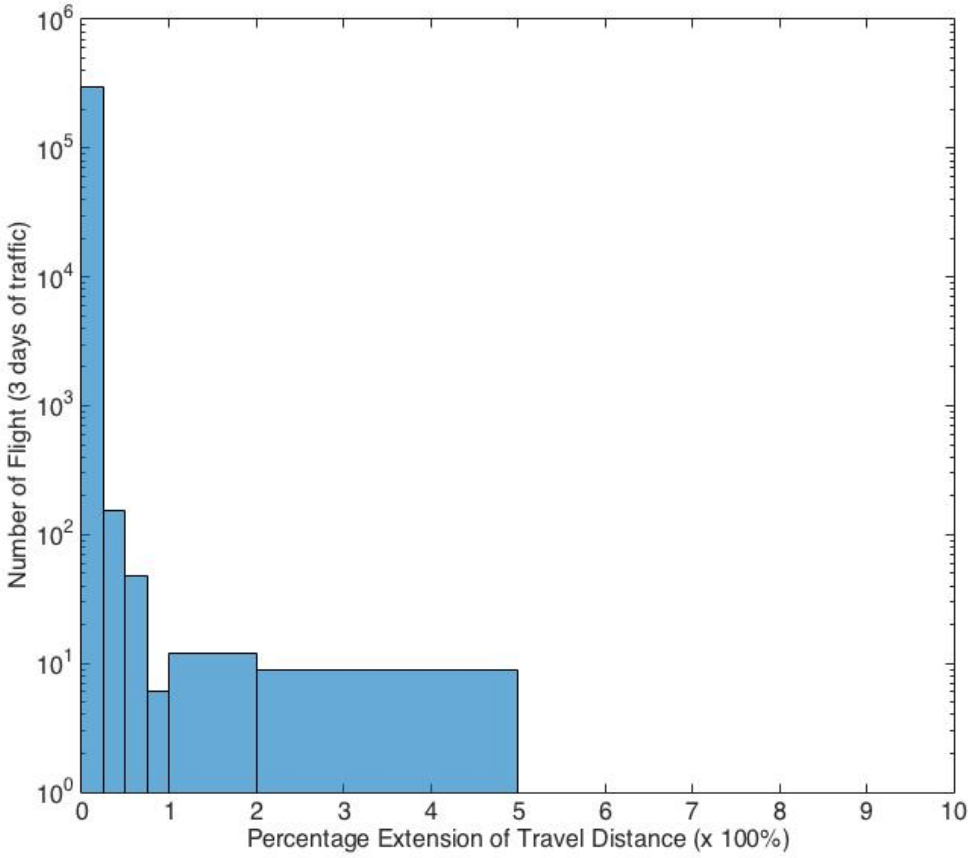

Figure 3.20: Distribution of Percentage Extension of Travel Distance over 3 days of traffic

Therefore, to summarize the findings on airspace capacity and answer the opening question of the chapter - Metropolitan airspace can get congested at varying densities depending upon the chosen CD&R technology and required safety to be achieved in the airspace. For example, for under 400 feet goods movement by sUAS in a region like the Bay Area, this happens at a daily traffic density of 10,000 flights per day at a collision distance of 2.5m.

Chapter 4

Airspace Productivity

While airspace remains uncongested, what type of onboard control increases productivity without compromising safety? This chapter evaluates two conflict detection and resolution approaches - pure speed control and pure direction control; and quantifies their impact on airspace productivity using three types of metrics - throughput, travel time extension and energy consumption. We simulate unmanned traffic over a representative square area and compute the productivity metrics. The inflow rate into the area is increased gradually and the corresponding outflow rates (throughput), travel time extensions and energy consumption for each type of control are measured. A representative power consumption model is developed for aircraft with both kinds of control. As stated in the previous chapter, we only focus on sUAS traffic in low altitude (under 400 feet) airspace. The chapter concludes with our findings on how each type of control impacts airspace productivity.

4.1 Introduction

With the expected introduction of unmanned aircraft to move goods[54] and people[71, 4, 69] and conduct other novel operations like structural monitoring, surveying, etc, future metropolitan airspace could be required to operate at traffic densities far greater than what it sees today. This airspace capacity as discussed in the previous chapter is limited by the allowable safety. However, given the allowable safety, how efficiently can the airspace be operated as a function of the onboard technologies? More precisely, how does the airspace productivity change as a function of on-board safety control?

To answer that, we choose two simple conflict detection and resolution approaches - pure speed control (aircraft can only change speed while maintaining direction to avoid other aircraft) and pure direction control (aircraft can avoid other aircraft only by turning but maintain their speed). We select a representative square area of 0.25 square kilometers (section 4.3), simulate uniformly distributed sUAS traffic over the study region, with increasing

inflow rate (section 4.4) and measure our three airspace productivity metrics for each CD&R - the throughput or outflow rate of the area, the percentage extension of travel time and the mean energy consumption of the sUAS traffic. We adjust the parameters of the two controls in the simulation to ensure that they are equally safe. We also assume that in the absence of the controls, the sUAS fly at their energy optimal speeds. Hence, when simulated with the CD&R, the energy consumed by the sUAS is measured as a multiple of the minimum energy consumed (without CD&R) (section 4.4).

Historically, manned airspace productivity has also been constrained by manual air traffic controller workload[64, 65, 50, 58]. The system has evolved with very stringent requirements on safety, as any loss of flight is catastrophic. Consequently, traffic flow management strategies have been developed to maximize the airspace throughput without compromising the high level of safety. The related impact of tactical resolutions on fuel consumption and traffic delays is also minimal as compared to the total fuel consumption and travel time of the entire trip, respectively. The approach to airspace productivity for unmanned operations may however need to be changed for three main reasons. First, the constraint of a manual controller is relaxed. Automated traffic management should be able to accommodate higher traffic densities and allow for higher throughput rates. It has been shown to do so to some extent even for manned aviation ([56, 57]). Second, not all crashes will be catastrophic. Most of the goods movement may instead result in property damage and not injury or death. Hence, this opens up the opportunity to explore new approaches to throughput for operations in the low-altitude airspace. Third, given the size, speed and energy requirements of the sUAS aircraft, tactical resolutions could consume a significant amount of the available energy and cause substantial delays thereby preventing a trip from even being completed.

Our throughput idea is inspired by the concept of the fundamental diagram[35], a component of kinematic wave theory. An extensive application of the concept in road transportation [30] relates the freeway traffic flow to the traffic density (figure 4.1). This has been researched for over seven decades and is well understood and utilized in road transportation[60]. Further, the expected future demand of over 100,000 flights per day[18] (just for package delivery in a single metropolitan region) is closer to volumes traditionally handled in road transportation. Hence, it provides a reasonable starting point for further research into evaluating throughput as a metric of airspace productivity for novel air traffic operations.

Intuitively, as inflow into a given airspace increases from zero, the throughput or outflow rate (i.e. number of aircraft traversing and exiting the airspace per unit time) increases as well. However as aircraft begin to excessively impede each other to avoid losses of separation, the traffic becomes congested and throughput decreases. The aircraft must slow down or deviate significantly from their intended path. Since the inflow is maintained and the outflow is reduced, this induces a corresponding rise in accumulation (density) and therefore a loss of steady state in the system. If continued, the system would eventually produce a gridlock. Once steady state is lost (outflow rate thereafter is always less than inflow rate), operating

beyond that regime will be inefficient, even if it is still safe. Therefore, this constrains the useful capacity of the given airspace even further.

In this chapter, we study whether such traffic behavior is actually exhibited by aircraft traversing an airspace. The study is restricted to sUAS traffic but can be extended by changing the modeling assumptions (speed, turn rates, power consumption models, etc) to account for any type of aircraft. We note that even for the chosen type of traffic, since there is no data available on actual aircraft that can enable these future operations, we use a generic power consumption model for our energy consumption evaluation. The model is however flexible to a wide class of capabilities. Hence, our analysis is conducted with a goal to inform future design decisions for these aircraft. Furthermore, capacity and subsequently productivity is a function of technology. Technology dictates the CD&R [59] capability and the allowable minimum separations between the aircraft. Hence, we evaluate this behavior for the two CD&R algorithms, for two different separation minima and use a simulation paradigm to produce the results.

The rest of this chapter is structured as follows. We first present a review of related work that motivates this effort under section 4.2. Section 4.3 lays out our approach in detail. Metrics, CD&R methods and the simulation platform are discussed under section 4.4. In 4.5 we present the results analyzing the throughput behavior exhibited by the CD&R methods at different separation minima and their corresponding energy consumption. Section 4.6 concludes this paper with our findings on airspace productivity.

4.2 Literature Review

The input to an airspace is the traffic density or demand that needs to be met. The airspace design (structure, air traffic management architecture, required on-board technological capabilities, etc.) dictates what portion of the demand is met and how efficiently. The portion of demand that can be met is basically airspace capacity. Intuitively, airspace productivity is the latter.

For traditional manned aviation productivity is dependent on the controller and pilot workload[64, 65, 50, 58]. Given air traffic complexity measures such as MAP[94], the maximum number of aircraft an ATC controller can handle at any given time and DD[62, 84], a weighted summation of factors that affect the air traffic complexity, metrics like the traffic flow rates[9, 10], system and route delays[86, 95], fuel consumption[11] and so on are computed for aircraft operating in a highly structured airspace with monitors, sectors and airways[85, 68, 52, 55]. These productivity parameters are estimated using fast-time and real-time simulation methods [88] in a highly subjective manner biased by the judgment of human air traffic controllers during the experiments, who are also assumed to be the bottleneck of the system.

As stated in the previous chapter, a second approach called the Eurocontrol Care-Integra models the ATM system as a combination of several information processing agents, each with an associated information processing load (IPL) [41]. The system reaches capacity when one of the agents overloads and the loads of all the other agents that capture the system efficiency are the productivity metrics. This is deterministic for machine agents but again needs subjective judgment for human agents. However, it finds the bottleneck in the system instead of assuming it. Road transportation practice uses a third approach that pins down the bottleneck by measuring the change in lane throughput as a function of the freeway traffic density (see Figure 4.1). Associated statistics on average speeds and fuel efficiency (the mpg numbers) are also the productivity measures for the road traffic.

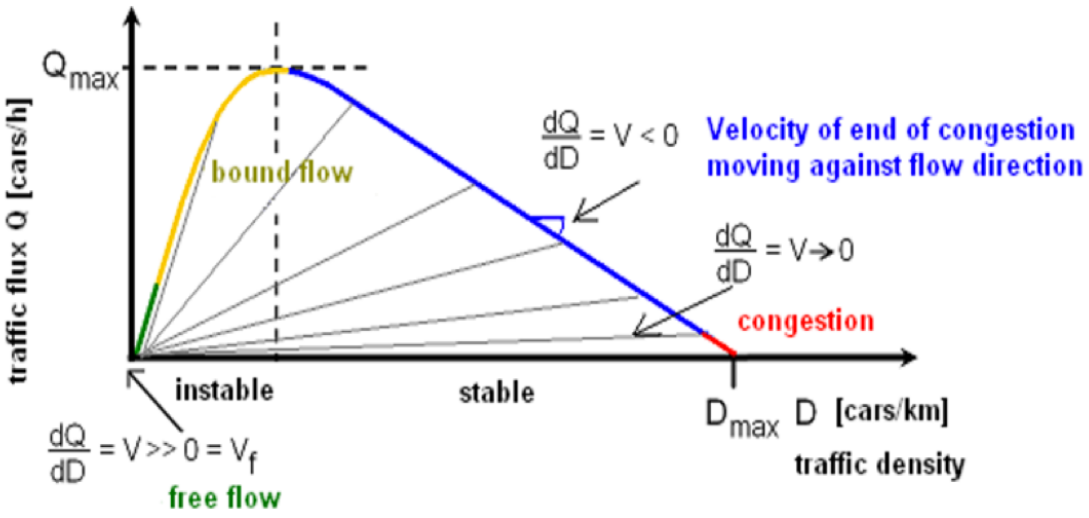

Figure 4.1: Fundamental Diagram of Traffic Flow

Our throughput productivity metric is inspired by the latter two approaches. Further, the fundamental diagram approach was recently studied for highly structured one-dimensional sUAS traffic flow in sky lanes in urban areas and shown to exhibit a threshold behavior[43]. We want to explore if anything similar is exhibited by unstructured free routed traffic in an area (2D) and eventually in an airspace volume in future.

UAM operations [69] may be free flight in nature; i.e. individual flights could be responsible for determining their own courses, independent of a global plan or system. UTM should therefore support user-preferred flight trajectories to the extent possible. Any chosen metrics should account for this. ATM architectures that transfer some of the separation responsibility to the cockpit for manned free flight were researched by Bilimoria et al. as part of their DAG-TM concept[34, 56, 57, 13]. First of all, this work points out that productivity is quite necessary in conjunction with capacity. In spirit, it captures the practical or useful capacity of the airspace. For a given representative area at a particular altitude, the available airspace is defined in [56] as the percentage of that area covered by aircraft with a defined

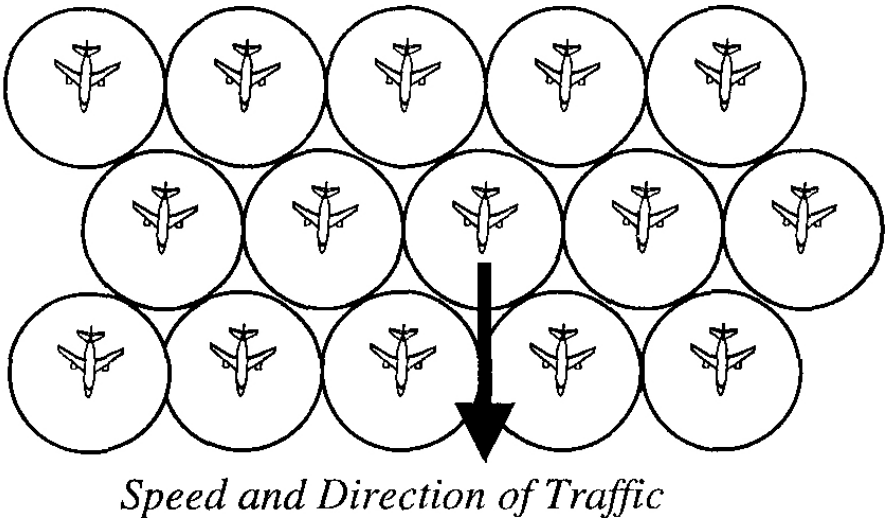

Figure 4.2: Optimal packing allowing only one flow direction [56]

protected zone around them. It establishes a 90.7% theoretical capacity, assuming a minimum separation of 5 nautical miles and under the consideration of a unidirectional uniform speed packing of the aircraft (Figure 4.2). The unidirectional consideration however means not everyone gets from origin to destination resulting in longer routes and hence higher fuel consumption. Hence, although the airspace has a high available capacity, practically it is quite restrictive and inefficient.

More importantly the above work presents Change in Direct Operating Cost as a promising metric to evaluate the airspace productivity for any UTM architecture for free flight. The direct operating cost is further broken down into the time cost (accounts for the effect of delays in trip) and the fuel cost (accounts for the changes in fuel consumption). We therefore focus on these as applicable for UAM operations.

Next comes modeling the on-board CD&R controls. CD&R methods utilized to measure airspace productivity in aviation literature have been primarily developed for large aircraft[59] flying at higher altitudes and lower densities than the expected future sUAS traffic. An example of a simple rule used by Krozel et al.[56] was shown in Figure 3.1. Smaller unmanned aircraft provide a unique opportunity for simpler conflict resolution algorithms. CD&R algorithms for such aircraft have also been extensively developed [59, 75, 89, 81, 49, 51, 66] but their impact has been primarily evaluated on airspace safety. The impact on airspace productivity hasn't been researched as well.

We note that all these methods use either speed control or direction control or a combination of both to ensure safe resolution of conflicts. Furthermore, each also has limits on the complexity of conflicts they can handle. We therefore abstract these two controls and

study their impact on airspace productivity independently. Proposed future operations [8] might primarily be done by aircraft that have VTOL capability and better maneuverability. Under these considerations, we chose two simple CD&R algorithms in this work. We discuss these further under section 4.4.

Owing to the nascency of the UAM industry, there isn't substantial aircraft performance data available unlike manned aviation. In turn, this means a lack of power consumption models for aircraft that will enable this industry. Liu et. al. [63] developed one of the first such models for sUAS. However, the theoretical basis for developing aircraft models and evaluating their power consumption models exists [45, 47, 46, 23]. Short of developing multiple aircraft models and extracting their power consumption curves, we instead use the theory to build a generic set of power consumption curves for a varied class of sUAS.

Finally, we need a simulator that can simulate sUAS traffic densities so that airspace productivity can be studied. Existing simulation and evaluation tools developed for ATM (like BlueSky, TMX, ACES, AEDT, FACET) may not fit for our purposes – they are designed to handle manned-aircraft with a much lower traffic density than our study. They take into account interactions with a variety of actors (air traffic controllers, etc.) that are not needed in low-altitude UTM questions of airspace productivity. The fast-time Fe3 simulator developed by NASA Ames[96] provides the capability of statistically analyzing the high-density, high-fidelity, and low-altitude traffic system. It can be used for effectively evaluating policies and concepts, and performing parameter studies in a higher-fidelity environment like the one in which we are interested. Hence, we use it in conjunction with a simple kinematic model-based Matlab simulator, developed by us as described in the previous chapter. We contributed to the development of Fe3 as part of this research.

4.3 Approach

Airspace productivity is a way of measuring the impact of useful capacity on traffic characteristics like flow rate, travel time and fuel efficiency. Analysis in the airspace capacity chapter and related work[18] suggested that demand for sUAS package deliveries could be as high as 100,000 flights per day in a metropolitan region like the San Francisco Bay Area. A threshold-based definition was used to study these estimates and establish airspace capacity for such a metropolitan region in terms of "flights per day" considering safety[19]. Such a macroscopic approach, although useful for long-term planning and design of an airspace system, may not necessarily provide a direct method of real-time control. On the other hand, the flow density relation is used as a tool to control road traffic by regulating inflow in real time and improve throughput. Hence, if a peak steady state throughput behavior is exhibited by air traffic, a similar air traffic control method could also be explored in future for operating the airspace at or close to capacity without causing any instability in the system.

There is no empirical data on sUAS traffic in the airspace today on which to base our methods. Hence, we start by considering a representative area, subjecting it to increasing steady state inflow rates of air traffic and measuring the mean outflow rate, which we call throughput of the airspace. As long as inflow rate and outflow rates match, we know that there is no build up in the system. However, once the outflow is less than the inflow, air traffic is building up in the system and therefore, sustained inflow will lead to loss of steady state.

It must be noted that for omni-directional free routed air traffic, it is not possible to reproduce an exactly similar behavior as a fundamental diagram for road traffic or sUAS traffic in an air highway. In these two cases, there is a global direction of flow. Hence, the outflow is never obstructed by inflow. In other words, vehicles leaving the system are not obstructed by vehicles trying to enter the system. They may impede or be impeded by traffic already in the system, which in turn could impede further inflow. In figure 4.1, for the blue and red regions, the inflow and the outflow (which is equal to the flux on y axis) are still the same even though the traffic is slowed down. In other words, all the states on the right of the peak are still steady states.

However, in the omni-directional uniformly distributed traffic case, there is no global direction of flow. Subsequently, for a high enough inflow, the outflow begins to be obstructed by the inflow. The trip exit rate then becomes lower than the trip entry rate creating a build up of traffic in the system which continues till the inflow is stopped. As a result the system loses steady state. To explain with the same figure 4.1, once the traffic is in the region beyond the peak, it will no more be in steady state as the density will keep increasing.

We simulate the sUAS traffic over a 0.25 square kilometers representative area. For comparison, this is as big as a 36 square blocks (6x6) region in a residential neighborhood or a similar sized downtown area (see figure 4.3). Two other productivity metrics are evaluated - percentage extension of travel time and mean energy consumption at each inflow rate. We present these in more detail in section 4.4.

We make the following operational assumptions about the aircraft and their operations: (a) All aircraft are sUAS with strictly VTOL capability; (b) Their flight plans are straight line paths from entry to exit on the boundary of the study area. These paths change as aircraft fly through the airspace and avoid conflicts with other aircraft using a given CD&R algorithm; and (c) All sUAS have best endurance and maximum speeds constrained by the capabilities of typical sUAS in use today. Our setup is two dimensional. Any losses of separation are horizontal. We plan to extend this to a volumetric study in the future. The detailed simulation setup and the chosen metrics and CD&R methods are described next.

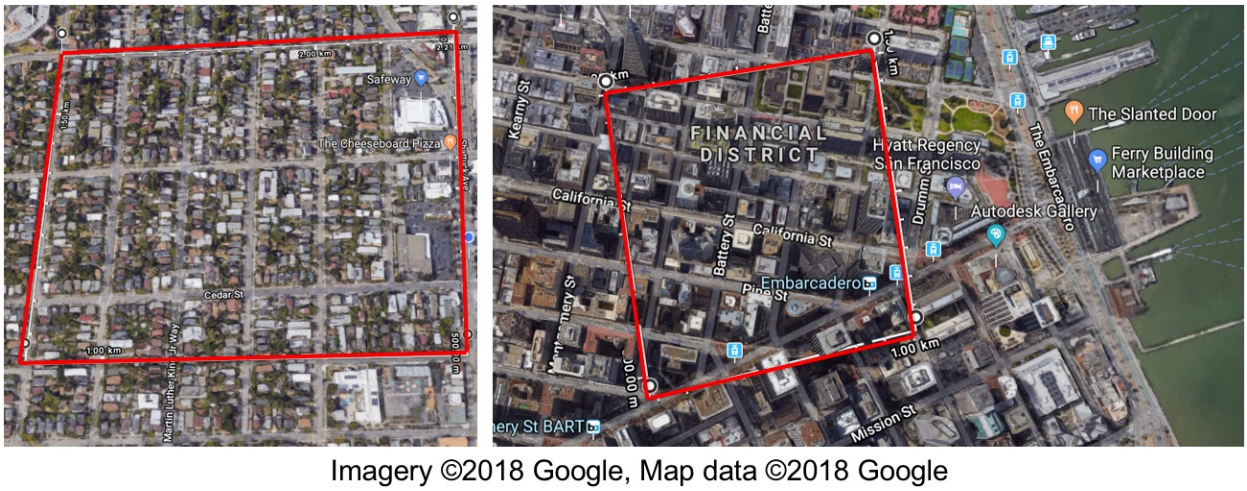

Figure 4.3: Representative area size comparison. Left - 6 x 6 small blocks in residential neighborhood (Berkeley). Right - A substantial portion of the San Francisco financial district.

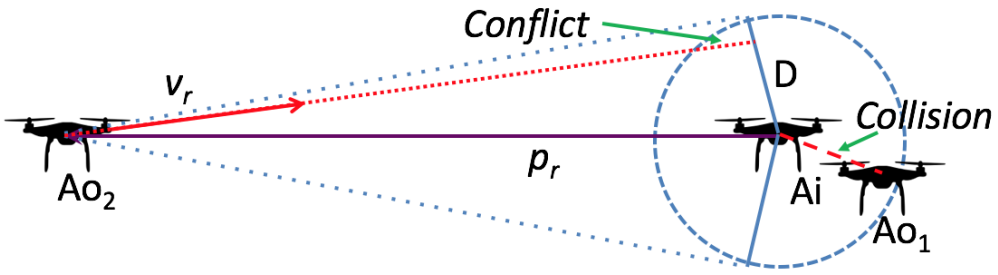

Figure 4.4: Conflict and Loss of Separation. Ao_2 & Ao_2 - Own sUAS, Ai - Intruder sUAS. The aircraft are shown in relative frame of reference

4.4 Simulation

We first restate the notion of a conflict and loss of separation (referred to earlier as a collision) as defined in chapter 3. Any sUAS should stay out of a minimum separation exclusion zone (a disc with radius D) around another sUAS. A loss of separation occurs when two sUAS come within this minimum separation. Given their projected paths in the horizontal plane, if an sUAS is predicted to eventually enter within the minimum separation of another sUAS, the two aircraft are said to be in conflict. Figure 4.4 illustrates a loss of separation occurring between two sUAS. As stated earlier, this means that two aircraft could be potentially in conflict even if they are too far apart to matter. Hence, we pick a detection range for each CD&R as a multiple of the minimum separation required for detecting and avoiding an intruder sUAS. This detection range is the parameter that we adjust in our simulation to ensure that the losses of separation for the two CD&R methods begin to occur with high

probability at similar inflow rates. Hence, they are adjusted to be equally safe.

We make the following additional assumptions. All aircraft are assumed to have the capability to hover and a maximum turn rate constraint of 6° per second. The turn rate assumed is twice the standard rate turn in manned aviation owing to the expected high maneuverability of future sUAS. The best endurance flight speed is assumed to be 30 ms^{-1} with a maximum value of 45 ms^{-1}. This is again based on the FAA part 107 regulations that restricts under 400 feet operations to a maximum speed of under 45 ms^{-1}. The sUAS in the simulator fly at the best range speed by default. The maximum acceleration that today's sUAS can achieve is about 2g. If 1g is used to overcome the weight, close to 1g is available for horizontal maneuvers while keeping the aircraft in safe operational limits. To avoid pushing aircraft to their maximum capability all the time, we limited the maximum acceleration/deceleration to 0.5g. The origins and destinations of aircraft are uniformly distributed along the edges of the representative area and are spaced such that two aircraft aren't forced to enter or exit within loss of separation distance of each other. These are randomly connected to form the flight paths such that no aircraft has an origin and destination on the same edge. This ensures that every aircraft enters the study area. Finally, we estimate the different metrics for two different separation minima - 5m and 10m.

We varied the inflow rates of the sUAS from one per minute to a hundred and twenty per minute. At each inflow rate, 1000 simulations were run to compute the metrics.

Metrics

Throughput/Outflow Rate

Our first metric - *Trip Exits per min* captures the average traffic outflow rate through the area (i.e. throughput). Measuring trip exits per second would be too small to capture substantial intended boundary crossings and measurements over an hour would be too long to provide any real-time control over an area.

Safety

Safe operation of the airspace is of utmost importance. Following the proposed requirements by MITRE[67] and its use in our prior macroscopic capacity estimation study, we choose the necessary safety metric as the *Total Losses of Separation* observed over the simulation interval. This metric is only used to tune the two CD&R to be equally safe and no further detailed analysis is done on this.

Extension of Travel Time

Both slowing down and taking longer routes for safety, increase travel times thereby affecting the system's productivity. We capture this by measuring the *Percentage Extension of Travel*

Time. This is a direct derivative of the *Change in Direct Operating Cost* as proposed by Krozel et al.[56].

Relative Energy Consumption

Any CD&R approach will deviate an aircraft from its intended flight trajectory, either in space, time or both. Assuming the aircraft is already flying at its best range speed (energy optimal), any such deviation would increase the total energy consumption. Hence, the increase in energy consumption of all flights in an airspace is another measure of the airspace productivity.

Measuring this is straight forward if the performance data of the aircraft is known. For commercial manned aviation, such data is readily available (for example - Eurocontrol's Base of Aircraft Data (BADA) and International Civil Aviation Organization (ICAO) Engine Exhaust Emissions Data Bank). However, there is a dearth of such data for aircraft that can enable UAM operations. Even models in literature for such aircraft are rather few. Approaches either develop models for individual rotors[2] or for small model aircraft[72, 79] at very low speeds[39] not necessarily adequate for UAM operations under consideration in this work. Liu et. al. [63] provides a model for an actual multicopter sUAS. The authors in [76] develop a theoretical power consumption model for a small convertible UAV that can be operated both in a hover and cruise mode utilizing the benefits of the two designs. We use insights from [63, 76], the theory on aircraft power consumption models [45, 47, 46, 23] and inputs from subject matter experts to develop a representative range of power consumption curves (figure 4.5) to cover a wide range of potential sUAS designs.

These curves are generated using 3 parameters. First parameter is the Best Endurance Speed (S_{BE}) (minimum power consumption). We assume this to be 30 ms^{-1}. For reducing time of flight, sUAS are expected to fly as fast as possible with some cushion for emergencies. With a maximum allowable low-altitude speed of under 45 ms^{-1}[27], we assume sUAS will be designed for a S_{BE} of at least two-thirds of it (30 ms^{-1}). The second parameter is the Power consumption at Hover (P_H). Based on insights from the above literature, we assume this to vary between 1.5 to 3 times the minimum power (We chose 4 values - 1.5, 2,2.5 and 3) . The third parameter is the power consumption at a cruise speed one and half times the endurance speed (P_{max}). Again based on theory and expert recommendation, we assume a variation between 1.5 to 2 times the minimum power consumption (We chose 3 values - 1.5, 1.75 and 2). For speeds between zero and S_{BE}, we assume a spline interpolation between P_H and minimum power (P_{min}) . For cruise speeds beyond S_{BE} power consumption growth will be at least quadratic [45]. The set of curves developed are shown in figure 4.5.

Since power is used as a multiple of minimum power, our energy consumption metric is also measured relative to the minimum energy for an sUAS trip. We assume that all sUAS in the simulation fly at their Best Range Speed (S_{BR}). On the power consumption curves, this

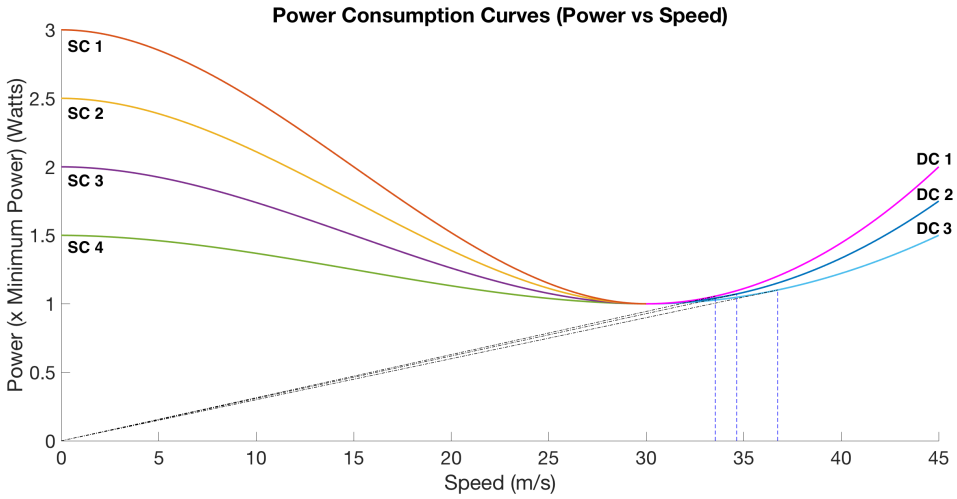

Figure 4.5: Power consumption curves. SC - used for Speed Control. DC - used for Direction Control. Minimum Energy lines - dashed black. Best Range Speed - dashed blue

is the point where the slope of the curves, to the right of best endurance speed, is minimized. Minimum energy consumed is therefore calculated from the sUAS shortest path from origin to destination. The best range speeds and their associated power consumption values are listed in table 4.1.

Table 4.1: Best Range Speed and Power Consumption

Curve (**Right of** $S_{BE} = 30ms^{-1}$)	**Best Range Speed** (ms^{-1})	**Best Range Power** (**X** P_{min})
DC 1	33.54	1.06
DC 2	34.65	1.07
DC 3	36.74	1.10

For direction control simulations, the sUAS fly at their best endurance speeds and only change direction to avoid other sUAS. The relative energy consumption therefore only depends on the extra distance travelled. Furthermore for the three power curves for direction control, the S_{BR} values are so close to each other that the extra distances travelled in our simulations were also very similar at least till the peak steady state flow was reached. Therefore for all our simulations, we picked their average (35 ms^{-1}) as the S_{BR} and used the DC 2 curve for the energy computation.

TO summarize, our fourth airspace productivity metric is *Relative Energy Consumption* measured relative to the minimum energy consumption. This metric is also a direct derivative of the *Change in Direct Operating Cost* as proposed by Krozel et al.[56].

CD&R methods

Approaches to CD&R may be broadly classified into three categories - force field based, trajectory projection based[22, 73] and offline look-up table-based[70]. However all of them use a combination of only two types of control, namely speed and direction. We therefore chose two simple CD&R methods that capture each of the two types of control and can together encompass most types of aircraft. This makes them flexible for future extensions of this study to different classes of aircraft.

First CD&R is avoidance by slowing down to hover and then speeding back up to the energy optimal speed when clear. This captures the effect of pure speed control and encompasses aircraft that can stop in flight. It uses a trajectory projection-based approach. Second is a pure direction control where the sUAS can only turn without changing speed. This is also a trajectory projection approach. Using the relative frame of reference as per figure 4.4, we know the direction of the sUAS when it is in conflict. To avoid the intruder, the minimum required manuever should make the own sUAS fly tangentially to the intruder's separation exclusion disc. This gives us the position and direction of the sUAS at that point. We generate the dubins path between these two states in the simulator constrained by the maximum turn rate and the sUAS flies that path. This is extendable to all aircraft with a stall speed constraint.

We used a kinematic model-based simulator in Matlab as described in chapter 3 to study the throughput behavior for speed and direction control. We only present these kinematic results in this chapter. In future, we propose to extend our study to dynamic aircraft models as implemented in the fast-time simulation platform Fe3[96]. Fe3 also incorporates vehicle communication and sensor models and wind models and other essential functionality necessary for a high fidelity verification. However, for this work we only used it as a good visualization tool (e.g. - see figure 4.6).

4.5 Results

In this section, we present our results for all the airspace productivity metrics. In all the figures, solid line and dotted line represent 5 meters and 10 meters minimum separation, respectively, unless stated otherwise. The black dash-dot line in all the figures is the steady state line (outflow rate = inflow rate). First, we describe the throughput metric in comparison with the safety metric. Figures 4.7 and 4.8 show the variation of throughput or the average area outflow rate measured as Trip Exits per min (plotted in blue) for speed control and direction control respectively. The losses of separation (plotted in orange) measured at each inflow rate are also plotted (on the right y axis) to show their variation along with throughput as the inflow rate is increased.

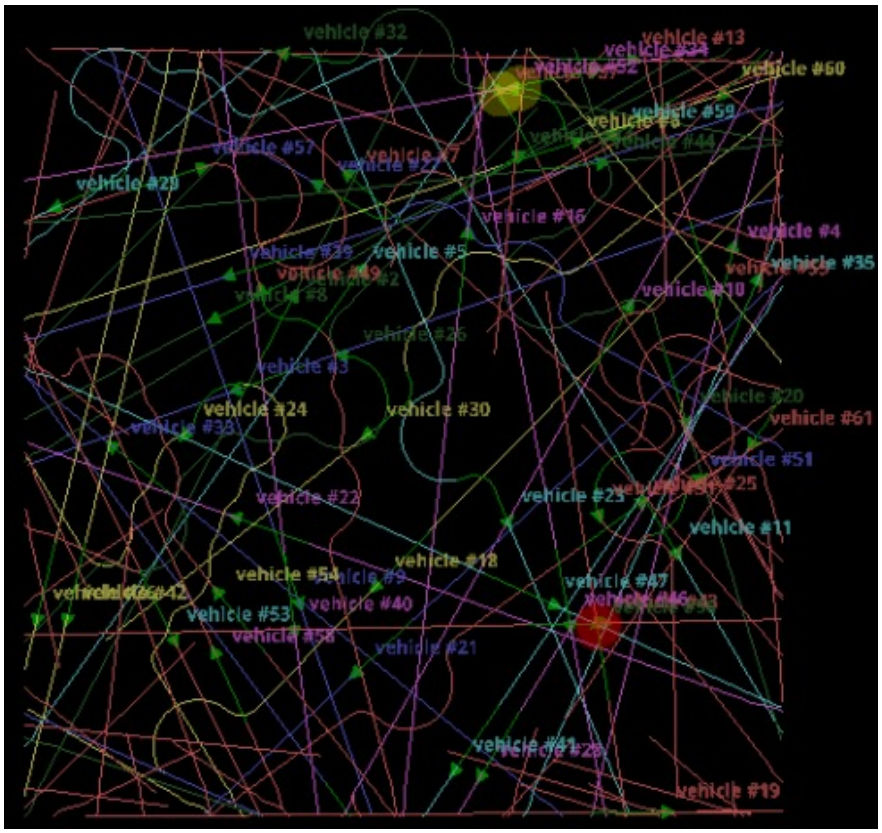

Figure 4.6: A sample visual of simulation with direction control in the Fe3 visualization tool. Traffic shown for first 3 minutes at an inflow rate of 20 flights/min.

At 10 m minimum separation, the outflow rate becomes less than the inflow rate beyond roughly 36 flights/min. The system therefore loses stead state. When the tolerance is higher at 5 m (smaller minimum separation), the best steady state outflow rate is also higher at 40 flights/min as the aircraft can be safely packed closer together. The airspace in the representative area therefore should not be operated beyond these rates. We also observe that similar throughput is achieved by both speed and direction control. They both perform equally well at keeping the airspace safe up till the best steady state flow. At 5 m separation, neither of them show any losses of separation on average. At 10 m separation, both speed and direction control cause around 2 losses of separation on average. The losses of separation rise rapidly beyond the steady state flow making the airspace quite unsafe.

These trends are further explained as follows. Speed control slows down aircraft to a stop without deviating them from their trajectory. Hence beyond peak steady state flow, first there is an excessive slowdown that reduces the throughput. Next, as more aircraft begin to stop while the inflow is still maintained, several aircraft don't have enough distance/time to stop safely. Hence, they start entering each others' minimum separation distances, especially

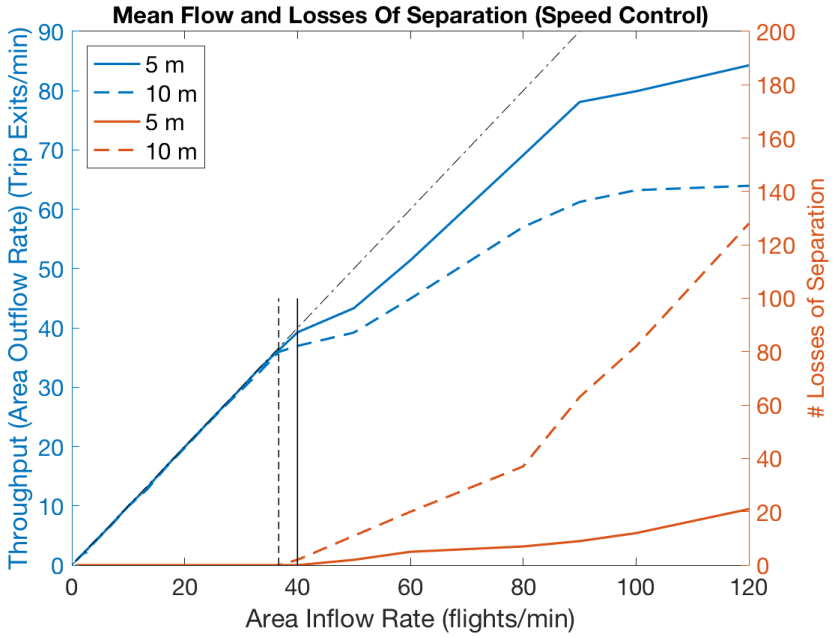

Figure 4.7: Throughput and Safety for Speed Control. Vertical lines indicate the peak steady state inflow rate.

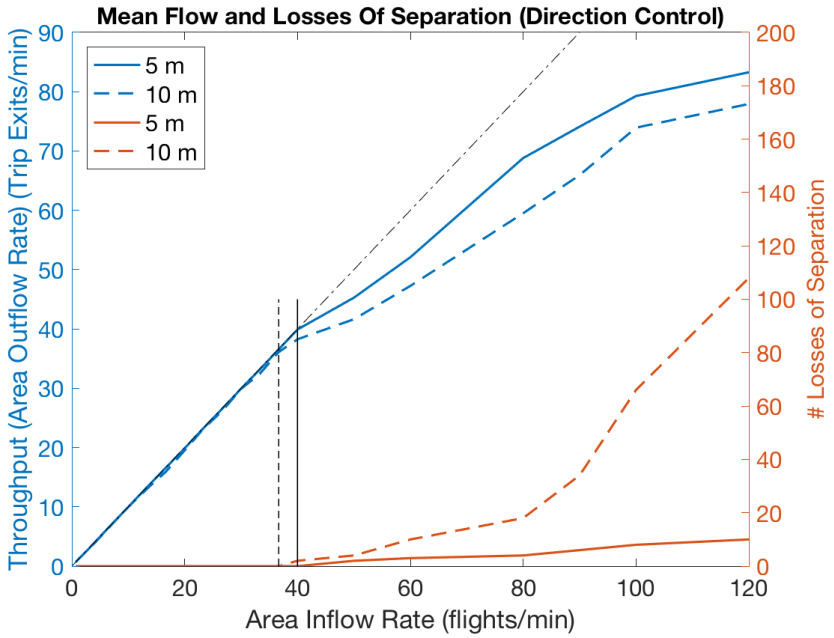

Figure 4.8: Throughput and Safety for Direction Control. Vertical lines indicate the peak steady state inflow rate.

closer to the boundaries. The number of losses of separation rises fast and exit rates continue to fall. However, the aircraft within separation minima are either stopped or moving very slowly. This is comparable to a jam on a freeway where cars are bumper to bumper but not crashing into each other. Hence, although operation in this regime is not in steady state, it is not necessarily unsafe. With direction control, higher minimum separation implies more deviation from the intended path. The losses of separation rise rapidly beyond peak steady state because excessive aircraft have accumulated in the system and the deviations start to overwhelm the aircraft operation limits.

Next, we compare throughput against the mean percentage extension of travel time in figures 4.9 and 4.10. Here speed control performs better than direction control. For 5 m separation, at best steady state flow, speed control extends the travel time by 1.6 percent on average compared to 6.9 percent for direction control. At 10 m separation the difference is even more pronounced. Direction control extends travel time by 13.7 percent compared to 1.34 percent for speed control, at the corresponding best steady state flow.

Once the system loses steady state, we observe that the travel time extension rises rapidly, for both speed and direction control. However for direction control it happens much faster. This could be explained by the fact that with pure direction control, sUAS are constantly moving without getting closer to the destination. With speed control, the sUAS are possibly hovering close to their destination till they can exit.

Finally we compare the relative energy consumption. For direction control we use the power consumption values from the DC 2 curve in figure 4.5. We note that below the peak steady state, both DC 1 and DC 2 produced similar energy consumption values as their best range power consumption values are very similar. Hence, we use only one direction control curve for comparison with the other four speed control energy measurements. The four speed control power curves produce visibly dispersed energy curves because the hover powers for each curve are quite spread apart.

First, we analyze the 5 m separation case as shown in figure 4.11. At and below the peak steady state flow, direction control has similar relative energy consumption as speed control with the most efficient power curve ($P_H = 1.5P_{min}$). This implies that if the sUAS has a highly efficient hovering capability, both speed and direction control perform equally well. Otherwise, direction control improves the airspace productivity (based on energy consumption) more than speed control.

Next, we study the 10 m separation case as shown in figure 4.12. Here the trend begins to change. At and below the peak steady state flow, speed control performs better if the sUAS has a highly energy efficient hovering capability ($P_H = 1.5P_{min}$). Otherwise, direction control is better than speed control. This difference is clearer in the zoomed in versions of these figures shown in figure 4.13. The specific relative energy consumption for the 5 m and

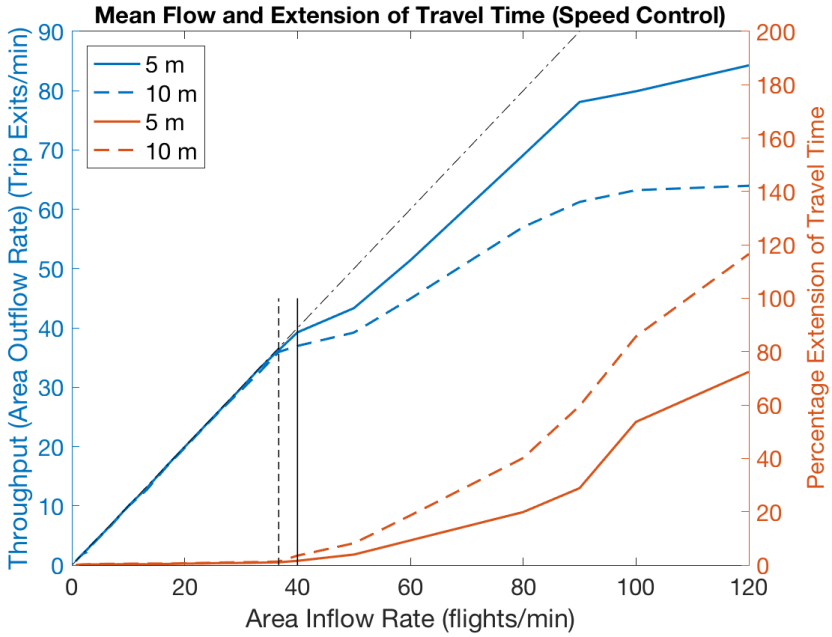

Figure 4.9: Throughput and Extension of Travel Time for Speed Control. Vertical lines indicate the peak steady state inflow rate.

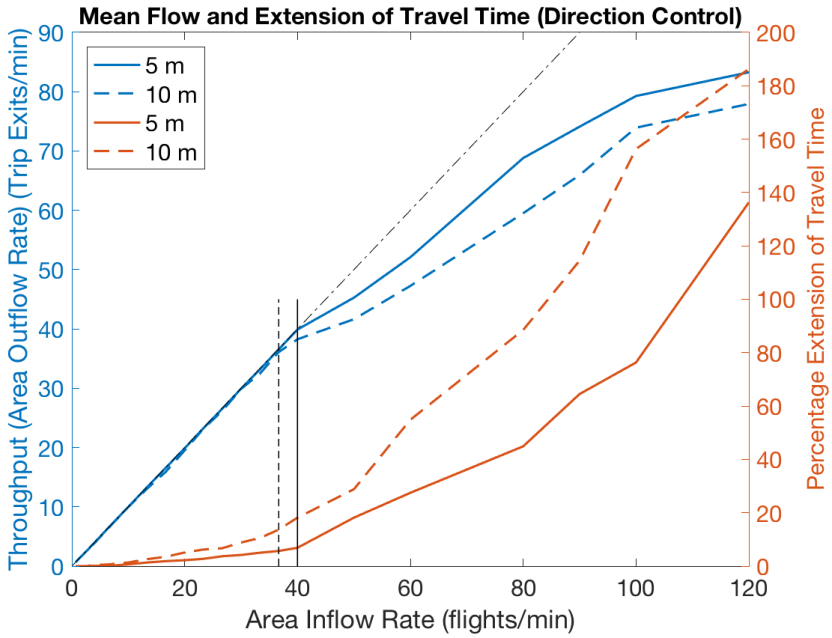

Figure 4.10: Throughput and Extension of Travel Time for Direction Control. Vertical lines indicate the peak steady state inflow rate.

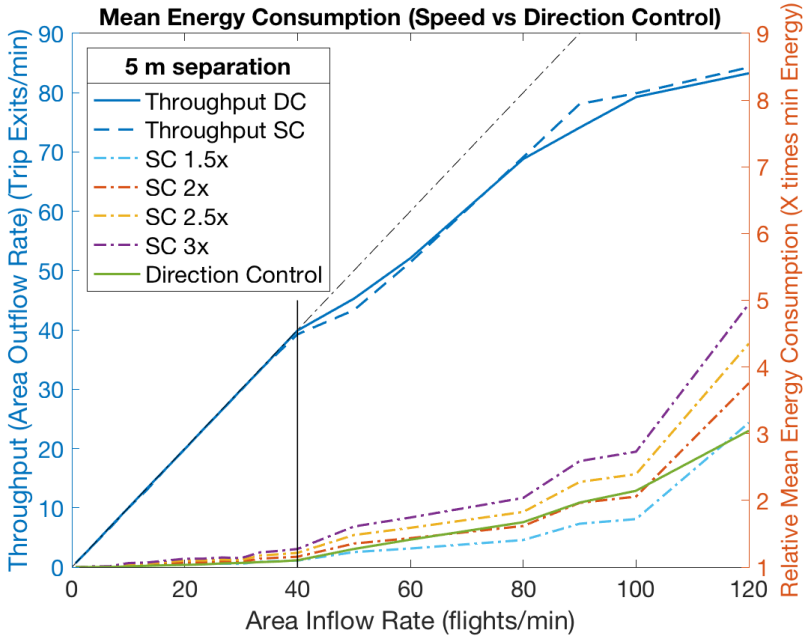

Figure 4.11: Throughput and Relative Energy Consumption for 5 m minimum separation. SC - Speed Control. DC - Direction Control. Vertical line - peak steady state inflow rate.

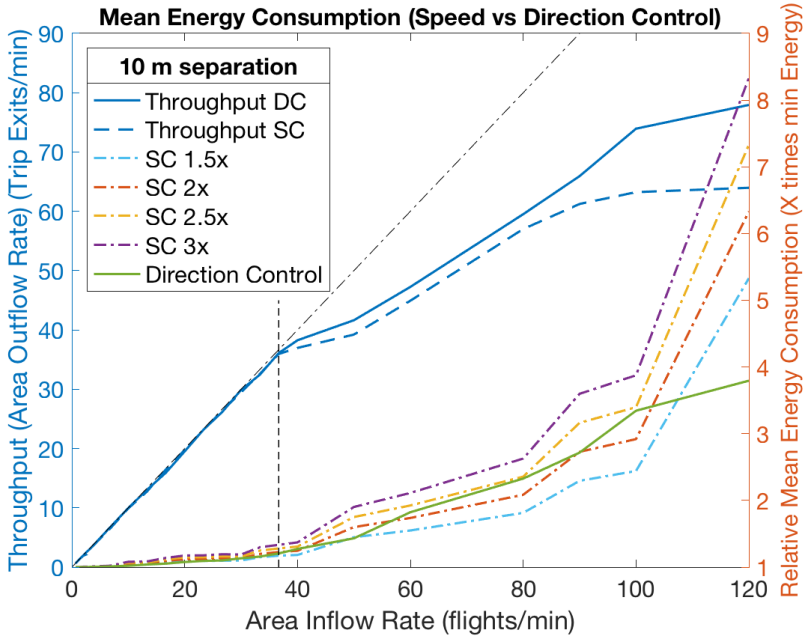

Figure 4.12: Throughput and Relative Energy Consumption for 10 m minimum separation. SC - Speed Control. DC - Direction Control. Vertical line - peak steady state inflow rate.

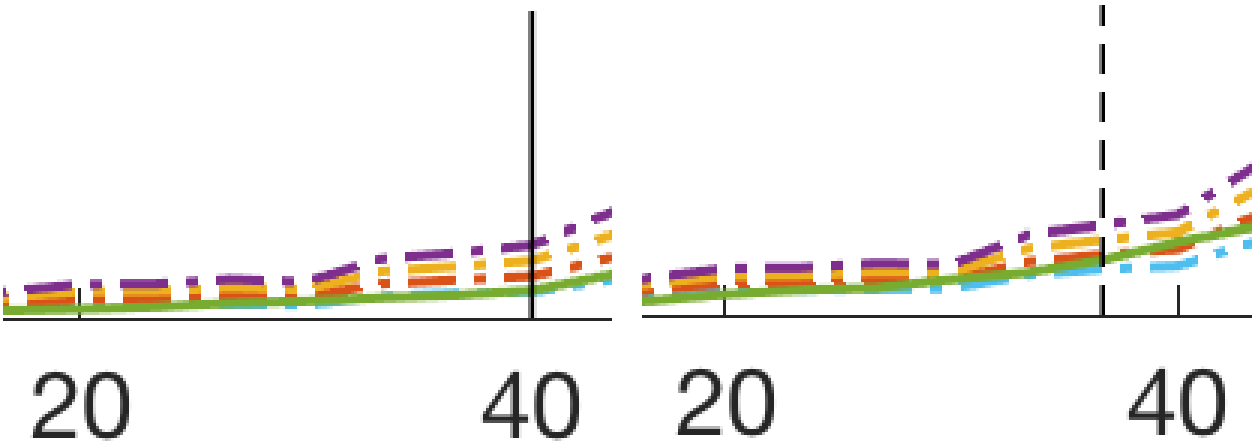

Figure 4.13: Zoomed in portions of figures 4.11 and 4.12 showing the differences in relative energy consumption near peak steady state flow. Left - 5 m separation. Right - 10 m separation.

10 m separation cases are listed in table 4.2.

Table 4.2: Relative Energy Consumption (x Min. Energy) at Peak Steady State Flow

Minimum Separation	**Direction Control**	**Speed Control ($P_H = kP_{min}$)**			
		k=1.5	**k=2**	**k=2.5**	**k=3**
5 m	1.10	1.10	1.16	1.21	1.27
10 m	1.20	1.17	1.22	1.28	1.33

Overall, we observe the following trends. Speed control and direction control produce similar throughput measured as peak steady state outflow rate when designed to be equally safe. At or below peak steady state, with respect to extension of travel time, speed control is better than direction control. However, when compared for their relative energy consumption, direction control beats speed control unless the sUAS have a highly efficient hovering capability.

4.6 Conclusions

We have evaluated two conflict detection and resolution approaches - pure speed control and pure direction control; and quantified their impact on airspace productivity using three types of metrics - throughput, travel time extension and energy consumption. We simulated sUAS traffic in low-altitude airspace over a representative square area and computed the above metrics at different inflow rates and two separation minima - 5 meters and 10 meters. We also utilized a representative generic power consumption model to capture the energy consumption of an sUAS with both kinds of control.

Our results show that at 10 m separation, speed control and direction control reach similar peak steady state at an inflow rate of 36 flights/min. This is improved further to 40 flights/min at a lower minimum separation of 5 m. Both controls are equally safe producing 2 or less losses of separation on average at peak steady state.

Speed control performs better on average in terms of extension of travel time with a saving of five percent over direction control at 5 m separation. The average time saving improves to over twelve percent at a higher minimum separation of 10 m. However, direction control outperforms speed control in terms of energy savings unless the sUAS have a highly efficient hovering capability.

Since the industry envisions an electric sUAS future, energy is more crucial than travel time because of the impact on battery weights. Hence, there would be a natural inclination towards utilizing the more energy efficient control. This suggests that direction control will be more preferred than speed control as an enroute CD&R approach. However, it is also desirable to incorporate speed control as an emergency feature for contingencies.

Therefore, to summarize the findings on airspace productivity and answer the opening question of the chapter - While airspace remains uncongested, without compromising safety, both direction control and speed control are equally good for under 400 feet goods movement, unless the sUAS are designed to be highly efficient while hovering, If the sUAS have a hover power consumption that is equal to or less than one and a half time the minimum power consumption, speed control increases airspace productivity more than direction control.

Chapter 5

Conclusion

Advancement and innovation in aircraft design over the past century has placed air transport as a potential competitive alternative to road, for hub-to-door and door-to-door urban services. In this dissertation, we evaluated that potential by studying the feasibility, capacity and productivity of the urban airspace. First, we measured the feasibility of air vs road for passenger and goods movement using three metrics - travel time, fuel cost and CO_2 emissions. Second, we measured the capacity of under 400 feet low-altitude urban airspace to move goods via free routed sUAS traffic constrained by safety. Third, we evaluated a pure speed control based CD&R against a pure direction control based one and quantified their impact on airspace productivity measured by three metrics - throughput, extension of travel time and energy consumption.

The airspace feasibility study suggests that air performs at par or better than road. For passenger movement, air is faster than road for all distances over a mile. Electric air movement fares better than gasoline road movement, on fuel cost and emissions, only for longer distances (specific transition distances are based on the circuity factor and are stated in chapter 2). For consolidated movement of goods also, electric air movement is at par or better than diesel delivery trucks, even after accounting for the increase in travel distance from the dis-aggregation effect of flying individual packages. Finally, for movement of unconsolidated goods, air again fares better than road on all three metrics.

The value of the above benefits to a consumer will however vary based on individual preferences and is a good direction for further exploration. For example, a 33 min time saving (produced by uncongested air against uncongested road with a circuity factor of 1.20) could be valued differently based on whether it is a work or leisure trip. When it is valued high, the consumer's willingness to pay will determine how much overhead costs can be tolerated by an air service provider, in addition to the fuel costs. A similar analysis would then be needed for comparing direct operating costs of air vs road.

It is also noteworthy that these benefits are in an urban area designed today to be highly efficient for road travel. What if the cities of tomorrow were designed to be highly efficient for movement by both air and road or just air? This dissertation therefore also motivates exploring newer urban designs and policy changes that support UAM. There are examples of cities which have already redesigned themselves to sustain non-automobile travel modes. Amsterdam (figure 5.1) in the Netherlands was redesigned to accommodate bike travel. Giethoorn in the same country, developed itself around canals instead of developing roads. Even redesigning for air is not that far fetched an idea as proven by the already developed fly in community at Spruce Creek, Florida (figure 5.3).

Figure 5.1: Roads in Amsterdam, Netherlands redesigned for bike travel

The airspace capacity chapter presents a threshold based approach to estimate capacity. Using a simulation paradigm, we estimated capacity for goods movement at or under 400 feet AGL altitude given a required level of safety. Based on a vertical avoidance CD&R algorithm, we estimated that around 10,000 free routed sUAS flights/day can be enabled in the San Francisco Bay Area low altitude airspace. Automated aircraft and air traffic management could vastly improve this capacity. Other metrics can be incorporated in our capacity estimation approach in future. A sample application for noise was studied in [16]. As more empirical data becomes available and better models of suitable airborne technologies

Figure 5.2: Houses in Giethoorn, Netherlands connected by canals instead of roads

Figure 5.3: Fly in Community - Spruce Creek, Florida, USA

are developed for future UAM operations, more theoretical approaches can be developed to substitute or compliment our simulation based study. As an example a sampling based

approach to speed up and diversify our simulation set up was explored in [82].

In the same chapter, we proposed conflict cluster size as an architectural separator between UTM and on-board CD&R. It determines the computational complexity (that acts as the unmanned surrogate for manned pilot and controller workload) of many CD&R algorithms. Air traffic management strategies that keep the cluster sizes low are useful to explore further. For example, we studied the impact of decentralized ground delay strategy on increasing the airspace capacity by decreasing the frequency of large clusters via ground delay[17]. We also explored how a simple airway structure can vastly reduce the complexity (see figure 5.4).

Our study ignored the impact of airspace constraints, static and dynamic obstacles and wind. Another area for exploration is therefore to incorporate each one of them. As a first step, a geometric approach to evaluate available airspace was explored as part of an international joint research collaboration recently[92]. We also note that although we focused on the low-altitude goods movement traffic, our approach and methods developed in this dissertation can be extended to other operations (both goods and people movement) spanning a wider section of airspace. It will have to incorporate the appropriate aircraft models, operational requirements and models of suitable technological capabilities, as and when they are better understood and developed with the progress of the UAM industry.

The airspace productivity analysis shows that direction control is more suitable than speed control for tactical resolution. We measured the impact of the two controls on productivity using the metrics - throughput, extension of travel time and relative energy consumption. Adjusted to be equally safe, both produced a peak steady state throughput of around 36 flight exits per minute from a 0.25 square kilometer area with a 10 m requirement on minimum separation. Relaxing the separation to 5 m improved that to 40 flights/min. At peak steady state flow, compared to direction control, speed control saved five percent and twelve percent more time at 5 m and 10 m separation, respectively. However, direction control consumes at least five percent less energy than speed control for either separation, unless the hover power consumption is at most one and a half times the minimum power consumption. In other words, unless the aircraft are designed to be highly efficient when slowing down to hover, direction control is better.

In our analysis, speed control doesn't produce any horizontal path deviations by design (although there are some vertical deviations as head on conflicts are assumed to be resolved vertically while slowing down). But direction control does deviate aircraft from their intended flight path horizontally. As a consequence, aircraft can get outside the study area, especially at the edges and then come back in. Although these exits and entries are not accounted for in the system inflow and outflow rates, they still imply that unlike speed control, direction control may require extra horizontal buffer airspace to operate effectively. Hence, the need and magnitude of such buffer airspace is worth exploring in future.

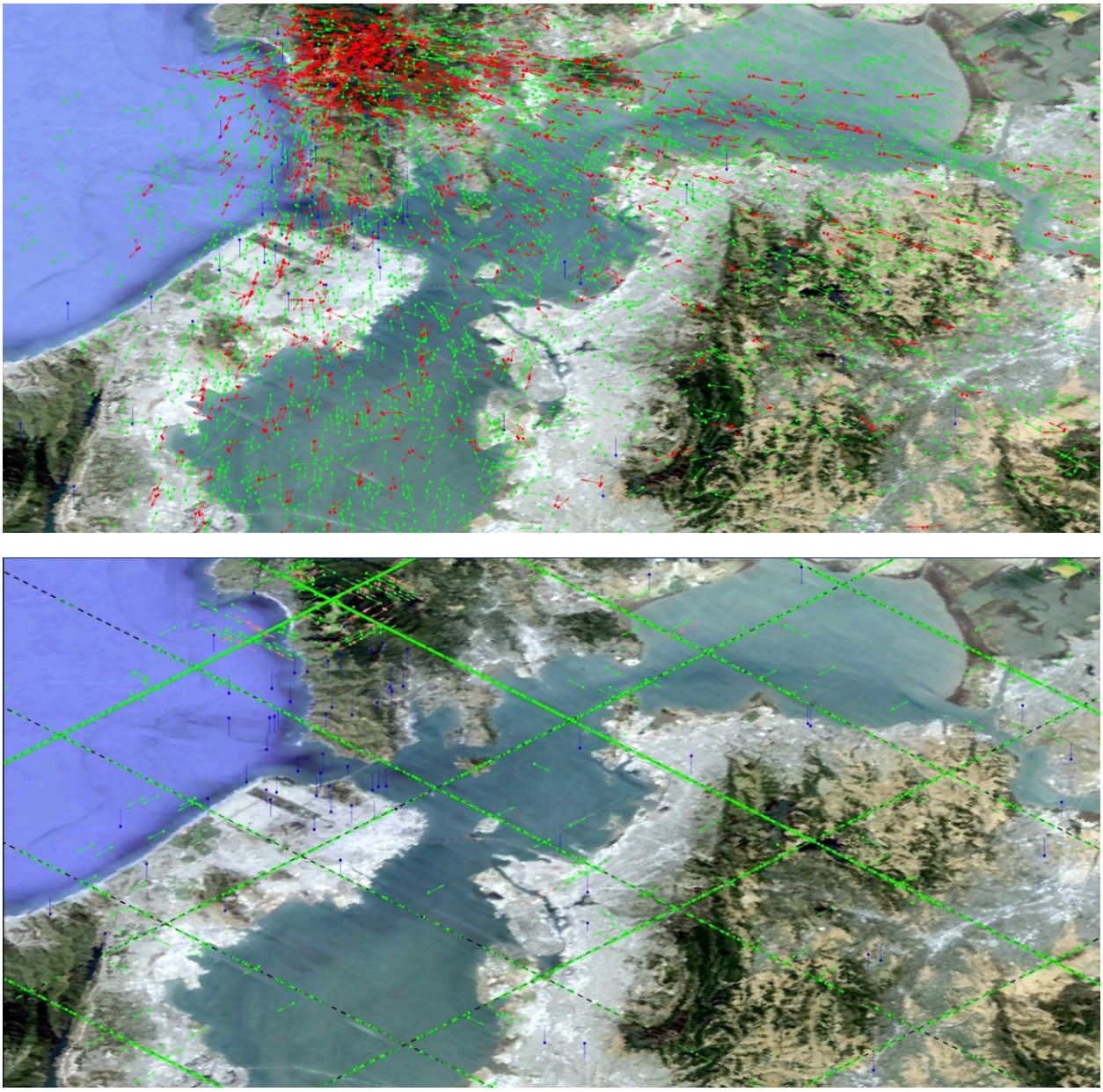

Figure 5.4: Zoomed perspective view of 100,000 sUAS flights/day over San Francisco Bay Area. Top - Free routed. Bottom - Structured. sUAS inside highways assumed procedurally separated even when densely packed. Arrow colors: Green - sUAS in flight, Blue - sUAS taking off or landing, Red - sUAS within conflict distance, Pink - sUAS within conflict distance outside the aerial highways but on parallel trajectories.

Our findings have implications for research in aircraft design to enable UAM operations of future. Three UAS designs are widely being explored owing to their maneuverability - multicopter, vectored thrust (tilt wing or tilt rotor) and lift + cruise (separate propellers for lift and cruise). Our findings suggest that the latter two are better suited for improving airspace productivity. Wings provide a higher lift to drag ratio than rotors and can attain higher speeds at lower power while being capable of direction control. The extra hover/slowing down capability provided by the latter two designs is useful for contingencies and is also operationally more suitable at terminals than enroute airspace.

Further, we also provide a paradigm to evaluate airspace design and air traffic management strategies. Those which improve the airspace productivity are more suitable. The methods and metrics used can therefore be extended to compare air traffic management architectures and more complex CD&R algorithms, thereby having an important role to play in establishing the right policies for urban airspace.

To summarize the findings of this dissertation we respond to the research questions raised in the introduction:

1. Is Air a feasible option for hub-door and door-door services of today?
   A: Yes, it fares at par or better than roads on travel time, fuel cost and CO_2 emissions, *if airspace is uncongested.*

2. When can airspace get congested in a metropolitan region? In other words, what is the metropolitan Airspace Capacity?
   A: Depends on the operational requirements and technological capabilities. For example - 10,000 free routed sUAS flights per day are possible in the low-altitude San Francisco Bay Area airspace for goods movement at or under 400 feet AGL altitude.

3. While airspace remains uncongested, what type of airborne control increases productivity without compromising safety? Is Speed control better or Direction control?
   A: Both are equally good but direction control is more preferable unless aircraft can be designed with high hover efficiency (Hover power $\leq$ Minimum power consumption.)

This work finds that air is indeed a competitive alternative to road for urban services. The UAM industry and research are primed to support the next revolution in urban transportation. For a metropolitan airspace such as the San Francisco Bay Area, the potential exists for a day, when there are far more aircraft in the urban airspace, than boats in the bay, if not more than cars on the highway (figure 5.5).

Figure 5.5: San Francisco Bay Area metropolitan airspace today.
A vast potential for the UAM revolution!

Bibliography

[1] US Environmental Protection Agency. *Light-Duty Automotive Technology, Carbon Dioxide Emissions, and Fuel Economy Trends: 1975 Through 2017 – Executive Summary*. `https://www.epa.gov/fuel-economy-trends/download-report-co2-and-fuel-economy-trends`. 2018.

[2] Dmitri Aleksandrov and Igor Penkov. "Energy consumption of mini UAV helicopters with different number of rotors". In: *11th International Symposium Topical Problems in the Field of Electrical and Power Engineering*. 2012, pp. 259–262.

[3] Juan J Alonso et al. "System-of-Systems Considerations in the Notional Development of a Metropolitan Aerial Transportation System.[Implications as to the Identification of Enabling Technologies and Reference Designs for Extreme Short Haul VTOL Vehicles With Electric Propulsion]". In: (2017).

[4] Kevin R Antcliff, Mark D Moore, and Kenneth H Goodrich. "Silicon Valley as an Early Adopter for On-Demand Civil VTOL Operations". In: *16th AIAA Aviat. Technol. Integr. Oper. Conf.* 2016, pp. 1–17.

[5] *ArcGIS USA Population Density*. `https://www.arcgis.com/home/index.html`. 2016.

[6] USA Argonne National Laboratory - Lemont Illinois. *GREET Net Database*. 2018.

[7] Ronald H Ballou, Handoko Rahardja, and Noriaki Sakai. "Selected country circuity factors for road travel distance estimation". In: *Transportation Research Part A: Policy and Practice* 36.9 (2002), pp. 843–848.

[8] A. Barr and G. Bensinger. *Google Is Testing Delivery Drone System*. Wall Street Journal. Aug. 2014.

[9] Alexandre M Bayen, Robin L Raffard, and Claire J Tomlin. "Adjoint-based control of a new Eulerian network model of air traffic flow". In: *IEEE transactions on Control systems technology* 14.5 (2006), pp. 804–818.

[10] Alexandre Bayen et al. "Langrangian delay predictive model for sector-based air traffic flow". In: *Journal of guidance, control, and dynamics* 28.5 (2005), pp. 1015–1026.

[11] Alexandre Bayen et al. "Optimal arrival traffic spacing via dynamic programming". In: *AIAA Guidance, Navigation, and Control Conference and Exhibit*. 2004, p. 5228.

[12] Karl D Bilimoria and Hilda Q Lee. "Analysis of aircraft clusters to measure sector-independent airspace congestion". In: *5th Aviation, Technology, Integration, and Operations Conference*. 2005.

[13] Karl D Bilimoria et al. "Performance evaluation of airborne separation assurance for free flight". In: *Air Traffic Control Quarterly* 11.2 (2003), pp. 85–102.

[14] Thomas B Billingsley, LP Espindle, and J Daniel Griffith. "TCAS multiple threat encounter analysis". In: *Massachusetts Institute of Technology, Lincoln Laboratory, Project Report ATC-359* (2009).

[15] V. Bulusu and V. Polishchuk. "A Threshold Based Airspace Capacity Estimation Method for UAS Traffic Management". In: *IEEE Systems Conference*. 2017.

[16] V. Bulusu, L. Sedov, and V. Polishchuk. "Noise estimation for future large scale small UAS operations". In: *NOISECON*. 2017. URL: `http://unmanned.berkeley.edu/#publications`.

[17] Vishwanath Bulusu, Leonid Sedov, and Valentin Polishchuk. "Decentralized self propagating ground delay for UTM: Capitalizing on domino effect". In: *Integrated Communications, Navigation, and Surveillance Conference, I-CNS*. **Best Track Paper and Best Conference Paper**. 2017.

[18] Vishwanath Bulusu, Raja Sengupta, and Zhilong Liu. "Unmanned Aviation: To Be Free or Not To Be Free? A Complexity Based Approach". In: *7th International Conference on Research in Air Transportation*. 2016.

[19] Vishwanath Bulusu et al. "Capacity estimation for low altitude airspace". In: *17th AIAA Aviation Technology, Integration, and Operations Conference*. 2017, p. 4266.

[20] V. Bulusu et al. "Cooperative and Non-Cooperative UAS Traffic Volumes". In: *International Conference on Unmanned Aircraft Systems ICUAS*. 2017.

[21] Randolph Cabell, Ferdinand Grosveld, and Robert McSwain. "Measured Noise from Small Unmanned Aerial Vehicles". In: *INTER-NOISE and NOISE-CON Congress and Conference Proceedings*. Vol. 252. 2. Institute of Noise Control Engineering. 2016, pp. 345–354.

[22] María Consiglio et al. "ICAROUS: Integrated configurable algorithms for reliable operations of unmanned systems". In: *Digital Avionics Systems Conference (DASC), 2016 IEEE/AIAA 35th*. IEEE. 2016, pp. 1–5.

[23] Anubhav Datta and Wayne Johnson. *An Assessment of the State-of-the-art in Multidisciplinary Aeromechanical Analyses*. Tech. rep. ELORET CORP MOFFETT FIELD CA NASA AMES RESEARCH CENTER, 2008.

[24] DJI. *DJI S900 Specifications*. URL: `https://www.dji.com/spreading-wings-s900/info#specs` (visited on 07/31/2019).

[25] US DOE EIA. *Household Vehicles Energy Use: Latest Data and Trends (November 2005)*. 2001.

[26] U.S. Department of Energy. *https://fueleconomy.gov/*. (Visited on 07/31/2019).

[27] *Federal Aviation Administration - Unmanned Aircraft Systems*. `https://www.faa.gov/uas/`. 2016.

[28] TN FedEx Memphis. *Q1 Fiscal 2016 Statistics*. Tech. rep. 2016.

[29] *Gartner Says Almost 3 Million Personal and Commercial Drones Will Be Shipped in 2017*. 2017. URL: `http://www.gartner.com/newsroom/id/3602317`.

[30] Nikolas Geroliminis and Carlos F Daganzo. "Existence of urban-scale macroscopic fundamental diagrams: Some experimental findings". In: *Transportation Research Part B: Methodological* 42.9 (2008), pp. 759–770.

[31] Ashish Goel, Sanatan Rai, and Bhaskar Krishnamachari. "Sharp thresholds for monotone properties in random geometric graphs". In: *Proceedings of the thirty-sixth annual ACM symposium on Theory of computing*. ACM. 2004, pp. 580–586.

[32] Anne Goodchild and Jordan Toy. "Delivery by drone: An evaluation of unmanned aerial vehicle technology in reducing CO2 emissions in the delivery service industry". In: *Transportation Research Part D: Transport and Environment* 61 (2018), pp. 58–67.

[33] Géraud Granger and Nicolas Durand. "A traffic complexity approach through cluster analysis". In: *ATM 2003, 5th USA/Europe Air Traffic Management Research and Development Seminar*. 2003.

[34] Steven M Green, KD Bilimoria, and Mark G Ballin. "Distributed air/ground traffic management for en route flight operations". In: *Air Traffic Control Quarterly* 9.4 (2001).

[35] BD Greenshields, Ws Channing, Hh Miller, et al. "A study of traffic capacity". In: *Highway research board proceedings*. Vol. 1935. National Research Council (USA), Highway Research Board. 1935.

[36] J. Hoekstra. "Designing for Safety: the Free Flight Air Traffic Management Concept". ISBN 90-806343-2-8, also published as NLR TP-2001-313. PhD thesis. National Aerospace Laboratory NLR, Netherlands, 2001.

[37] Jacco M Hoekstra, Ronald NHW van Gent, and Rob CJ Ruigrok. "Designing for safety: the 'free flight' air traffic management concept". In: *Reliability Engineering & System Safety* 75.2 (2002), pp. 215–232.

[38] Jacco M Hoekstra et al. "How do layered airspace design parameters affect airspace capacity and safety?" In: *ICRAT2016-7th International Conference on Research in Air Transportation*. 2016.

[39] Gabriel Hoffmann et al. "Quadrotor helicopter flight dynamics and control: Theory and experiment". In: *AIAA guidance, navigation and control conference and exhibit*. 2007, p. 6461.

[40] Jeff Holden and Nikhil Goel. "Uber Elevate: Fast-Forwarding to a Future of On-Demand Urban Air Transportation". In: *Uber Technologies, Inc., San Francisco, CA* (2016).

[41] Alison J Hudgell and RM Gingell. "Assessing the capacity of novel ATM systems". In: *4th USA/Europe Air Traffic Management R&D Seminar*. 2001.

[42] UPS Inc. *Third Quarter 2015 Full Financial Tables*. Tech. rep. 2015.

[43] Dae-Sung Jang et al. "Concepts of Airspace Structures and System Analysis for UAS Traffic flows for Urban Areas". In: *AIAA Information Systems-AIAA Infotech*. 2017, p. 0449.

[44] Matt R Jardin. "Analytical relationships between conflict counts and air-traffic density". In: *Journal of guidance, control, and dynamics* 28.6 (2005), pp. 1150–1156.

[45] Wayne Johnson. *Helicopter theory*. Courier Corporation, 2012.

[46] Wayne Johnson. "NDARC-NASA Design and Analysis of Rotorcraft". In: (2015).

[47] Wayne Johnson. *Rotorcraft aeromechanics*. Vol. 36. Cambridge University Press, 2013.

[48] Wayne Johnson and Christopher Silva. "Observations from Exploration of VTOL Urban Air Mobility Designs". In: (2018).

[49] Kwang-Yeon Kim, Jung-Woo Park, and Min-Jea Tahk. "UAV collision avoidance using probabilistic method in 3-D". In: *Control, Automation and Systems, 2007. ICCAS'07. International Conference on*. IEEE. 2007, pp. 826–829.

[50] Alexander Klein et al. "Airspace capacity estimation using flows and weather-impacted traffic index". In: *2008 Integrated Communications, Navigation and Surveillance Conference*. IEEE. 2008, pp. 1–12.

[51] Mykel J Kochenderfer and JP Chryssanthacopoulos. "Robust airborne collision avoidance through dynamic programming". In: *Massachusetts Institute of Technology, Lincoln Laboratory, Project Report ATC-371* (2011).

[52] P Kopardekar. "Dynamic density: A review of proposed variables". In: *FAA internal document. overall conclusions and recommendations, Federal Aviation Administration* (2000).

[53] Parimal Kopardekar. *Unmanned Aerial System Traffic Management System*. Talks at Google. 2016.

[54] Parimal H Kopardekar. *Unmanned Aerial System (UAS) Traffic Management (UTM): Enabling Low-Altitude Airspace and UAS Operations*. Tech. rep. NASA Ames Research Center, Apr. 2014.

[55] Parimal H Kopardekar et al. "Airspace complexity measurement: An air traffic control simulation analysis". In: *International Journal of Industrial Engineering: Theory, Applications and Practice* 16.1 (2009), pp. 61–70.

[56] Jimmy Krozel, Mark Peters, and Karl Bilimoria. "A decentralized control strategy for distributed air/ground traffic separation". In: 2000.

[57] Jimmy Krozel et al. "System performance characteristics of centralized and decentralized air traffic separation strategies". In: *Fourth USA/Europe air traffic management research and development seminar*. 2001.

[58] J Krozel et al. "Airspace capacity estimation with convective weather constraints". In: *AIAA Guidance, Navigation, and Control Conference*. 2007.

[59] James K Kuchar and Lee C Yang. "A review of conflict detection and resolution modeling methods". In: *IEEE Transactions on intelligent transportation systems* 1.4 (2000), pp. 179–189.

[60] R Kühne and N Gartner. "Years of the Fundamental Diagram for Traffic Flow Theory: Greenshields Symposium, vol. E-C149 of Transportation Research Circular, Traffic Flow Theory and Characteristics Committee". In: *Transportation Research Board of the National Academies* 46 (75).

[61] M. Lammert. *Twelve-Month Evaluation of Diesel Hybrid Electric Van*. URL: `https://www.nrel.gov/docs/fy10osti/44134.pdf` (visited on 07/31/2019).

[62] Irene Vincie Laudeman et al. "Dynamic density: An air traffic management metric". In: (1998).

[63] Zhilong Liu, Raja Sengupta, and Alex Kurzhanskiy. "A power consumption model for multi-rotor small unmanned aircraft systems". In: *2017 International Conference on Unmanned Aircraft Systems (ICUAS)*. IEEE. 2017, pp. 310–315.

[64] Arnab Majumdar, Washington Ochieng, and John Polak. "Estimation of European airspace capacity from a model of controller workload". In: *Journal of Navigation* 55.03 (2002), pp. 381–403.

[65] Arnab Majumdar et al. "En-route sector capacity estimation methodologies: An international survey". In: *Journal of Air Transport Management* 11.6 (2005), pp. 375–387.

[66] Daniel Mellinger, Alex Kushleyev, and Vijay Kumar. "Mixed-integer quadratic program trajectory generation for heterogeneous quadrotor teams". In: *Robotics and Automation (ICRA), 2012 IEEE International Conference on*. IEEE. 2012, pp. 477–483.

[67] MITRE. "SUAS gaps being worked by SARP". In: *UTM Convention*. Researc Panel Presentation. 2016. URL: `http://www.utm2016.com/Uploads/Presentations/%20UTMRDPanelcompress.pdf`.

[68] Richard H Mogford et al. *The Complexity Construct in Air Traffic Control: A Review and Synthesis of the Literature*. Tech. rep. DTIC Document, 1995.

[69] Mark D Moore et al. "High Speed Mobility through On-Demand Aviation". In: (2013).

[70] Eric R Mueller and Mykel J Kochenderfer. "Multi-rotor aircraft collision avoidance using partially observable Markov decision processes". PhD thesis. Stanford University, 2016.

[71] Eric Mueller, Parimal Kopardekar, and Kenneth H Goodrich. "Enabling Airspace Integration for High-Density On-Demand Mobility Operations". In: *17th AIAA Aviation Technology, Integration, and Operations Conference*. 2017, p. 3086.

[72] Yash Mulgaonkar et al. "Power and weight considerations in small, agile quadrotors". In: *Micro-and Nanotechnology Sensors, Systems, and Applications VI*. Vol. 9083. International Society for Optics and Photonics. 2014, 90831Q.

[73] César Muñoz et al. "DAIDALUS: detect and avoid alerting logic for unmanned systems". In: *Digital Avionics Systems Conference (DASC), 2015 IEEE/AIAA 34th*. IEEE. 2015, 5A1–1.

[74] Electric VTOL News. *A^3 Vahana*. URL: `http://evtol.news/aircraft/a3-by-airbus/` (visited on 07/17/2019).

[75] Jung-Woo Park, Hyon-Dong Oh, and Min-Jea Tahk. "Uav collision avoidance based on geometric approach". In: *SICE Annual Conference, 2008*. IEEE. 2008, pp. 2122–2126.

[76] Duc-Kien Phung and Pascal Morin. "Modeling and energy evaluation of small convertible uavs". In: *IFAC Proceedings Volumes* 46.30 (2013), pp. 212–219.

[77] Thomas Prevot et al. "UAS traffic management (UTM) concept of operations to safely enable low altitude flight operations". In: *16th AIAA Aviation Technology, Integration, and Operations Conference*. 2016, p. 3292.

[78] *Revising the Airspace Model for the Safe Integration of Small Unmanned Aircraft Systems*. (Date last accessed 01-April-2016). URL: `http://utm.arc.nasa.gov/docs/Amazon_Revising%20the%20Airspace%20Model%20for%20the%20Safe%20Integration%20of%20sUAS[6].pdf`.

[79] James F Roberts, Jean-Christophe Zufferey, and Dario Floreano. "Energy management for indoor hovering robots". In: *2008 IEEE/RSJ International Conference on Intelligent Robots and Systems*. IEEE. 2008, pp. 1242–1247.

[80] *San Francisco County Transportation Authority: City Performance Scorecards*. 2017. URL: `https://sfgov.org/scorecards/transportation/congestion`.

[81] Tom Schouwenaars et al. "Mixed integer programming for multi-vehicle path planning". In: *European control conference*. Vol. 1. 2001, pp. 2603–2608.

[82] L. Sedov, V. Polishchuk, and V. Bulusu. "Sampling-based capacity estimation for unmanned traffic management". In: *2017 IEEE/AIAA 36th Digital Avionics Systems Conference (DASC)*. **Best Paper Award**. Sept. 2017, pp. 1–10.

[83] United Parcel Service. *UPS 2017 Corporate Sustainability Report*. 2017.

[84] Banavar Sridhar, Kapil S Sheth, and Shon Grabbe. "Airspace complexity and its application in air traffic management". In: *2nd USA/Europe Air Traffic Management R&D Seminar*. 1998, pp. 1–6.

[85] Dengfeng Sun, Alexis Clinet, and Alexandre M Bayen. "A dual decomposition method for sector capacity constrained traffic flow optimization". In: *Transportation Research Part B: Methodological* 45.6 (2011), pp. 880–902.

[86] Dengfeng Sun, Issam S Strub, and Alexandre M Bayen. "Comparison of the performance of four Eulerian network flow models for strategic air traffic management". In: *Networks and Heterogeneous Media* 2.4 (2007), p. 569.

[87] Emmanuel Sunil et al. "Metropolis: Relating airspace structure and capacity for extreme traffic densities". In: *11th USA/EUROPE Air Traffic Management R&D Seminar*. 2015.

[88] Gonzalo Tobaruela, Arnab Majumdar, and Washington Y Ochieng. "Identifying Airspace Capacity Factors in the Air Traffic Management System". In: *Proceedings of the 2nd International Conference on Application and Theory of Automation in Command and Control Systems*. 2012, pp. 219–224.

[89] Claire Tomlin, George J Pappas, and Shankar Sastry. "Conflict resolution for air traffic management: A study in multiagent hybrid systems". In: *IEEE Transactions on automatic control* 43.4 (1998), pp. 509–521.

[90] Rachael E Tompa et al. "Collision avoidance for unmanned aircraft using coordination tables". In: *Digital Avionics Systems Conference (DASC), 2016 IEEE/AIAA 35th*. IEEE. 2016, pp. 1–9.

[91] Federal Highway Administration U.S. Department of Transportation. *2017 National Household Travel Survey*. Tech. rep. 2017.

[92] Parker D Vascik et al. "A Geometric Approach Towards Airspace Assessment for Emerging Operations". In: *Submitted to AIAA Journal of Air Transportation Special Issue on best papers from ATM Seminar* (2019). **Best Paper in UAS Track**.

[93] *VTOL For All, Tag: electric*. 2016. URL: `http://vtolforall.com/tag/electric/`.

[94] Jerry D Welch et al. "Macroscopic workload model for estimating en route sector capacity". In: *Proc. of 7th USA/Europe ATM Research and Development Seminar, Barcelona, Spain*. 2007, p. 138.

[95] Daniel B Work and Alexandre M Bayen. "Convex formulations of air traffic flow optimization problems". In: *Proceedings of the IEEE* 96.12 (2008), pp. 2096–2112.

[96] Min Xue and Joseph Rios. "Initial Study of An Effective Fast-time Simulation Platform for Unmanned Aircraft System Traffic Management". In: *17th AIAA Aviation Technology, Integration, and Operations Conference*. 2017, p. 3073.